STRESS RESPONSES IN GRAPEVINE: GENE EXPRESSION PROFILING UNDER FOUR STRESSORS AND GENOME EDITING APPROACHES FOR PHYTOPLASMA RESISTANCE

Rebeka Strah

Doctoral Dissertation
Jožef Stefan International Postgraduate School
Ljubljana, Slovenia

Supervisor: Prof. Dr. Marina Dermastia, National Institute of Biology, Ljubljana, Slovenia
Co-Supervisor: Prof. Dr. Maruša Pompe Novak, National Institute of Biology, Ljubljana, Slovenia, and University of Nova Gorica, Vipava, Slovenia

Evaluation Board:
Prof. Dr. Kristina Gruden, Chair, National Institute of Biology, Ljubljana, Slovenia, and Jožef Stefan International Postgraduate School, Ljubljana, Slovenia

Assoc. Prof. Dr. Nataša Mehle, Member, National Institute of Biology, Ljubljana, Slovenia, and Jožef Stefan International Postgraduate School, Ljubljana, Slovenia, and University of Nova Gorica, Vipava, Slovenia

Prof. Dr. Johan Burger, Member, Department of Genetics, Stellenbosch University, Republic of South Africa

MEDNARODNA PODIPLOMSKA ŠOLA JOŽEFA STEFANA
JOŽEF STEFAN INTERNATIONAL POSTGRADUATE SCHOOL



Rebeka Strah

STRESS RESPONSES IN GRAPEVINE: GENE EXPRESSION PROFILING UNDER FOUR STRESSORS AND GENOME EDITING APPROACHES FOR PHYTOPLASMA RESISTANCE

Doctoral Dissertation

ODZIV VINSKE TRTE NA STRES: PROFILIRANJE IZRAŽANJA GENOV OB ŠTIRIH STRESNIH DEJAVNIKIH IN UREJANJE GENOMA ZA ODPORNOST PROTI FITOPLAZMI

Doktorska disertacija

Supervisor: Prof. Dr. Marina Dermastia

Co-Supervisor: Prof. Dr. Maruša Pompe Novak

Ljubljana, Slovenia, 2026

Acknowledgments

Many facets of support combined to make this PhD possible. My colleagues, family, and friends provided care and guidance. I also gratefully acknowledge the funding received from Slovenian Research and Innovation Agency (ARIS; grant numbers J1-7151, J4-2544, J1-60018, P4-0165 and P4-0463), bilateral funding within the call for Scientific & Technological Cooperation between Austria and Slovenia (ARIS grant number BI-AT/23-24-005 and Austria's Agency for Education and Internationalisation (OeAD-GmbH) grant Sl 25/2023), Arimnet 2 project EnViRoS (grant number 618127), and the short-term scientific mission funded by the COST action INTEGRAPE (CA17111). Finally, the infrastructure used in this work was supported by ARIS grant IO-0004.

I would like to express my sincere gratitude to my supervisor, Marina Dermastia, who believed in me from my first steps into the world of plant research. Her continued guidance and support made my research possible. I also thank her for making it possible to do part of my research at University of Verona.

I was also privileged to have Maruša Pompe Novak as my co-supervisor. I want to thank her for the knowledge she imparted to me, the patience and care with which she shared it, her unrelenting drive and her ability to inspire the same drive in me.

Besides my supervisors, I want to thank the members of my committee: Prof. Dr. Kristina Gruden, Assoc. Prof. Dr. Nataša Mehle, and Prof. Dr. Johan Burger, for their insightful comments that encouraged me to see my research from different perspectives.

I also sincerely thank our collaborators. Prof. Dr. Paolo Sivilotti and Assoc. Prof. Dr. Rachele Falchi from the University of Udine, Prof. Dr. Ignacio Buesa from Instituto Valenciano de Investigaciones Agrarias, Prof. Dr. Aaron Fait and Dr. Chao Song from Ben-Gurion University of the Negev, and Prof. Dr. Michaela Griesser and Dr. Sarhan Khalil from BOKU University in Tulln, who all conducted experiments and provided plant materials that made my research possible. Dr. Günter Brader from Austrian Institute of Technology led field trials and also provided Zweigelt canes that were used in our experiments. Finally, I thank Maja Cigoj, who provided Chardonnay canes for our experiments.

My sincere thanks also go to Prof. Dr. Mario Pezzotti from the University of Verona, who provided me with an opportunity to join his working team for six months, and Prof. Dr. Sara Zenoni and Dr. Edoardo Bertini, who patiently taught me the intricacies of transcriptomic analysis.

Many thanks also to my NIB colleagues. I am especially thankful to OMICS group for valuable discussions, Živa for teaching me the complexities of transcriptomic analysis, Vesna for her astounding ability to keep up with my production of dirty glassware, Maja and Valentina for their support that helped me grow both as a researcher and as a person, and the fresh air team that helped keep my brain running on long days both during and after work.

Last, I want to thank my family, especially my sisters, who stick with me through good and bad, from near and far. Thanks also to Sara, Pia, Gregor, and all my friends. Your precious support made my successes possible.

Claude was used for grammar and sentence-level clarity edits. The author reviewed every change and remains responsible for the final text.

Abstract

Viticulture faces production challenges from multiple environmental factors, ranging from changing weather patterns and nutrient deficiencies to pathogen pressure. In this thesis, we deepened the understanding of how grapevine responds to water deficit, increased soil salinity, different aspects of iron deficiency, and infection by '*Candidatus* Phytoplasma solani', by investigating transcriptomic responses in various genotypes. A multifactorial linear model was used to combine transcriptomic and metabolomic data with midday stem water potential to evaluate the responses of Cabernet Volos and Fleurtai, both cultivars originally bred for disease resistance, to prolonged water deficit. The responses were categorized into three groups. The most numerous were core responses shared by both genotypes, including osmoprotectant accumulation and downregulation of biotic defense. The other two categories comprised the gene expression and metabolite abundance signatures unique to each genotype. Salinity stress was evaluated in the leaves and berry skins of Tempranillo vines grafted onto rootstocks M1, M4, and 1103 Paulsen. None of the tested rootstocks were associated with major salinity-induced transcriptomic disturbances in the scion. Rootstocks 3309 C and Fercal were used to investigate iron deficiency responses. The effects of iron deficiency were first studied in combination with different nitrogen sources; the response was more severe when only nitrate was supplied, compared to the application of equal amounts of nitrate and ammonium. This held true for both rootstocks; however, the more susceptible 3309 C consistently showed a lower capacity to engage core Fe deficiency-related genes and lower induction of auxin responses and root growth. Iron deficiency was induced by two different mechanisms: directly, through low-Fe treatments, or indirectly, by adding bicarbonate to Fe-sufficient media. For both genotypes, indirect Fe deficiency presented a greater challenge, and the more tolerant Fercal exhibited a greater ability to engage genes related to Fe transport and root development. Gene expression changes in grapevines infected with '*Ca.* P. solani' were detected in the early growing season, before symptom onset, and included major shifts in photosynthesis and energy metabolism, protein synthesis, and disturbances in lignification-related genes, which persisted into the late growing season as symptoms appeared. Two genes involved in salicylic acid response regulation, *VviDMR6-1* and *VviDLO1*, were found to be significantly regulated in this investigation and were therefore selected as candidate targets for genome editing, with the long-term aim of potentially reducing grapevine susceptibility to this pathogen. DNA-free genome editing was performed on protoplasts isolated from embryogenic callus, using polyethylene glycol-mediated transfection to deliver in vitro-assembled Cas9-gRNA ribonucleoprotein complexes into the cells. Plants were successfully regenerated from both Chardonnay and Zweigelt. Zweigelt showed a much higher propensity to regenerate into whole plants than Chardonnay, while successful editing was more frequent in Chardonnay than in Zweigelt. Six of the eight edited lines obtained in our experiments carried a single nucleotide insertion resulting in a frameshift and a premature stop codon. However, all the lines have been edited on only one allele. The phenotype effect will be evaluated in future investigations.

Povzetek

Vinogradniki se pri pridelavi soočajo s številnimi okoljskimi izzivi, od spreminjajočih se vremenskih vzorcev in pomanjkanja hranil do pritiska povzročiteljev bolezni. V tej disertaciji smo s proučevanjem transkriptomskih odzivov pri različnih genotipih poglobili razumevanje odziva vinske trte na pomanjkanje vode, povečano zasoljenost tal, različne vidike pomanjkanja železa ter okužbo s fitoplazmo '*Candidatus* Phytoplasma solani'. Za oceno odziva sort Cabernet Volos in Fleurtai na dolgotrajno pomanjkanje vode smo z multifaktorskim linearnim modelom povezali transkriptomske in metabolomske podatke s poldnevnim vodnim potencialom stebla. Odzive smo razvrstili v tri skupine. Najštevilnejši so bili osnovni odzivi, skupni obema genotipoma, med njimi kopičenje osmoprotektantov in znižana izraženost genov, povezanih z biotsko obrambo. Preostali dve kategoriji sta zajemali vzorce izražanja genov in vsebnosti metabolitov, značilne za posamezen genotip. Stres zaradi zasoljenosti smo ovrednotili v listih in kožicah jagod trt sorte Tempranillo, cepljenih na podlage M1, M4 in 1103 Paulsen. Nobena od preizkušenih podlag ni bila povezana z večjimi transkriptomskimi motnjami cepiča zaradi zasoljenosti. Za proučevanje odziva na pomanjkanje železa smo uporabili podlagi 3309 C in Fercal. Učinke pomanjkanja železa smo najprej proučevali v kombinaciji z različnimi viri dušika; odziv je bil hujši, kadar je bil dodan zgolj nitrat, v primerjavi z enakimi količinami nitrata in amonija. To je veljalo za obe podlagi; bolj občutljiva podlaga 3309 C pa je dosledno kazala manjšo zmožnost aktivacije osnovnih genov, povezanih s pomanjkanjem železa, ter šibkejšo indukcijo avksinskih odzivov in rasti korenin. Pomanjkanje železa smo povzročili z dvema različnima mehanizmoma: neposredno, v obravnavah z nizko vsebnostjo železa, ali posredno, z dodatkom bikarbonata v gojišča z zadostno vsebnostjo železa. Pri obeh genotipih je posredno pomanjkanje železa predstavljalo večji izziv, pri čemer je bolj tolerantna podlaga Fercal izkazovala večjo zmožnost aktivacije genov, povezanih s transportom železa in razvojem korenin. Spremembe v izražanju genov pri trtah, okuženih s '*Ca.* P. solani', so bile zaznane že zgodaj v rastni sezoni, še pred pojavom simptomov, in so vključevale večje spremembe v fotosintezi in energijskem metabolizmu, sintezi beljakovin ter motnje v genih, povezanih z lignifikacijo; te spremembe so se nadaljevale tudi pozneje v rastni sezoni, ko so se pojavili simptomi. V tej raziskavi smo ugotovili, da sta bila značilno regulirana dva gena, vključena v uravnavanje odziva salicilne kisline, *VviDMR6-1* in *VviDLO1*, zato smo ju izbrali kot kandidata za urejanje genoma, z dolgoročnim ciljem morebitnega zmanjšanja dovzetnosti vinske trte za tega povzročitelja bolezni. Urejanje genoma brez uporabe DNA smo izvedli na protoplastih, izoliranih iz embriogenega kalusa, pri čemer smo s transfekcijo, posredovano s polietilenglikolom, v celice vnesli in vitro sestavljene ribonukleoproteinske komplekse Cas9-gRNA. Rastline smo uspešno regenerirali iz obeh sort, Chardonnaya in Zweigelta. Zweigelt je izkazoval veliko večjo nagnjenost k regeneraciji v cele rastline kot Chardonnay, medtem ko je bilo uspešno urejanje genoma pogostejše pri Chardonnayu kot pri Zweigeltu. Šest od osmih urejenih linij, pridobljenih v naših poskusih, je vsebovalo insercijo enega nukleotida, ki je povzročila premik bralnega okvirja in prezgodnji stop kodon. Vse linije pa so bile urejene le na enem alelu. Fenotipski učinek bo ovrednoten v prihodnjih raziskavah.

Contents

List of Figures **xiii**

List of Tables **xv**

Abbreviations **xvii**

Symbols **xxi**

1 Introduction **1**
1.1 Grapevine Response to Abiotic Stress ... 1
1.1.1 Drought ... 1
1.1.2 High salinity ... 3
1.1.3 Iron deficit ... 5
1.2 Grapevine Responses to Biotic Stress ... 6
1.2.1 Plant immune responses ... 6
1.2.2 The role of *DMR6* ... 7
1.2.3 '*Candidatus* Phytoplasma solani' infection ... 8
1.3 Grapevine Genome Editing ... 9
1.4 Research Hypotheses ... 10

2 Materials and Methods **12**
2.1 Plant Material ... 12
2.1.1 Water deficit experiments ... 12
2.1.2 High salinity experiments ... 13
2.1.3 Iron deficiency experiments ... 13
2.1.3.1 Effect of nitrogen source ... 14
2.1.3.2 Direct and indirect iron deficit ... 14
2.1.4 Phytoplasma infection experiments ... 14
2.2 RNA Isolation and High-Throughput Sequencing ... 15
2.3 RNA Sequencing and Data Analysis ... 15
2.3.1 Differential gene expression analysis ... 15
2.3.2 Differential metabolite abundance analysis and transcript and metabolite correlation ... 17
2.4 Protoplast Genome Editing ... 18
2.4.1 Embryogenic callus induction ... 18
2.4.2 In vitro guide RNA synthesis ... 19
2.4.3 Protoplast isolation ... 22
2.4.4 Protoplast transfection ... 22
2.4.5 Plant regeneration ... 24
2.4.6 Editing confirmation ... 24

3 Results **28**

3.1 Water Deficit Response in Cabernet Volos and Fleurtai ... 28
3.1.1 Type 1 ... 30
3.1.2 Type 2 ... 31
3.1.3 Type 3 ... 31
3.2 High Salinity Responses in M1, M4 and 1103 Paulsen Rootstocks ... 34
3.3 Iron Deficit in Fercal and 3309 C ... 39
3.3.1 Nitrogen source and iron availability ... 39
3.3.2 Direct and induced iron deficiency ... 44
3.4 '*Candidatus* Phytoplasma solani' Infection in cv. Zweigelt ... 46
3.5 DNA-Free Genome Editing of *DMR6* Genes in cv. Chardonnay and cv. Zweigelt 51
3.5.1 Embryogenic callus induction ... 51
3.5.2 Protoplast isolation and cultivation ... 51
3.5.3 Plant regeneration ... 52
3.5.4 Genome editing confirmation ... 58

4 Discussion **61**
4.1 Water Deficit Induces a Metabolic Shift and Transcriptional Reprogramming .. 61
4.1.1 Shared responses to water deficit (Type 1) ... 62
4.1.2 Cabernet Volos-specific responses (Type 2) ... 63
4.1.3 Fleurtai-specific responses (Type 3) ... 63
4.2 Tolerant Rootstocks Limit Major Salinity-Induced Transcriptomic Disturbances in the Scion ... 64
4.3 Iron Deficiency Responses Vary Between Genotypes ... 65
4.3.1 Nitrogen source impacts the response to Fe deficiency ... 65
4.3.2 Bicarbonate-induced iron deficiency elicits a stronger response ... 66
4.4 '*Ca.* P. solani' Induces Significant Responses Before Symptom Appearance ... 68
4.5 Genome Editing of Grapevine Protoplasts Depends on the Genotype ... 69

5 Conclusions **73**

Appendix A Supplementary Material **77**
A.1 Supplementary Material for Section 3.4 ... 77

References **87**

Bibliography **109**

Biography **113**

List of Figures

Figure 2.1: Gene expression and metabolite abundance categories. 17
Figure 2.2: Rooted Chardonnay canes 18
Figure 2.3: Defoliated Chardonnay inflorescence (left) and pollen in the tetrad developmental stage (right). 19
Figure 2.4: *VviDMR6-1* and *VviDLO1* sequences. 20
Figure 3.1: Principal Component Analysis (PCA) of transcripts and metabolites in water deficit experiment. 29
Figure 3.2: Raffinose synthesis pathway with transcript and metabolite measurements in water deficit experiment. 30
Figure 3.3: Response of caffeoylquinate synthesis pathway with transcript and metabolite measurements in water deficit experiment 33
Figure 3.4: Gene expression overview in berry skin samples of grapevine cv. Tempranillo grafted onto three different rootstocks and exposed to salinity stress. 35
Figure 3.5: Gene expression overview in leaf samples of grapevine cv. Tempranillo grafted onto three different rootstocks and exposed to salinity stress. 36
Figure 3.6: Subset of significantly enriched gene sets identified by GSEA of grapevine cv. Tempranillo grafted onto three different rootstocks and exposed to salinity stress. 37
Figure 3.7: Expression of genes involved in anthocyanin synthesis in berry skins of grapevine cv. Tempranillo grafted onto three different rootstocks and exposed to salinity stress. 38
Figure 3.8: Expression of genes involved in anthocyanin synthesis in cv. Tempranillo in salinity-treated leaves. 39
Figure 3.9: Expression response of auxin- and ABA-responsive genes in Fercal and 3309 C in iron deficiency. 43
Figure 3.10: Changes in expression of genes involved in TCA cycle and abundance of organic acids in Fercal and 3309 C in iron deficiency 46
Figure 3.11: Principal component scatterplot of gene expression in '*Ca.* P. solani'-infected grapevine samples. 47
Figure 3.12: Chardonnay embryogenic callus induction. 51
Figure 3.13: Zweigelt embryogenic callus induction 51
Figure 3.14: Protoplasts in solid culture expressing GFP. 52
Figure 3.15: Plant regeneration from protoplasts. 52
Figure 3.16: Boxplots of embryo germination (A), plant regeneration (B) and regeneration efficiency (C) in Chardonnay and Zweigelt. 56
Figure 3.17: Boxplots of transfection treatment effects on embryo germination (A), plant regeneration (B) and regeneration efficiency (C) in Zweigelt. 58
Figure 3.18: Example alignment of sequencing chromatograms of a successfully edited line. 59
Figure 3.19: Representative results of each successful mutation detected in the edited lines. 60

List of Tables

Table 2.1: Guide RNA sequences designed for *VviDMR6-1* and *VviDLO1* and their predicted properties. 21
Table 2.2: List of transfection treatments. 23
Table 2.3: Primers for amplification of editing target regions. 26
Table 2.4: Sequencing primers 27
Table 3.1: Expression of iron deficiency- and nitrogen-responsive genes in Fercal and 3309 C. 41
Table 3.2: Expression of direct and indirect iron deficiency-responsive genes in Fercal and 3309 C 45
Table 3.3: Subset of significantly enriched processes in '*Ca.* P. solani'-infected grapevine identified by GSEA. 48
Table 3.4: Expression changes of selected genes from '*Ca.* P. solani'-infected grapevine. 50
Table 3.5: BAP effect on plant germination and regeneration in Chardonnay and Zweigelt. 53
Table 3.6: Embryo germination and plant regeneration in Chardonnay. 54
Table 3.7: Embryo germination and plant regeneration in Zweigelt....55
Table 3.8: Effect of transfection treatment type on germination, regeneration, and regeneration efficiency in Zweigelt. 57
Table 3.9: A list of successfully edited recovered lines and their corresponding editing targets. 59

Abbreviations

ABA	...	Abscisic acid
ADP	...	Adenosine diphosphate
AHA1	...	ATPase homolog 1
AHA2	...	Plasma membrane H^+-ATPase 2
AKT1	...	Arabidopsis K+ transporter 1
ANN4	...	Annexin IV
ANS	...	anthocyanin synthase
AREB/ABF	...	Abscisic acid-responsive element binding protein/ abscisic acid-responsive element binding factor
ATP	...	Adenosine triphosphate
ATPase	...	Adenosine triphosphatase
AUX	...	Auxin
BAM	...	Barely any meristem
BAP	...	6-benzylaminopurine
bHLH	...	Basic helix–loop–helix
BTS	...	Brutus
BTSL	...	Brutus-like
C4H	...	Cinnamate-4-hydroxylase
4CL	...	4-Coumarate:CoA ligase
Cas9	...	CRISPR-associated protein 9
CBL	...	Calcineurin B-like
CHI	...	Chalcone-flavanone isomerase
CHS	...	Chalcone synthase
CLC	...	Chloride channel
CLE25	...	Clavata 3 /embryo surrounding region 25
CRISPR	...	Clustered Regularly Interspaced Short Palindromic Repeats
CTAB	...	Cetyltrimethylammonium bromide
cv	...	cultivar
DAHPS	...	3-deoxy-D-arabino-heptulosonic acid 7-phosphate synthase
DFR	...	Dihydroflavonol 4-reductase
DHQS	...	3-dehydroquinate synthase
DLO	...	DMR6-like oxygenase
DMR6	...	Downy mildew resistant 6
DNA	...	Deoxyribonucleic acid
DREB2A	...	Dehydration-Responsive Element-Binding protein 2A

EC	...	Electrical conductivity
ET	...	Evapotranspiration
F3’5’H	...	Flavonoid 3'5'-hydroxylase
F3’H	...	Flavonoid 3'-hydroxylase
F3H	...	Flavanone 3-hydroxylase
FDR	...	False discovery rate
FER1	...	Ferritin 1
FRO2	...	Ferric reduction oxidase 2
GABA	...	Gamma-aminobutyric acid
GC-MS	...	Gas chromatography-mass spectrometry
GDSL	...	Glycine–aspartate–serine–leucine
GFP	...	Green fluorescent protein
gRNA	...	Guide RNA
GSEA	...	Gene Set Enrichment Analysis
HDH	...	Histidine-Aspartate-Histidine
HKT1	...	High-affinity K+ transporter
HSPs	...	Heat shock proteins
IAA	...	Indole-3-acetic acid
IMA	...	Iron man
IREG3	...	Iron-regulated protein 3
IRT1	...	Iron-regulated transporter 1
JA	...	Jasmonic acid
JAMT	...	Jasmonic acid carboxyl methyltransferase
KAT1	...	Potassium channel in Arabidopsis thaliana 1
LOX	...	Lipoxygenase
MAPK	...	Mitogen-activated protein kinase
MES	...	2-(N-morpholino) ethanesulfonic acid
MS	...	Murashige and Skoog
NADH	...	Reduced nicotinamide adenine dinucleotide
NCED	...	9-cis-epoxycarotenoid dioxygenase
NHX1	...	Sodium/Hydrogen exchanger 1
NLR	...	Nucleotide-binding leucine-rich repeat receptor
NAA	...	1-naphthaleneacetic acid
NPF2.4	...	Nitrate transporter 1/peptide transporter family
NR2	...	Nitrate reductase 2
NRT1:2	...	Nitrate transporter 1:2
NSCCs	...	Non-selective cation channels
NYYPPCP	...	Asparagine–Tyrosine–Tyrosine–Proline–Proline–Cysteine–Proline
OMT	...	O-methyltransferase
OPT3	...	Oligopeptide transporter 3
OsHKT2;1	...	Class 2 Oryza sativa high-affinity K+ transporter
P5CR	...	Pyrroline-5-carboxylate reductase
PAL	...	Phenylalanine ammonia-lyase

PAM	...	Protospacer Adjacent Motif
PCA	...	Principal component analysis
PCR	...	Polymerase Chain Reaction
PEG	...	Polyethylene glycol
PMU	...	Potential mobile unit
PP2C	...	Type 2C protein phosphatase
PR5	...	pathogenesis-related protein 5
PRR	...	Pattern recognition receptor
PsbS	...	Photosystem II subunit S
PSI	...	Photosystem I
PSII	...	Photosystem II
PYL	...	Pyrabactin resistance-like
PYR	...	Pyrabactin resistance
RCAR	...	Regulatory component of ABA receptor
RNA	...	Ribonucleic acid
RNP	...	ribonucleoprotein particles
ROS	...	Reactive oxygen species
SA	...	Salicylic acid
SAMT	...	Salicylic acid carboxyl methyltransferase
SAP	...	Secreted AY-WB Protein
SAR	...	Systemic acquired resistance
SAUR	...	Small Auxin Up-Regulated RNA
SCaBP8	...	SOS3-like calcium-binding protein 8
SecY	...	Protein translocase subunit SecY
sgRNA	...	Single-guide RNA
SLAC1	...	Slow anion channel-associated 1
SLAH	...	Slow-type anion channel
SnRK2	...	Sucrose non-fermenting 1-related protein kinase 2
SOS	...	Salt overly sensitive
Stamp	...	Stolbur antigenic membrane protein
TCA	...	Tricarboxylic acid
TCP	...	TEOSINTE BRANCHED 1, CYCLOIDEA, PROLIFERATING CELL FACTOR
TIR-NBS-LRR	...	Toll/interleukin-1 receptor–nucleotide-binding site–leucine-rich repeat
TMM	...	Trimmed mean of M-values
tuf	...	Elongation factor Tu
UFGT	...	Anthocyanidin 3-O-glucosyltransferase
VIT1	...	Vacuolar iron transporter 1
vmp1	...	Variable membrane protein 1
VvFER1	...	Ferritin1
VviNCED1	...	Vitis vinifera 9-cis-epoxycarotenoid dioxygenase 1 gene
VviNCED2	...	Vitis vinifera 9-cis-epoxycarotenoid dioxygenase 2 gene

WRDY/FLRL	...	Tryptophan–Arginine–Aspartate–Tyrosine/ Phenylalanine–Leucine–Arginine–Leucine
WRKY	...	Tryptophan–arginine–lysine–tyrosine
WS	...	Water-stress
WW	...	Well-watered
YSL6	...	Yellow stripe-like 6
ZAT11	...	Zinc finger of Arabidopsis thaliana 11
ZIF1	...	Zinc-induced facilitator 1

Symbols

Ψ_s	...	Stem water potential
EC_{25}	...	Electrical conductivity at 25 °C
ET_c	...	Crop evapotranspiration
ET_o	...	Reference evapotranspiration
Log_2FC	...	Log_2 fold change

Chapter 1

Introduction

1.1 Grapevine Response to Abiotic Stress

Grapevine (*Vitis vinifera* L.) is cultivated across the globe between the 30th and 50th parallels, spanning Mediterranean and continental climate zones, as well as a variety of soil types. Once planted, a commercial vineyard is expected to remain productive for decades. The perennial nature of grapevine therefore requires that the plants tolerate a wide variety of environmental challenges, including the new challenges brought about by climate change.

Although grapevine is considered a relatively drought-resilient crop, irrigation of vineyards is becoming increasingly necessary due to the progressively hotter summers and reduced rainfall during the growing season brought about by climate change in recent years. The need for irrigation typically arises during periods of overall water scarcity, placing additional strain on already diminishing water supplies. One way to reduce water consumption is the use of drought-resistant cultivars. Since obtaining such cultivars through conventional breeding can take several years, testing already existing cultivars for drought resistance emerges as a promising alternative [1].

Using reclaimed water is another option for providing irrigation without depleting the supply of potable water. However, reclaimed water usually contains higher ion concentrations and in the long term contributes to soil salinization, which could render vineyards unproductive. Salinity-tolerant rootstocks are a promising solution to soil salinization.

Grafting onto tolerant rootstocks is also a common solution to the problem of iron deficiency. This is a frequent nutrient deficiency in calcareous soils in the Mediterranean, alpine, and karst regions of Europe, as elevated soil pH reduces iron availability to plants.

1.1.1 Drought

Reduced water availability initiates a series of protective responses in plants, beginning with stomatal closure to reduce water loss through transpiration. This process is largely regulated by abscisic acid (ABA), which is considered the main regulator of drought response in plants, although it is also involved in many other processes. ABA is synthesized from β-carotene through a series of enzymatic reactions, in which cleavage of 9-*cis*-violaxanthin by 9-*cis*-epoxycarotenoid dioxygenase (NCED) is the first dedicated step [2].

Cells perceive ABA through binding to PYR/PYL/RCAR receptors inside the cell. This causes inactivation of clade A type 2C phosphatases (PP2Cs), which are inhibitors of ABA signaling. PP2Cs block ABA signaling by sequestering SnRK2s (Snf1-related kinases 2) and inhibiting their kinase activity [3]. ABA binding to PYR/PYL/RCAR receptors

therefore releases SnRK2s to activate downstream targets, including AREB/ABF transcription factors and ion channels.

SnRK2s induce stomatal closure by activating the S-type efflux anion channel SLAC1 (slow anion channel-associated 1) and inhibiting the inward K^+ channel KAT1 (potassium channel in *Arabidopsis thaliana* 1), both of which are preferentially expressed in guard cells. This causes simultaneous Ca^{2+} influx and Cl^-/K^+ efflux, followed by water loss, loss of turgor, and finally stomatal closure, which persists as long as ABA remains present in its active form [4].

Stomatal closure is a rapid response, followed by transcriptional reprogramming to adapt to the new circumstances. This reprogramming is governed by SnRK2 activation of AREB/ABF transcription factors, which induce gene expression by recognizing ABA-responsive elements [5]. Plants also possess ABA-independent drought-responsive genes containing dehydration-responsive elements, recognized by dehydration-responsive element-binding transcription factors, such as DREB2A [6].

There are strong indications that ABA is the main signal communicating water deficit from roots to leaves. This hypothesis is supported by measurements showing increased expression of *VviNCED1* and *VviNCED2* in drought-stressed roots of Cabernet Sauvignon, but not in the leaves [7]. This finding led to the development of partial rootzone drying as an irrigation technique in viticulture, in which part of the root system is left unirrigated to stimulate stomatal closure and increase the water-use efficiency of the vines [8]. At the same time, leaves can produce ABA in mesophyll cells under water deficit, and loss of cell volume has been proposed as a trigger for ABA synthesis in leaves [9]. Water loss also leads to increased xylem tension and embolisms that occlude the conduits and reduce hydraulic conductivity. This cavitation has been proposed as a hydraulic signal that can trigger stomatal response, although the relationship is not straightforward, as stomatal closure often occurs before embolism [10, 11]. Whatever the hydraulic signal may be, increased ABA content in leaves has been proposed to maintain stomatal closure and prevent premature reopening in this scenario [11]. Finally, water deficit in the soil is also signaled long-distance by the small signaling peptide CLE25 (CLAVATA3/embryo surrounding region-related 25). It is expressed in vascular tissues and roots upon dehydration and then moves from roots to leaves, where it is recognized by BAM (BARELY ANY MERISTEM) receptors. This induces ABA synthesis and accumulation [12].

Stomatal closure mitigates water loss but simultaneously decreases gas exchange. This leads to a reduction in leaf internal CO_2 levels and declining photosynthesis rates, culminating in reduced growth of the aerial parts. This favors water retention and long-term survival of the perennial plant [13]. Reduced photosynthetic capacity also diminishes the plant's ability to dissipate light energy, leading to photodamage of photosystem II (PSII) reaction centers [14, 15]. Plants counteract the effects of excess light through non-photochemical quenching, which dissipates the energy absorbed by PSII as heat [16, 17]. This process involves the photosystem II subunit S (PsbS) and the violaxanthin-antheraxanthin-zeaxanthin cycle (also known as the xanthophyll cycle) [18]. Excess light can also be dissipated via cyclic electron flow around photosystem I (PSI) and the photorespiration pathway [19, 20].

Inevitably, the excess light energy resulting from stomatal closure leads to overproduction of reactive oxygen species (ROS) in the chloroplast, which can be detoxified by ROS-scavenging enzymes. Superoxide radicals are first converted into O_2 and H_2O_2 by superoxide dismutases. H_2O_2 is then further detoxified either by catalases in the peroxisomes or by enzymes of the ascorbate-glutathione cycle in the chloroplasts and cytosol [21]. ROS can also be scavenged by non-enzymatic defenses, comprising molecules that are normal cell constituents but may begin accumulating increasingly under ROS

pressure. These molecules include glutathione, ascorbic acid, α-tocopherol, carotenoids, and flavonoids [22]. Among the flavonoids, anthocyanins occupy a dual protective role in the plant cell, functioning both as ROS scavengers and as light-absorbing pigments [23].

Plants also alleviate water loss by accumulating compatible solutes—low molecular weight organic molecules that can accumulate in the cell at relatively large concentrations without toxic effects, thereby aiding osmotic adjustment. In plant tissues, these are commonly proline, glycine betaine, and raffinose family oligosaccharides. Reduced cell volume due to water loss crowds the cellular components, and the higher leaf temperatures caused by reduced transpiration can lead to increased protein damage and aggregation. Plants repair this damage using heat shock proteins (HSPs), constitutively present molecular chaperones that participate in protein stabilization, folding, assembly, and disassembly. They also reduce further damage by accumulating small HSPs, which are stress-inducible and protect other proteins from stress-induced damage [24, 25].

Grapevines employ all these responses effectively, as they are considered a drought-tolerant crop [26]. In fact, moderate water deficit is sometimes deliberately used in premium red wine production. It has recently also been applied in white wine production to reduce water consumption without negatively affecting grape quality [27]. Stem water potential (Ψ_s) is a common measure of water status in grapevine. When producers impose a water-deficit regime, they commonly target Ψ_s levels between -1.2 and -1.4 MPa, which can decrease stomatal conductance and reduce yield but is not severe enough to cause leaf turgor loss or embolism in grapevine. If Ψ_s drops below -1.6 MPa, vines are at risk of xylem cavitation, leaf loss, or even mortality [26, 28].

Studies on the stomatal behavior of grapevine under water-deficit conditions have shown considerable variation among cultivars. Cultivars were initially grouped into two categories based on observed strategies. The isohydric strategy describes plants that maintain Ψ within a defined range under water deficit by limiting transpiration at relatively low stress levels. The anisohydric strategy describes plants that maintain transpiration rates while tolerating increasingly negative Ψ, down to the point at which embolism may occur [29, 30]. However, further studies have shown that this separation is not clear-cut. Categorizing cultivars into either group is further complicated by the fact that grapevine is normally grafted, and the rootstock appears to significantly influence the scion's stomatal behavior [31]. Large-scale experiments have indicated that the same cultivar may employ either an iso- or anisohydric strategy depending on stress severity [32, 33], and that this response can be significantly impacted by the chosen rootstock [34].

1.1.2 High salinity

Salinity stress partially overlaps with drought stress in its effects on plants. The osmotic effect occurs because increased ion concentration in the soil makes water uptake more difficult, leading to stomatal closure and turgor loss. The osmotic effect usually occurs first and is followed by the ionic effect, as the plant can no longer exclude or prevent the uptake of excess ions and begins to accumulate them in its tissues [35].

Roots are the first organ exposed to salinity. In the short term, a reduction in biomass and length is common, followed by more prominent anatomical changes during long-term exposure, including uneven thickening and increased suberization and Casparian strip thickening in woody species [36]. The first effect observed in leaves is stomatal closure and reduced turgor, resulting in decreased photosynthesis rates and increased ROS accumulation. During longer salinity exposure, plants take up sodium (Na^+) and chloride (Cl^-) ions, which follow the water column to the site of transpiration, where they accumulate. The resulting salt injury is usually observed first in older leaves, which have

been transpiring longer, and is apparent as leaf yellowing and eventual death [37]. Na^+ and Cl^- ion accumulation cause toxicity through different mechanisms.

Cl^- cooperates with K^+ in osmoregulation and turgor maintenance. It is also a cofactor in the oxygen-evolving complex of PSII and its assembly, and is therefore essential for photosynthesis [38, 39]. Excess Cl^- can reduce the uptake of nitrates and phosphates, leading to nutrient imbalances [40]. Cl^- accumulation in leaves causes chlorosis and necrosis, likely by accumulating excessively in the thylakoid lumen and causing chloroplast swelling and destruction [41, 42]. Na^+ ions are comparatively less toxic and can replace the function of K^+ in osmotic adjustment to a certain extent but can disrupt basic K^+ physiological functions if the K^+/Na^+ ratio is unfavorable [43]. Excess Na^+ can disrupt enzyme activation, protein synthesis, and stomatal functioning [44].

The water deficit caused by increased salinity is signaled by ABA, similarly to the drought stress. However, the osmotic component of salt stress is perceived by the roots as increased Na^+ and causes perturbation in cytosolic Ca^{2+} levels, which then spreads as a wave from the apex or application site to the basal part of the root [45]. This Ca^{2+} wave is accompanied by a ROS wave that is probably generated by RBOHD (respiratory burst oxidase homolog D), which propagates the signal rapidly throughout the whole plant and has been shown to play an important role in salt stress response signaling [46]. The Ca^{2+} signal is generated by the annexin ANN4, a Ca^{2+}-permeable transporter that mediates such increases under different stress conditions. In cooperation with SCaBP8 (SOS3-like calcium-binding protein 8) and SOS2, the calcium signal is decoded to induce the salt overly sensitive (SOS) pathway, the core signaling pathway for plant salt stress response [47]. The first component is SOS3/CBL4, a CBL-type (calcineurin B-like) Ca^{2+} sensor that activates the CBL-interacting protein kinase SOS2/CIPK24 by forming the SOS3-SOS2 complex [48]. This complex then phosphorylates SOS1, a Na^+ antiporter that facilitates efflux from the root cytoplasm into the rhizosphere to minimize uptake, as well as xylem loading and long-distance transport under severe stress [49, 50]. CBL10 is another Ca^{2+} sensor directly linked to Na^+ homeostasis, regulating its uptake into the vacuole for storage and detoxification [51].

Plants regulate ion content and localization using several transport proteins. Cl^- is actively taken up by the roots under non-stress conditions and is transported symplastically. It is loaded into the root xylem by the passive transporter NPF2.4 (nitrate transporter 1/peptide transporter family) and by the SLAH1–SLAH3 (slow-type anion channel) complex. To prevent excessive uptake, plants mainly regulate Cl^- xylem loading through the expression levels of these transporters [52, 53]. When uptake cannot be prevented, plants sequester Cl^- in the roots, away from photosynthetically active tissue. It is transported to the vacuole across the tonoplast by the ClC family of anion transporters via Cl^-/H^+ antiport [54, 55].

As mentioned above, Na^+ uptake is largely coupled with nitrate uptake. Nonselective cation channels (NSCCs) lack cation selectivity and have been suggested as the main importers [56]. Additionally, because of its similarity to K^+, Na^+ can be taken up by high-affinity potassium transporters, such as OsHKT2;1 in rice, and by the low-affinity potassium channel AKT1 [57, 58]. However, Na^+ exclusion is highly regulated. In addition to SOS1, which exports Na^+ from the cytoplasm to the extracellular space, plants also possess the high-affinity potassium transporter HKT1, which regulates its loading into the phloem sap in shoots and its unloading from xylem vessels into the xylem parenchyma cells [59, 60]. Na^+ can also be sequestered into the vacuole by the NHX1 (sodium/hydrogen exchanger) antiporter [61].

Grapevine is moderately sensitive to salinity stress. Since it is commonly grafted, using salinity-tolerant rootstocks is a common practice to compensate for the scion's sensitivity. The ability to exclude Cl^- is an important part of this tolerance. Own-rooted plants of the

tolerant rootstock genotype 140 Ruggeri absorb a similar amount of Cl^- as the more sensitive K51-40 but are better able to partition it into the roots, away from the photosynthetic apparatus [62]. Henderson et al. [63] compared the transcriptomes of the aforementioned rootstocks and demonstrated that 140 Ruggeri's ability to exclude Cl^- derives from constitutive expression of various anion transporters, which is observable even under non-stressed conditions. Na^+ exclusion capability holds similar importance for grapevine salt tolerance. The high-affinity Na^+-selective transporter HKT1;1 appears to be the most relevant in grapevine, since certain alleles confer increased Na^+ exclusion capability and are found in many salinity-tolerant rootstock genotypes [64, 65].

Sensitive grapevine cultivars can show decreased yields when irrigated with water of conductivity 1.5 dS/m. Using tolerant genotypes as rootstocks can raise this limit to as much as 4 dS/m [66]. This tolerance can be conferred by increased vigor, ion exclusion, and ion retention capabilities. Examples of such tolerant rootstocks are 1103 Paulsen and M4 [66, 67, 68].

1.1.3 Iron deficit

Iron (Fe) is an essential micronutrient for most living organisms because of its role as a cofactor in a wide range of enzymes. In plants, it is necessary for many biological processes, including chlorophyll synthesis, photosynthesis, respiration, oxidative stress responses, and nitrogen assimilation [69]. It is fairly abundant in most soils relative to plant needs; however, it is mostly present in the poorly soluble ferric (Fe^{3+}) form, rather than the more readily available ferrous (Fe^{2+}) form [70]. Poor Fe solubility in soil is usually the limiting factor leading to deficiency, especially in alkaline and calcareous soils, where high pH further reduces iron solubility [71]. Plants growing in calcareous soil can also absorb bicarbonate, which alkalizes the xylem sap and reduces iron transport efficiency. In addition to inducing nutrient imbalances, high soil pH weakens cell membrane stability and disrupts intracellular pH regulation [72]. Soil pH can also be influenced by fertilizer choice. Nitrate (NO_3^-) is a common nitrogen source in viticulture but can raise soil pH and reduce iron availability [73]. For this reason, it is commonly paired with ammonium (NH_4^+), which helps iron mobilization in the soil, as well as its remobilization and redistribution from the cell walls of roots and older leaves to younger leaves [74].

Iron deficiency commonly manifests as interveinal chlorosis, primarily in young leaves, eventually leading to necrosis and severe yield losses. Non-graminaceous plants rely on a reduction-based strategy to acquire iron, commonly referred to as Strategy I [75]. In this strategy, the soil surrounding the roots is acidified by proton ATPases, such as AHA1, which solubilize Fe^{3+}. Fe^{3+} is then reduced to Fe^{2+} by membrane-bound ferric chelate reductases such as FRO2, and can subsequently be transported into root cells by the high-affinity iron transporter IRT1 [76]. In Arabidopsis, iron solubilization is additionally supported by roots extruding phenolic compounds and organic acids, such as coumarins and malate, which can form complexes and aid in reduction [77]. The exact composition of root exudates is species-specific. Grapevine exudates contain higher amounts of phenolic compounds and citrate, which assume a role similar to that of coumarins [78].

It is not entirely clear how plants sense iron deficiency. The BTS (BRUTUS) and BTS-LIKE proteins are currently considered the best candidates. They are considered negative regulators of iron uptake, sensing the presence of sufficient iron through hemerythrin domains that bind iron-oxygen. When iron binds to this site, the BTS and BTSL proteins are stabilized and target several bHLH transcription factors for degradation via ubiquitination [79]. BTS and BTSL targets include the bHLH subgroup IVb and IVc transcription factors, which are the top-level regulators of many iron-deficiency-response genes [80, 81]. Iron Man (IMA) peptides are a component of a positive feedback loop in

iron acquisition. Their expression is induced by the group IVb/c factors bHLH121 and bHLH105, whereupon IMAs also become ubiquitination targets. In the current model, IMAs protect BTS and BTSL targets from degradation, thereby intensifying the iron deficiency response [82].

Split-root experiments have demonstrated that soil iron content is communicated systemically. When one part of the root system is exposed to iron-depleted conditions and the other to iron-sufficient conditions, iron-acquisition responses are activated in the iron-sufficient parts and shut down where iron was absent [83, 84]. However, the initial signal of iron deficiency or sufficiency originates from the leaves [85, 86]. It is unclear what this signal is; however, foliar iron application experiments have implicated oligopeptide transporter 3 (OPT3) as an important contributor to this communication. OPT3 is a phloem-specific iron transporter that loads iron, in its ionic form, into the leaf phloem. This regulates leaf iron demand, since *opt3-3* mutants show iron starvation symptoms under iron-sufficient conditions, even while their xylem and leaf iron content is higher than in WT plants [87]. Moreover, foliar iron application did not alleviate iron deficiency symptoms and responses in *opt3-3* knockdown plants, but grafting functional OPT3 Arabidopsis shoots onto *opt3-3* knockdown roots was sufficient to attenuate iron deficiency responses [88]. It appears that the inability to unload iron from the phloem renders it unavailable, causing deficiency signals to travel back to the root.

Direct iron deficiency caused by a lack of iron, and indirect iron deficiency caused by the presence of bicarbonate, induce similar core responses in plants. However, bicarbonate stress is not simply another form of iron deficiency and induces distinct responses; plants are able to discriminate between the different causes of iron deficiency. For example, in cucumber (*Cucumis sativus* L.), root ferric chelate reductase activity is increased by iron deficiency under mildly acidic conditions and by increased alkalinity under full iron supply, but not by iron deficiency under alkaline conditions [89].

The use of iron-deficiency-tolerant rootstocks is one of the simplest methods to prevent these issues in viticulture. Grapevine rootstock varieties possess a wide range of susceptibility. Examples of susceptible genotypes include 101-14 and Couderc 3309 (3309 C), while 140 Ruggeri, 110 Richter, Fercal, and M1 are tolerant. The main difference between tolerant and susceptible varieties is that the former can activate iron-uptake mechanisms more vigorously. This has been shown at the level of gene expression [78], enzyme activity, root exudate composition and acidification capacity [89, 90, 91].

1.2 Grapevine Responses to Biotic Stress

1.2.1 Plant immune responses

Plant immune responses rely on both the innate immunity of individual cells and systemic signaling that spreads from infection sites. They can be perceived by receptors either outside or inside the cell, separating the response into either extracellularly or intracellularly triggered immunity [92]. On the cell surface, plants recognize pathogen-associated molecular patterns (PAMPs) via pattern-recognition receptors (PRRs). In the cell, they recognize pathogen effectors, also termed avirulence (Avr) proteins via resistance (R) proteins, which are commonly nucleotide-binding domain leucine-rich repeat receptors (NLRs) [92].

Both extracellularly and intracellularly triggered immunity are highly intertwined and activate convergent downstream responses, including Ca^{2+} influx, ROS bursts, mitogen-activated protein kinase (MAPK) activation, induction of defense-related genes, and phytohormone production [93, 94]. While they share similar transcriptional signatures,

intracellularly triggered immunity responses are typically stronger and more sustained [95]. Intracellularly triggered immunity can culminate in hypersensitive response (HR)—a form of localized cell death that restricts pathogen spread [96]. When R proteins are expressed at high levels, intracellularly triggered immunity instead results in extreme resistance, where infection is effectively blocked without visible cell death [97].

Extracellularly and intracellularly triggered immunity also mutually potentiate one another. Pathogen effectors can increase the abundance of proteins that contribute to extracellularly triggered immunity, while the loss of extracellularly triggered immunity results in reduced cell death compared with the combined activation of both pathways [98]. Furthermore, several extracellularly triggered immunity coreceptors have been shown to be essential for full activation of intracellularly triggered immunity [99, 100], while, conversely, signaling via intracellularly triggered immunity components is required for extracellularly triggered immunity [101, 102]. The combined response of extracellularly and intracellularly triggered immunity exceeds the sum of the individual responses. In addition to higher abundance of BIK1, RbohD, and MPK3, which are the core components of extracellularly triggered immunity, a qualitative change also occurs through phosphorylation of RbohD and MAPKs and generation of apoplastic ROS. These synergistic effects occur at both the transcriptional and post-transcriptional levels [99, 100]. Extracellularly triggered immunity also amplifies the HR triggered by several effectors, through MAPK and Rboh activity [99].

Downstream of initial pathogen detection, the appropriate defense response is coordinated primarily through salicylic acid (SA), jasmonic acid (JA), and ethylene (ET) signaling pathways [103]. Plant defense against biotic stress is generally divided into two types which depend on the pathogen lifestyle: responses to biotrophs, which require living host tissue, and responses to herbivores and necrotrophs, which feed on and proliferate in dead tissue. Defense against biotrophs is mostly SA-dependent, while herbivory and necrotrophy responses rely mainly on JA and ET signaling. This distinction is referred to as trophic divergence [104].

SA additionally enables the activation of systemic acquired resistance (SAR), a phenomenon in plant immune signaling in which a signal is transduced from infected sites throughout the whole plant, raising basal defense responses. SA accumulation in both infected and distal tissues is required to induce SAR; however, the mobile signal carrying this information is N-hydroxypipecolic acid, which is synthesized in response to SA accumulation [105, 106].

1.2.2 The role of *DMR6*

The presence of SA sustains the immune response in plants, but this comes at the expense of growth. Therefore, levels of bioactive SA are tightly controlled through processes such as hydroxylation, glycosylation, methylation, and amino acid conjugation [107, 108]. DMR6 (downy mildew resistant 6) and DLO (DMR6-like oxygenase) are a group of plant 2OG-Fe(II) oxygenases that act as SA hydroxylases and suppressors of plant immunity. They convert SA to 2,5-dihydroxybenzoic acid (gentisic acid) and 2,3-dihydroxybenzoic acid (pyrocatechuic acid), respectively [109]. They possess a characteristic HDH motif, involved in catalytic iron binding; an NYYPPCP motif, which interacts with the 2-oxoglutarate substrate; and a WRDY/FLRL motif, specific to DMR6- and DLO-type oxygenases, believed to bind SA [110].

SA presence increases DMR6 and DLO1 gene expression in Arabidopsis to enable its detoxification after infection or treatment. However, their role in negative regulation makes them susceptibility genes. In Arabidopsis, DMR6 is expressed in tissues surrounding the infection site, while DLO1 is expressed in veins close to those regions. Overexpressing either

gene makes the plant more susceptible to infection, while *dmr6* and *dlo1* knockout mutants show reduced susceptibility to multiple pathogens. Moreover, double *dmr6/dlo1* mutants exhibit almost complete resistance, but also a severe growth penalty [111]. Similar roles of DMR6 and DLO have also been confirmed in crops such as potato [112], eggplant, sweet basil [113], and grapevine [110]. Each species has a different number of homologs of both genes, with distinct patterns of expression across tissues and conditions.

Grapevine possesses two DMR6 (*VviDMR6-1*, *VviDMR6-2*) and three DLO homologs (*VviDLO1*, *VviDLO2*, *VviDLO3*), each with different basal levels of expression across organs. *VviDMR6-1* is expressed in roots; *VviDMR6-2* and *VviDLO2* in mature leaves; *VviDLO1* almost exclusively in anthers; and *VviDLO3* in anthers and ovaries. All are responsive to treatment with an SA analog, but only *VviDMR6-1* and *VviDLO1* were induced by grapevine downy mildew (*Plasmopara viticola*) infection. *VviDMR6-1* was especially active in guard cells surrounding local infection [110].

Knockout studies in grapevine have demonstrated that the effect of DMR6 on downy mildew susceptibility is genotype-specific. CRISPR/Cas9-mediated knockouts of *VviDMR6-1*, *VviDMR6-2*, or both were generated in two table varieties, Sugraone and Crimson Seedless. Although all knockout plants showed increased SA levels and no growth penalty, only Crimson Seedless showed reduced susceptibility to downy mildew in leaf-disk assays. Moreover, resistance *in planta* was found only in the double *VviDMR6-1/VviDMR6-2* mutant [114].

When *VviDMR6-1* was knocked out in the 41B rootstock, the resulting lines showed reduced growth, increased SA levels, and decreased downy mildew susceptibility [115]. Another knockout study, by Holm et al. [116] confirmed the importance of genetic background for the final phenotype. *VviDMR6-1* was knocked out in the rootstock Richter 110, and SA levels were only slightly elevated in these mutants; however, this still resulted in a strong but incomplete reduction in downy mildew susceptibility. Surprisingly, the authors also showed that the *VviDMR6-1* knockout increased stomatal regulation and drought resistance, likely by priming the plants against abiotic stress [116].

1.2.3 '*Candidatus* Phytoplasma solani' infection

'*Candidatus* Phytoplasma' is a genus of plant-pathogenic bacteria that infect a wide range of host plants and are transmitted by phloem-feeding insects of the suborder Auchenorrhyncha. They reside in phloem tissue and cause various symptoms, including leaf reddening or yellowing, stunting, abnormal branching and flower formation, incomplete lignification, and dieback [117]. Host plants of '*Candidatus* Phytoplasma solani' ('*Ca.* P. solani') range from wild species and ornamentals to crops, and it can be transmitted by various polyphagous vectors. This host versatility means that '*Ca.* P. solani' causes significant losses in agriculture, affecting economically important crops including maize, potato, tomato, pepper, strawberry, and grapevine [118, 119].

The phytoplasmas' parasitic lifestyle has allowed for significant genome reduction, retaining only the most essential functions. These include core metabolism, DNA replication and repair, and the Sec-dependent secretion system [120, 121]. Potential mobile units (PMUs) are an interesting feature of phytoplasma genomes. They are transposon-like genetic elements that vary widely in size and contain genes involved in replication and transposition, as well as various secreted proteins believed to be phytoplasma effectors. These regions show high heterogeneity and mosaicism, as well as evidence of large-scale rearrangements and horizontal gene transfer between phytoplasma species. It is believed that these highly variable regions are what enable '*Ca.* P. solani' to adapt to such a wide host range [121].

Phytoplasmas rely on effector proteins to survive in their hosts, though only a small number have been studied in detail. The most widely characterized, SAP11 and SAP54, have been shown to target transcription factors regulating plant development, which explains the striking symptoms observed in infected plants [122, 123, 124]. This is a markedly divergent strategy from that of most other plant-pathogenic organisms, which usually target immune system regulatory hubs or vulnerable points of entry. Marrero et al. [125] constructed a protein-protein interaction network of phytoplasma effectors and transcription factors, which indicated that targeting developmental transcription factors may be a phytoplasma-specific strategy.

Various omics approaches have shed light on how '*Ca.* P. solani' interacts with grapevine, from gene expression to metabolite abundance. Both primary and secondary metabolism are affected, together with hormonal and stress signaling pathways. Decreased expression of photosynthesis-related genes corresponds with decreases in leaf chlorophyll and carotenoid content, as well as decreased activity of Rubisco and nitrate reductase [126, 127, 128, 129]. Although photosynthesis is decreased, leaf sucrose and total soluble sugars increase in infected plants, suggesting a disturbance in source-sink relations. This can occur due to feedback inhibition of photosynthesis, as blocked phloem flow causes sugar accumulation [130, 131]. Phloem flow blockage can be caused by high phytoplasma titers in plant tissues and increased callose deposition, which is commonly accompanied by disruption of sugar transporter expression [132, 133]. Sugar accumulation is often paired with increases in flavonoids [129, 134]. The antioxidative properties of flavonoids can help alleviate ROS stress induced by infection; however, their accumulation may also be a by-product of the greater availability of carbon skeletons resulting from both sugar accumulation and the decreased lignin synthesis typical of phytoplasma infection [130, 131].

The immune responses that phytoplasmas induce in their hosts are also intriguing. A significant decrease in jasmonic acid (JA) and the resulting suppression of JA-related defenses is common, and has been linked to phytoplasmas manipulating this specific pathway via the SAP11 effector. SAP11 destabilizes TCP transcription factors and down-regulates expression of lipoxygenase, an enzyme involved in JA biosynthesis [135]. Decreased JA reduces the plant's herbivory defenses; indeed, it has been demonstrated that Arabidopsis plants infected with Aster Yellows phytoplasma, or expressing SAP11, produce less JA upon wounding and attract the insect vector more strongly, causing it to lay more eggs and produce more nymphs. All of these effects are beneficial for phytoplasma spread [136].

Simultaneously, since phytoplasmas act as biotrophic pathogens living in the phloem sieve elements, they trigger the SA response. This can further suppress the JA response due to SA-JA antagonism. An increase in SA is a common occurrence in phytoplasma infection, followed by increased *VviDMR6* expression, to the extent that it can serve as a good predictor of disease severity [137]. However, it appears that the SA response alone is not sufficient to overcome the infection, as increased JA accumulation has been found to be indicative of grapevine recovery [138].

1.3 Grapevine Genome Editing

Genetic engineering advances have opened many possibilities for both research and crop improvement. *Agrobacterium tumefaciens*-mediated delivery of transgenes into plant genomes is a well-established method in plant genetic engineering and has also been expanded to deliver the CRISPR/Cas9 complex, enabling precise editing of chosen targets [139]. This induction of precise changes is termed genome editing. It still requires insertion of a transgene (for example, the Cas9 protein and guide RNA) into the plant genome,

which can increase the occurrence of off-target effects, disrupt the function of other genes depending on the genomic context of the insertion, and is also disadvantageous for crop improvement in the EU, where the use of transgenic plants is highly restricted [140].

Genome editing in plants has also been achieved through a so-called DNA-free delivery system, first demonstrated in *Arabidopsis thaliana*, tobacco (*Nicotiana attenuata*), rice (*Oryza sativa*), and lettuce (*Lactuca sativa*) [141]. In this method, complexes of Cas9 and synthetically produced guide RNA, also called ribonucleoprotein particles (RNPs), are assembled in vitro and delivered into plant protoplasts via polyethylene glycol-mediated transfection. The protoplasts are then regenerated into whole plants with genes edited at the specified sites. In contrast to *Agrobacterium*-mediated delivery, in which the editing complex is constitutively expressed in the plant, RNPs perform editing for only a limited time, until they are degraded by natural cellular processes. This results in lower editing efficiency; however, it avoids the intentional introduction of foreign DNA into the plant genome and prevents chimerism, since plants are regenerated from single cells.

Despite these advances in plant genetic engineering, the recalcitrant nature of woody species, including grapevine, impedes the smooth transfer of methods developed in herbaceous plants. To achieve the best efficiency in grapevine, genetic engineering methods are most commonly applied to embryogenic callus [142], which is typically obtained from flowers cultured on auxin- and cytokinin-rich media [143, 144]. The success rate of this procedure depends on medium selection and varies greatly with genotype. Embryogenic callus can be transformed by co-cultivation with *Agrobacterium*, or it can be enzymatically digested to produce protoplasts, which are then transfected with RNPs [116, 145]. The callus or protoplasts must then be regenerated into whole plants. This is the bottleneck step in obtaining transformed plants, and one that is also strongly cultivar-dependent. Tissue browning and mortality are common in both approaches; however, callus co-cultivation has a higher success rate than protoplast regeneration, which to date has been reported by only a small number of groups.

1.4 Research Hypotheses

In this doctoral dissertation, we aimed to increase the knowledge about how grapevine responds to water deficit, high salinity, iron deficiency, or '*Candidatus* Phytoplasma solani' infection, and identify the key processes involved in these responses by studying gene expression. With this, we aimed to identify targets for the DNA-free genome editing approach. Furthermore, we aimed to improve the procedure of DNA-free editing of grapevine protoplasts and regenerate whole genome-edited grapevine plants.

Objectives of the research were:

1. Obtain insight into the responses to water deficit in two novel grapevine cultivars
2. Obtain insight into the responses to high salinity in different grapevine rootstocks
3. Obtain insight into the responses to iron deficit in different grapevine rootstocks
4. Obtain insight into how grapevine responds to '*Candidatus* Phytoplasma solani' infection
5. Produce genome-edited grapevine plants targeting *VviDMR6-1* and *VviDLO1*

We tested the following hypotheses:

1. Differential gene expression analysis will show differences in water deficit responses between cultivars.
2. Differential gene expression analysis will show differences in salinity responses among different rootstock genotypes.
3. Differential gene expression analysis will show differences in iron deficiency responses among different rootstock genotypes.
4. Differential gene expression analysis will reveal the grapevine transcriptomic response to '*Candidatus* Phytoplasma solani' infection in the early growing season.
5. DNA-free genome editing via protoplast transfection will be achievable in grapevine cvs. Chardonnay and Zweigelt.

Results corresponding to the first hypothesis are explained in Results Section 3.1 and have been published in Strah et al. [146]. Results corresponding to the second hypothesis are explained in Results Section 3.2 and have been published in Buesa et al. [147]. Results corresponding to the third hypothesis are explained in Results Section 3.3 and have been published in two articles by Khalil et al. [148, 149]. Results corresponding to the fourth hypothesis are explained in Results Section 3.4 and have been published in Dermastia et al. [150]. Results corresponding to the fifth hypothesis are explained in Results Section 3.5 and have not yet been published.

Chapter 2

Materials and Methods

2.1 Plant Material

2.1.1 Water deficit experiments

The water deficit experiments were performed by our collaborators at the University of Udine, Italy. The study was carried out in 2018 and 2019 at the experimental farm "A. Servadei" in a vineyard planted in 2011 with two grapevine cultivars: the white-berry genotype Fleurtai (Tocai friulano × 20/3) and the red-berry genotype Cabernet Volos (Cabernet Sauvignon × 20/3). Both varieties were selected through a breeding program for the introgression of resistance markers tied to genes *REN1*, *Rpv3* and *Rpv12* to powdery and downy mildew and were registered for cultivation in Italy since 2015 [151]. The vines were arranged in two North-South-oriented rows, pruned to a single Guyot training system with a vertical shoot positioned trellis, retaining 8–9 buds per vine. For each genotype, 24 plants were used, divided into two plots assigned to the well-watered (WW) and water-stress (WS) treatments, respectively. Within each treatment, four subplots of three vines each were used in both years of the experiment for physiological measurements and sampling. WW were irrigated weekly to maintain stem water potential (Ψ_s) above -0.6 MPa throughout the whole season, while WS was induced by withholding irrigation starting 10 days after flowering; emergency irrigation was applied to WS plants only when Ψ_s reached -1.2 MPa for Fleurtai and -1.4 MPa for Cabernet Volos. The ground was covered with ethylene-vinyl-acetate film to ensure adequate water deficit in case of summer rainfall. The film was further covered with 3–4 cm of soil to avoid microclimate alteration by soil heating and radiation reflection.

In both seasons, plant water status was measured around midday at ten time points evenly distributed throughout the water-stress periods by our collaborators at the University of Udine. Ψ_s was determined according to the procedure described in Braidotti et al. [152]. Four fully expanded leaves per treatment (one per subplot) were bagged and covered with aluminum foil 1 h before measurement, then excised with a razor blade. A Scholander pressure bomb (Soil Moisture Co., Santa Barbara, CA, USA) was used to measure Ψ_s.

For transcriptomic and metabolomic analysis, three leaves per plot were collected by selecting fully expanded leaves between the 6th and 10th nodes; these were wrapped in aluminum foil, flash-frozen in liquid nitrogen, and stored at –80 °C. Leaf samples were subsequently ground to a fine powder and stored at –80 °C for further analysis. The transcriptomic analysis we performed is described in Methods Section 2.2, while the metabolomic analysis by GC-MS was performed by our collaborators at the Ben-Gurion University of the Negev in Israel and is described in detail by Strah et al. [146]. Samples

were collected at six time points in both seasons, from the onset of water-stress imposition (T0) to harvest: 12, 18, 31, 50, 58, and 65 days after T0 in 2018, and 16, 28, 37, 50, 57, and 63 days after T0 in 2019. Samples for transcriptomic analysis were selected based on Ψ_s measurements to capture the most physiologically relevant time points: 12, 31, and 65 days after T0 in 2018, and 28 and 50 days after T0 in 2019.

2.1.2 High salinity experiments

The high-salinity experiment was undertaken by our collaborators at the Valencian Institute for Agricultural Research (IVIA) in 2019, in a vineyard located at IVIA's experimental station in Moncada, Valencia, Spain. Cv. Tempranillo scions were grafted onto three rootstocks: M1 clone 1 (106/8 × *Vitis berlandieri*), M4 clone 1 (41B × *Vitis berlandieri*), and 1103 Paulsen clone VCR119 (*Vitis berlandieri* cv. 'Resseguier' nr. 2 × *Vitis rupestris* cv. 'Du Lot'). Vines were planted in 2018 at a spacing of 0.88 × 2.50 m and trained to a simple Guyot cordon on a vertical trellis. Crop load was constrained to four clusters per vine, yielding an average of 1.75 kg per vine (7.9 t ha^{-1}). There were no differences in initial shoot fruitfulness or yield at harvest among treatments.

The vineyard was drip irrigated at 100% of crop evapotranspiration (ET_c), calculated from crop coefficients reported for cv. Tempranillo by López-Urrea et al. [153], and reference evapotranspiration (ET_o) derived using the Penman–Monteith equation. Irrigation was applied through 2 l h^{-1} pressure-compensated emitters spaced at 0.88 m along a single drip line, beginning 50 days after budburst, when (Ψ_s) had reached –0.8 MPa. Vine water requirements were subsequently met through irrigation lasting 2–3 h, applied 3–5 days per week. Mineral nutrients were supplied throughout the season via fertigation, up to cumulative rates of 30, 20, and 60 kg ha^{-1} of N, P_2O_5, and K_2O, respectively.

Two sets of irrigation water were prepared by dissolving reagent-grade calcium and sodium chlorides in partially desalinated water. Each irrigation water set had a different electrical conductivity at 25 °C (EC_{25}). The control water had an EC_{25} of 0.8 dS m^{-1} with 2.7, 0.3, and 3.3 mmol l^{-1} of NaCl, Ca^{2+}, and Cl^-, respectively, whereas the saline water had an EC_{25} of 3.5 dS m^{-1} with 12.7, 6.5, and 25.7 mmol l^{-1} of NaCl, Ca^{2+}, and Cl^-, respectively.

During the experiment, the soil in the alleyways was tilled, and spontaneous weeds in the vine rows were controlled with glyphosate herbicide applications. The experiment followed a complete factorial design to assess the performance of the three rootstocks under two water-quality levels (control and salinity). All treatments had three replicates, resulting in 18 subplots of 10 vines each, randomly distributed throughout the vineyard. For water relations, gas exchange measurements, and transcriptomic analyses, the 8th vine in each subplot served as the biological replicate.

After 100 days of treatment, leaf and berry samples were collected from each biological replicate. Leaves were cut from the plant, wrapped in aluminum foil and flash frozen in liquid nitrogen and later ground to a fine powder with a mortar and pestle in liquid nitrogen. Twenty berries per plant were cleaned with cloth and distilled water before being cut from the plant and flash-frozen in liquid nitrogen. While still frozen, the berry skins were peeled away with a scalpel, ground to a fine powder with a mortar and pestle in liquid nitrogen and stored at –80 °C until further processing.

2.1.3 Iron deficiency experiments

The iron deficiency experiments were conducted by our collaborators at BOKU University in Tulln, Austria, in a glasshouse facility under semi-controlled conditions: a photoperiod of 16 h light / 8 h darkness, light intensity of 350–500 µmol m^{-2} s^{-1}, temperature of 22–30 °C during the day and 18–25 °C at night, and relative humidity of 60–70%. Two ungrafted

rootstock genotypes were used: Fercal (*Vitis berlandieri* × *Vitis vinifera*) and 3309 C (*Vitis riparia* × *Vitis rupestris*). One-year-old woody cuttings of ungrafted rootstocks with two buds were rooted in 2021 in a mixture of perlite and peat substrate. Two experiments were conducted on the rooted cuttings: a hydroponic experiment testing the effects of different nitrogen forms on iron availability, and a pot experiment comparing direct iron deficiency with low iron availability induced by bicarbonate. At the end of both experiments, root tips were collected, flash-frozen in liquid nitrogen and stored at –80 °C until further processing.

2.1.3.1 Effect of nitrogen source

For the hydroponic experiment, 4-week-old rooted cuttings were pruned to maintain one main shoot per plant (10–15 cm) and transferred to a hydroponic pot system (5 plants per pot) filled with 7.5 L of modified half-strength Hoagland nutrient solution [154]. Treatments began 10 days after acclimation to the new growth conditions. Six mM of N was supplied at different nitrate:ammonium ratios; either as nitrate only (NO_3^-/NH_4^+ 1:0) or as nitrate and ammonium (NO_3^-/NH_4^+ 1:1) under both Fe-sufficient and Fe-deficient conditions. This produced four treatments, maintained for the 28-day experimental period:

(1) N1A0/+Fe: 6 mM NO_3^-/NH_4^+ (1:0) + 50 µM NaFe(III)-EDTA
(2) N1A0/–Fe: 6 mM NO_3^-/NH_4^+ (1:0) + 0 µM NaFe(III)-EDTA
(3) N1A1/+Fe: 6 mM NO_3^-/NH_4^+ (1:1) + 50 µM NaFe(III)-EDTA
(4) N1A1/–Fe: 6 mM NO_3^-/NH_4^+ (1:1) + 0 µM NaFe(III)-EDTA

Nutrient solutions were renewed weekly, and evapotranspiration losses were replenished with water every second day. All pots were continuously aerated, and pH was monitored daily (portable pH meter Hi 991300, Hanna Instruments, Woonsocket, RI, USA) and adjusted to 5.7–6.0 with either 1 M NaOH or 1 M HCl.

2.1.3.2 Direct and indirect iron deficit

For the pot experiment, 6-week-old rooted cuttings were transplanted individually into 3 L pots filled with fine quartz sand (0.5–2 mm) as substrate. Plants were watered manually each day with modified half-strength Hoagland nutrient solution, starting at 100 mL and increasing to 300 mL as the plants grew. After a 10-day acclimation period, three treatments were applied for 30 days:

(1) Control (+Fe): 0 mM $KHCO_3$ + 50 µM NaFe(III)-EDTA
(2) Direct Fe deficiency (–Fe): 0 mM $KHCO_3$ + 0 µM NaFe(III)-EDTA
(3) Induced Fe deficiency (+Fe+BIC): 10 mM $KHCO_3$ + 50 µM NaFe(III)-EDTA

The Fe concentration followed the recommendation of Covarrubias et al. [155], with NaFeEDTA used to mimic the low Fe availability and solubility characteristic of calcareous soils. K concentration was not compensated for in the control and –Fe treatments, as there was no way to supply pure K; adding it in forms such as K_2SO_4, KH_2PO_4, or KNO_3 would have altered sulfate, phosphate, or nitrate levels in the nutrient solution.

2.1.4 Phytoplasma infection experiments

The samples used to study the effect of '*Candidatus* Phytoplasma solani' infection were collected by our collaborators from the Austrian Institute of Technology (AIT), Tulln, Austria, from a commercial vineyard in Klosterneuburg. The grapevines were grafted on Kober 5 BB and planted in 2006. Four phytoplasma-infected grapevines cv. Zweigelt (syn. Rotburger) and their four healthy neighbors were selected for the study, according to the development of their symptoms in the previous season (2016). The first fully developed leaves were sampled from several canes of each vine in June and September 2017 and then

in June 2020. The leaf veins were cut out of the leaves sampled, flash-frozen in liquid nitrogen, ground to a fine powder, and stored at -80°C. In 2017, all four of the selected phytoplasma-infected grapevines showed severe symptoms in September. The presence of '*Ca.* P. solani' was confirmed by PCR with *SecY*, *Stamp*, *tuf*, and *vmp1* specific primers as described by Aryan et al. [156]. Three of the four infected grapevines had recovered by 2020, showing no visible symptoms, and the phytoplasma was no longer detected.

2.2 RNA Isolation and High-Throughput Sequencing

Total RNA was isolated from powdered samples of leaves, leaf veins, and berry skins using an adapted CTAB (cetyltrimethylammonium bromide) buffer protocol [157], followed by additional purification via column-based approaches. CTAB buffer (100 mM Tris-HCl, pH 8.0, 2 M NaCl, 25 mM EDTA, 2.0% (w/v) CTAB, 2.5% (w/v) PVP40, 2.0% (v/v) β-mercaptoethanol) was warmed to 65 °C and added to the frozen powdered material. An equal volume of chloroform:isoamyl alcohol (24:1) was added, and the sample was vortexed and centrifuged for 10 min at 10,000 × g at 4 °C. The upper aqueous phase was collected and transferred to a new tube, and 1.5 volumes of pure ethanol were added to precipitate RNA at 4 °C for 30 min. The precipitate was then purified using Direct-zol™ RNA Miniprep Plus kit (Zymo Research) according to the manufacturer's instructions, subjected to DNase digestion to remove residual DNA (DNase I Set, Zymo Research), and further purified with the RNA Clean & Concentrator kit (Zymo Research). RNA quality and quantity were evaluated using a 2100 Bioanalyzer and RNA 6000 Nano Kit (Agilent Technologies).

2.3 RNA Sequencing and Data Analysis

Sequencing library preparation, paired-end Illumina HiSeq 4000 sequencing, adaptor trimming and low-quality sequence removal were provided by Novogene (Hong Kong, China). We mapped the resulting 150 bp paired end reads to the 12X.2 version of the PN40024 grapevine reference genome (https://urgi.versailles.inra.fr/files/Vini/Vitis%2012X.2%20annotations/) using CLC Genomics Workbench 12.0 (Qiagen), with the following parameters: mismatch cost 2, insertion or deletion cost 3, length fraction 1.0, similarity fraction 0.95, and maximum number of hits for a read 1. The reads were annotated with the VCost.v3 annotation [158] and exported as raw counts. This procedure was used for samples of water deficit experiments, salinity experiments, and phytoplasma infection experiments.

The samples of root tips described in Methods Section 2.1.3 were processed by our collaborators at BOKU University as described by Khalil et al. [148, 149]. Root tips were ground in liquid nitrogen, and 100 mg was used for total RNA extraction with the Spectrum Plant Total RNA Kit (Merck KGaA, Darmstadt, Germany). Samples were sent for RNA-Seq, which was conducted as a commercial service by Novogene Europe (Novogene, Cambridge, UK) using paired-end 150-bp sequencing on an Illumina NovaSeq 6000 platform. STAR aligner software was used to align fastq sequences to the reference genome, while quality checks were performed with FastQC, Qualimap, and MultiQC.

2.3.1 Differential gene expression analysis

Analysis of the exported raw counts was performed in R v4.0.2 [159], using the limma package v3.45.8 [160]. Genes with low expression were filtered out, retaining only those

with more than 50 counts in at least four samples. Data were normalized to library size using trimmed mean of M-values (TMM) normalization from the edgeR package v3.28.1 [161]. Gene expression was log transformed fit to a linear model where each coefficient corresponded to a treatment mean. Comparisons between treatment groups are obtained as contrasts of the fitted linear models and are expressed as log fold-changes (Log_2FC). P-value was obtained from t from testing the hypothesis that Log_2FC differs from 0 and then corrected for multiple comparisons via the Benjamini-Hochberg false discovery rate correction. Normalized, log-transformed total count values were used to perform principal component analysis (PCA), and PCA plots were visualized with the ggbiplot package v0.55 [162]. Hierarchical clustering analysis (used on high salinity samples) was performed using the pheatmap package v 1.0.12, applying 1-Pearson correlation as distance measure and Complete Linkage as the linkage method. Gene Set Enrichment Analysis (GSEA) was performed as described by Subramanian et al. [163] on normalized log-transformed expression data, using the GoMapMan gene ontology as gene sets [164]. GSEA results with a false discovery rate FDR < 0.25 were considered statistically significant [163].

Data from the water-deficit experiments (Methods Section 2.1.1) were analyzed using a linear-model approach developed by Strah et al. [146], which integrated Ψ_s, gene expression, and metabolite abundance measurements. The script is available at https://github.com/NIB-SI/FaDSeqSes. For each sample, Ψ_s was estimated by linear interpolation of measured values. Gene expression was analyzed using the lmFit function from the R limma package [160], applying a multifactor linear model incorporating genotype and Ψ_s. The rate of change in expression for each gene was represented by the slope of the model. Genes with absolute slope values greater than 1.5 were considered to show a strong change in expression, those with absolute slope values below 0.5 were considered unchanged, and those with absolute slope values between 0.5 and 1.5 were considered to show a moderate change.

Based on gene expression and metabolite abundance profiles, three categories of altered expression or abundance were defined, each corresponding to specific threshold values for the regression slopes in the two genotypes. The first category, Type 1, comprised genes that were either up- or down-regulated by low Ψ_s in both genotypes; in this category, the regression line of at least one genotype had an absolute slope greater than 1.5, and the other genotype's slope exceeded 0.5. Type 2 comprised genes that were up- or down-regulated in Cabernet Volos but not in Fleurtai, while Type 3 comprised genes up- or down-regulated in Fleurtai but not in Cabernet Volos. In both Type 2 and Type 3, the absolute slope for the first genotype exceeded 1.5, while that of the other genotype remained below 0.5. A schematic summary of the characteristics of each category is shown in Figure 2.1.

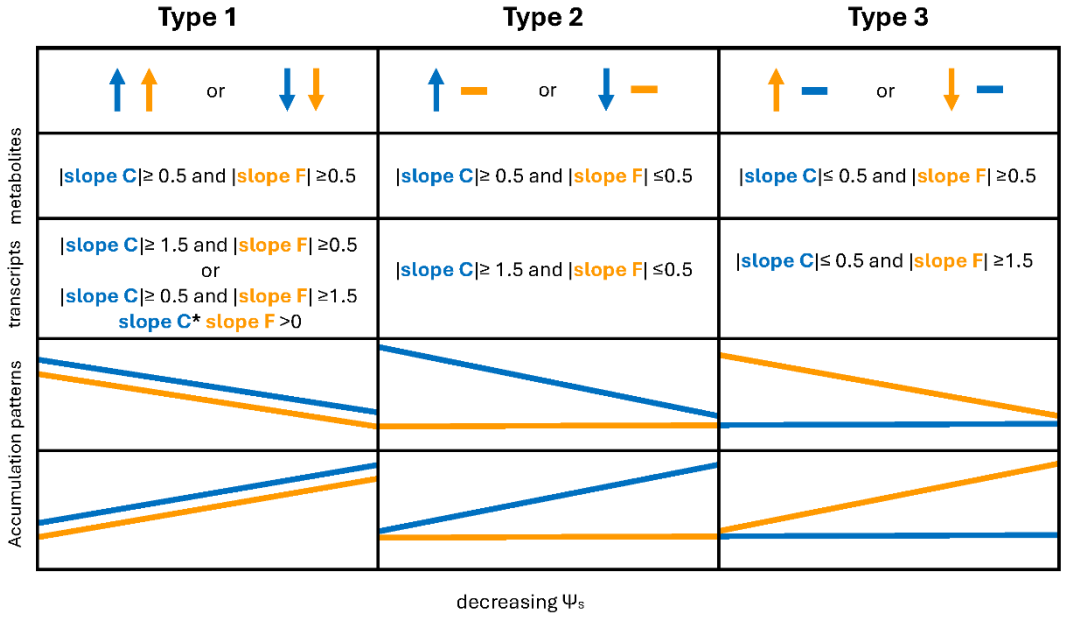


Figure 2.1: Gene expression and metabolite abundance categories. The slope of the regression line describes the relationship between gene expression or metabolite abundance and Ψ_s. Type 1 represents genes and metabolites that respond similarly in both genotypes; Type 2 represents genes and metabolites that respond only in Cabernet Volos; and Type 3 represents genes and metabolites that respond only in Fleurtai. The metabolite and transcript panels show the formulae used to categorize transcripts and metabolites into the three types, while the abundance pattern panels show the general slope pattern characteristic of each type. C, Cabernet Volos; F, Fleurtai. Republished from Combined omics data reveal multilevel response to water deficit in grapevine disease-resistant varieties, Strah et al. 2026, Frontiers in Plant Science, 17:1818883, 10.3389/fpls.2026.1818883, according to Creative Common Attribution ("CC BY") license.

2.3.2 Differential metabolite abundance analysis and transcript and metabolite correlation

Metabolites were classified using the same three categories (Type 1, 2, and 3), though with different thresholds to account for the lower slopes of their regression lines. In Type 1, the regression lines of both genotypes had absolute slopes greater than 0.5; in Types 2 and 3, the absolute slope of the first genotype exceeded 0.5, while that of the other genotype remained below 0.5. To compare metabolite abundance between the two genotypes, the difference in metabolite amount between Fleurtai and Cabernet Volos was calculated under low-stress ($\Psi_s = 0$) and moderate-stress ($\Psi_s = -1$) conditions.

Pearson's correlation was used to assess the relationship between transcript and metabolite abundance as Ψ_s declined. To focus on the most biologically relevant comparisons, correlations were calculated only for the subset of genes belonging to the same GoMapMan functional categories (BINs) as the metabolites.

2.4 Protoplast Genome Editing

2.4.1 Embryogenic callus induction

Embryogenic callus was induced from cv. Zweigelt and cv. Chardonnay clone VCR4. One-year-old canes were collected in December 2021. Zweigelt canes were collected by our collaborators at the AIT from a vineyard in Klosterneuburg, Austria, and we collected Chardonnay canes from a vineyard in Črniče, Slovenia. Canes were stored at 4 °C for a month to break dormancy.

For rooting, canes were cut into 20-30 cm segments, all but one bud was removed, and cuttings were dipped in a 3 g/L indole acetic acid solution for 5 s. The cuttings were then potted in sandy medium and placed into a heating bed maintained at 27 °C. The heating bed was covered pot height to prevent heat loss, and the heating beds were kept in 4 °C cold storage to keep the buds cool. Cuttings were left to root for 5 weeks.

For flowering induction, rooted cuttings (Figure 2.2) were transferred to a substrate mixture of perlite, vermiculite and humus (6:3:1) and moved to a growth chamber with a 16 h photoperiod at 27 °C. Cuttings were watered with half-strength Hoagland solution [154] every other day. First young leaves were removed as they emerged (Figure 2.3). Pollen developmental stage was monitored periodically under a microscope by crushing anthers in acetocarmine. Inflorescences were harvested when pollen reached the tetrad stage, surface-sterilized for 10 min in a 3% sodium hypochlorite solution with a few drops of Tween-20 and rinsed with sterile water.



Figure 2.2: Rooted Chardonnay canes

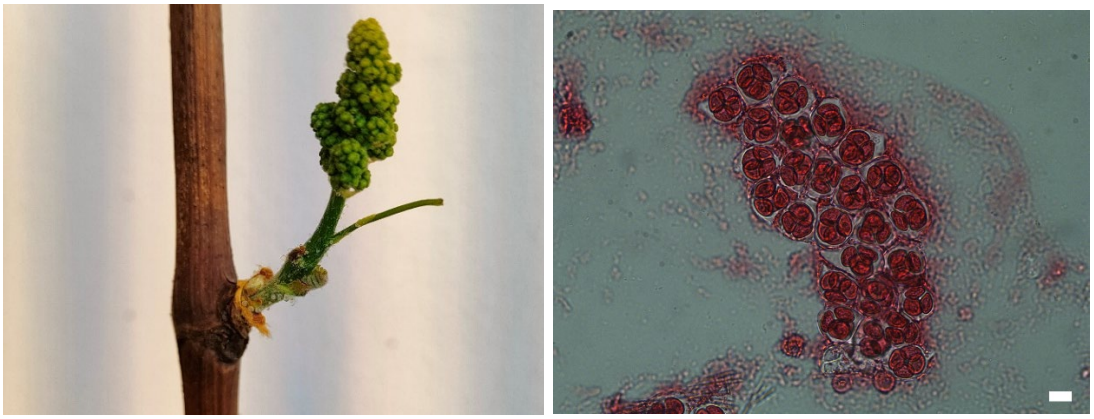


Figure 2.3: Defoliated Chardonnay inflorescence (left) and pollen in the tetrad developmental stage (right). Pollen image was taken under 40x magnification, the scale in the bottom right corner represents 16 µm.

Explants of pistils and stamens were prepared aseptically from the sterilized inflorescence and transferred to callus induction medium MSII [144]. The explants were grown at 27 °C in darkness for six months and checked periodically for embryogenic callus induction under a stereomicroscope. Any induced embryogenic callus was transferred to callus proliferation medium C1 [165] and kept in the same conditions. The callus was transferred to fresh medium every 4-5 weeks by selecting the proembryogenic masses under a stereomicroscope. Images were taken with the MZF LIII stereomicroscope (Leica, Germany) using a Plan Apo 1.0× objective.

2.4.2 In vitro guide RNA synthesis

We obtained sequences of the *VviDMR6-1* and *VviDLO1* genes from the PN40024 grapevine reference genome and annotated the exons, the catalytic site consisting of the 2-oxoglutarate-binding stretch and the HDH triplet, shown in Figure 2.4. Both genes have four exons, and most of the catalytic site is located on the third exon. For this reason, we selected the first two exons and the first half of the third exon as target regions for genome editing.

To design our guide RNA targets, we used the CRISPOR web tool [166], selecting the *Vitis vinifera* 12x as the target genome and NGG as the protospacer-adjacent motif. The tool provided several scores to select the most promising targets. Specificity scores indicate the likelihood of off-target effects in the genome of choice. Efficiency scores indicate how likely DNA cleavage is to occur at the specified site. Outcome scores indicate how likely the cleavage is to result in frameshift mutations. Properties of the selected targets are listed in Table 2.1. The selected guide RNA was then synthesized in vitro using the Precision gRNA Synthesis Kit (Invitrogen, USA) according to the manufacturer's instructions and stored at -80 °C until use.

vvDMR6-1

ATGGAATCAAAGGTGTTGTCCACCGGAATCCGGTACTTGACCTTGCCACAAAGTTACATCAGGCCAGAGCCGGAGAGGCCGAG
ACTCTCCCAAGTGAGTGAGTGTAAACATGTCCCCATAATCGACCTCGGCAAGGACGTAAACAGGGCCCAACTCATCCAACACA
TCGCCGATGCTTGCAGGCTCTATGGTTTTTTCCAGGTCTCCAAACAAAACCATATATATATATATATATGTTAGTAGTTTGAG
ACTGACTCCATGGATGAACTGATTTAATTTTTGTGCCAGGTGATCAATCATGGGGTAGCTGCAGAAATGATGGAGAAAATGTT
GGAGGTGGCCGATGAGTTCTACAGACTGCCGGTGGAGGAGAAGATGAAGCTGTATTCCGATGATCCCACCAAGACAATGAGGT
TGTCAACCAGCTTTAATGTGAATAAGGAGAAGGTCCATAACTGGAGAGATTATCTCAGACTCCATTGTTATCCTCTGGATCAG
TACACGCCTGAGTGGCCTTCCAATCCTCCTTCCTTCAAGTAAGTCTTTGATTTCTTCTCCTAAGTTATCTCTCTTTTGTATG
AATTTGATTTCTTATTCTCGAACCTGTTCTAGCAACTTTCAACTTTCTGCCTAATTCGTCCTCATCCTACTTTCAATGGTAGA
AGTAGGAATAGAAGTAATTATTATTAAATCACATTAAAATATGTTTTAAAAAAATTTCTCCATCATAGGTGTTGTAAGTCGAA
TATAAAAATCATTATTTTCTTATTTTGTATATACAAACTAAGACTTTAGTTTCGACCTCTTCTTGTTTTCAACAATAGAAAAA
CAAAAACAAAAGTAACTAAAGTCAAAAATCATACAAACAAACGTTGAAACTAGCATAAAACTTTAATTTTAATGTTTAAAAAA
CTCTTTTAGGTCATAGATGTTGTAAATTGATTATGAAAGAAACAAAAAATTTTATGTCTTCTTGTTTTGTATGTACTACCAAA
AATTTTATTTATTATAATATTCATGTACTACACCTAATATTCATGTACTACACGAGACAATGATTCTGATGATCACATGAAAT
AATGAATTATAATATCATAAATCTCATAATATATCAAATATTATGAACGAAACTCAATCATGTTATTTTATTTTCTTAAATTC
GTAATACTTGATGTCATGCACAATAGAAAAAAATTAAATTTTATATGATAAATAAGCAAAGTACATTGAATGAATCTATAAAG
TGGTGAAATAGATTCCTTTTTGTCTTTTAGCTAACTTTAGTGATATTGCAAATTTTGGGTCGAAATCTCATTGGGCATGTAGT
TATTCAAAAGGTATCACCTTAATTCTTAATTCAATGAATTTGATTTAGAGAATCCCTTAAAGTTAACCATGTGGTACATATTT
TTATAAAAATTCCAATAGTTGGATTTTATCGACATCTAGAATATCAGAACCAAACTTTTTGTCACATCAAAATAAGAAAAATAG
TATTACCACTTTTATTTTTATTTATATAATTAAAAATATAAGATACAAAAATTATATTTATTGAATTACATATTTGACTCGGT
AAATTTGTGTGATAAAACCTATATCGTTGTATGATATACAAATAAATGAGATTAAAAGTTTGTTTGACGGTAGTTTTAAAAAA
TGTTTTTAACTTAAAAAATATGAAGTATTTGACAAATTTATAAAATATTTTTAAAAATATGAAAAAATCATTAATAATATTTT
TAAGATAAACACTTAATAAACGATTCTCGTACAAATATTTTTAAAGCAAATACTTCAACTAAAAACACTTTTAAGTATCATCG
GATATAAACATATGGATATATAATAAAAACCCGATATACAAATTATGTCTTTTTAATATATTATTGAAAAAGTATCACTAAAT
TGAAAGTCCCATATAATAATTATTTGAAAAATATTATGTTATTAATTAGGTATTATATTAAAATCAAATTTTAAATCCTTAAA
AGATATGAATAAATTCAGTTGTTGAAAAAAAAAAACACAACGACTGAATTTCAAAAGAAAATGGTAATGAGATTTAGGTATAT
CTATGATAACGTAAGTGATAAACTACCTTATTAAATATGTTGAGCAATTTTTGACGCTTTTGAGCTGCTAATGGCTCCAAAAG
TCTTACTTTTGGACGGTGATGACGACATCAAATGGTGTGGGCACATAGATTTGTCAGTTTTTTGACATGATACCAATTTTATA
GTGTTTTCTAATTGACAATGGATTGAATTAGAATCCGCGTCGACGTAAGCAAATTGAATTATGTGTACATGATGAATAGGTGA
CGTGTACAATTTTTCATGGGCCCAGGTAGACTCCACTAGAAGCCCCAAAAAGAGTGGTTGGGTCAATAGGATATATGAATAAG
CCAAAAAAGCCAATTTTTTTATTTTTTATTTTTTTGTTAATGAATAAAGTTTTAATAAAAAAGAGTTTAATACATGCTTCAAA
CCTCGTTTACTTTACACTTGAATTTAATTTTATTATTTTATATGTTAATCTCGTTTATTTATATTTGATTTCATTTCTTCATT
TGATTTAGATTTTACTGTATATTTTGAATGATTTAAATTACATCATTAATAAATATTGATCTGATATCTTAAAATTTTTTAAT
TCTCTAATTAAAATTATGATTTTAACTTTGACTTCTAACTAAAATCAAGAAAAAATTCTCGAACAAATCCTAATTCAAAAATT
TGTTGTATTCTTAGGGAAATTGTGAGTAGTTATTGCAAAGAGGTAAGAGAACTTGGGTTCAGACTACAAGAAATGATATCAGA
GAGTTTAGGCTTGGAAAAGGATCATATAAAGAATGTTTTTGGTGAACAAGGGCAACACATGGCTGTAAACTATTATCCGCCAT
GTCCACAACCCGAGCTCACTTATGGATTGCCAGGACACACAGACCCCAACGCCCTTACCATTCTTCTTCAAGACCTACGAGTG
GCAGGTCTTCAAGTTCTCAAGGATGGTACTTGGCTCGCTATCAAGCCACATCCCGGTGCTTTTGTCGTCAATATAGGCGATCA
ATTACAGGTACAATAAGAGTTCATTTGATAGTGATTTTAAAATAATTAAAAGCATTTCCTAATATTTAGAAGTACTTTCGGGT
TTTAATATTTGCCCGGTTTTTAAAATTTAAAAATTTGTTTTAATGATGGAAATGGGCATGTGCTAATAAAGGGTTGCTGACAA
GTTAGTATGATTATAGGCTGTGAGTAATGGGAAATACAAAAGTGTATGGCATAGGGCCGTTGTGAATGCAGAGAGTGAAAGGC
TATCAGTGGCTTCTTTCCTCTGCCCATGCAATGATGCAGTAATTGGCCCTGCAAAGCCTCTCACAGAAGATGGATCTGCACCC
ATTTACAAGAATTTCACATATGCTGAGTATTACAAGAAGTTCTGGGGCAGGGACTTGGATCAAGAACATTGCTTGGAACTATT
CAAGAACTA

vvDLO1

ATGGCCAATGCAAAGCTTCTGTTGTCTGACCTTGCATCCAGTATAGACTGTGTTCCTTCAAGATATGTTCGACCC
GTGAACGACCGCCCAAACCTTGATGAGGTTCAGTCCTCATTGGATGGCTCCATTCCCCTCATCGACCTCCAAGAC
CTCCATGGTCCTAGCCGCTCCCATGTTATCAAGCAGATAGCTGAAGCCTGCCAGATTGATGGTTTTTTTCGGGTA
CATGTCGATATCTGTATTACTCTTGTATCTCTCCTTGCTTTGACATGATTCTTCTTGTTTTTGTTTCTCTCAAGG
TCAAGAACCATGGAATACCGGAGAGTGTGATCCATGGCATGTTGAGCATAACAAAGGAGTTTTTCCATTTACCGG
AAAGTGAAAGGTTGAAGAACTACTCCGACGACCCTTTGAAGACTATGAGACTCTCTACTAGTTTCAATGTGAAAA
CCGAGCAGGTGTCCAACTGGAGAGATTTCCTGAGACTCTATTGCTACCCTTTAGAGGATTACATTCAGGAATGGC
CCTCCAACCCTCCATCTTTCAGGTATAACTTAATTTTCTAGCAGAGATGTGTAGTTATTGTAATTAGTATATGTA
CAAGTACTGATAAGATTCTTGTGTGGCCTTGTGGCCTTGCACAGAGAAGTTGTGGCCGAGTATTGCAAGGAGGCT
AGAAAATTAGCATTACTACTGCTTGAAGCAATATCCGAAAGCTTAGGACTAGAGAGGAACCACATAGATAAGGCG
CTGGGAAAGCACAGCCAGCAGATGGCCCTCAACTACTACCCACCTTGTCCTCAACCAGAGCTGACGTTTGGCTTA
CCTGGCCATGCTGATCCTAATGCCCTCACAATCCTCCTTCAAGACGATGTGCCCGGTTTGCAGGTGCTCAAAGAT
GGAAAATGGGTGGCCATCCACCCTATTCCAAATACTTTCATTGTCAACATTGGTGATCAAATCCAGGTGATGGAG
ACAAAAGTATTAACAAGACAATGTCACATTCTGATATTACAGATCAACAATATCTGATTAATGATTAATCCACTG
GATGTTTGCAGGTACTTAGCAATGATTGCTACAAGAGTGCGGTCCATAGGGCCGTGGTGAACTGCCAGAAGGAGA
GGATCTCCATTCCAACCTTTTATTGCCCATCACCAGATGCAGTTATAGGACCAGCTCCGGGACTGGTCGACCATG
GTCATCCTGCCCTTTACAGGAAATTTACATACAGTGAGTACTTTGGGAAATTCTGGAACAGGGGCCTTGCTACTC
AATCCTGCTTGGACATGTTCAAGACGTAG

Exon Catalytic site

Figure 2.4: *VviDMR6-1* and *VviDLO1* sequences. Exons are highlighted in grey and nucleotides coding for catalytic site containing the 2-oxoglutarate-binding stretch and the HDH triplet are marked in red.

Table 2.1: Guide RNA sequences designed for *VviDMR6-1* and *VviDLO1* and their predicted properties. The sequences are listed without PAM. Specificity scores indicate the likelihood of off-target effects. Efficiency scores indicate a likelihood of cleavage in DNA. Outcome scores predict the likelihood of frameshift-inducing mutations. Off-target counts were predicted from the grapevine 12x genome sequence.

				Specificity			Efficiency scores			Outcome prediction	
Guide name	Target Sequence	Exon	Orientation	MIT Score	CFD Score	Off-target count	Doench '16-Score	Moreno Mateos Score	Doench RuleSet3 Score	Out-of-Frame Score	Lindel Score
VviDMR6-1											
sgRNA_DMR6-1_1	GGTCAAGTACCGGATTCCGG	1	-	100	100	4	69	53	106	52	79
sgRNA_DMR6-1_2	GGTGTTGTCCACCGGAATC	1	+	100	100	1	48	61	-43	58	76
sgRNA_DMR6-1_3	TGAGTTCTACAGACTGCCGG	2	+	100	100	0	70	63	92	42	78
sgRNA_DMR6-1_5	TGTGAGTAGTTATTGCAAAG	3	+	97	97	20	63	35	22	70	86
sgRNA_DMR6-1_47	CCTGATGTAACTTTGTGGCA	1	-	97	99	10	61	28	5	75	85
sgRNA_DMR6-1_95	TGGCAATCCATAAGTGAGCT	3	-	99	99	9	54	30	-85	66	86
sgRNA_DMR6-1_193	TGGGAGAGTCTCGGCCTCTC	1	-	98	99	8	47	66	-44	55	79
VviDLO1											
sgRNA_DLO1_1	AGGTTTGGGCGGTCGTTCAC	1	-	100	100	1	50	77	-16	71	83
sgRNA_DLO1_2	GGTTTGGGCGGTCGTTCAC	1	-	100	100	1	50	77	-16	71	83
sgRNA_DLO1_3	ATGCCATGGATCACACTCTC	2	-	99	99	8	57	62	-8	60	84
sgRNA_DLO1_4	GTGGCCGAGTATTGCAAGG	3	+	97	99	10	64	45	74	65	91
sgRNA_DLO1_5	CCGAAAGCTTAGGACTAGAG	3	+	99	99	11	56	53	10	76	90

2.4.3 Protoplast isolation

The starting material for protoplast isolation was cv. Chardonnay and cv. Zweigelt embryogenic callus described in Methods Section 2.4.1. The protocol was adapted from Bertini et al. [167], Najafi et al. [168] and Strah et al. [169].

Embryogenic callus was transferred to C1 [165] medium and cultivated in the dark at a constant 27 °C. After one week, protoplasts were isolated by digestion in protoplast digestion solution (Cellulase Onozuka RS 2% (w/v), Macerozyme R-10 1% (w/v), Pectolyase Y-23 0.05% (w/v), $CaCl_2$ x $2H_2O$ 1470.1 mg/l, 2-(N-morpholino) ethanesulfonic acid (MES) 97.2 mg/l, and mannitol 91.09 g/l). Digestion lasted three to five hours and was monitored periodically under a microscope to estimate the degree of cell wall removal, based on the number of intact, perfectly spherical individual cells observed. Once a satisfactory level of digestion was reached, the process was stopped by diluting with protoplast wash solution ($CaCl_2$ x $2H_2O$ 147.01 mg/l and mannitol 91.09 g/l), and protoplasts were strained through a 70 µm nylon mesh to remove debris. Protoplasts were counted using Neubauer counting chambers and separated into aliquots of 1.5×10^5 cells each.

2.4.4 Protoplast transfection

Directly prior to transfection, Cas9/sgRNA RNP complexes were assembled by mixing the in vitro-assembled sgRNA from Methods Section 2.4.2 with TrueCut™ Cas9 Protein v2 (Invitrogen, USA) at a 1:1 mass ratio and incubating at room temperature for 10 min. For each transfection, 60 µg each of sgRNA and Cas9 were used. To transfect the protoplasts, cells were resuspended in 200 µl of MMG solution (MES 780.8 mg/l, mannitol 72.83 g/l, and $MgCl_2$ 1428.16 mg/l), followed by the addition of an appropriate volume of the RNP complex and an equal volume of PEG solution (PEG 4000 40% (w/v), mannitol 72.83 g/l, and $CaCl_2$ x $2H_2O$ 14.701 g/l). Protoplasts were incubated for 20 min, then rinsed in W5 solution (MES 390.4 mg/l, NaCl 8.999 g/l, glucose 54 g/l, KCl 372.76 mg/l, and $CaCl_2$ x $2H_2O$ 55.88 g/l).

A combination treatment was also performed, using sgRNAs targeting *VviDMR6-1* and *VviDLO1* in the same transfection reaction. As a positive transfection control, 60 µg of the pB7WGF2 plasmid [170], carrying a GFP (green fluorescent protein) gene under the constitutive 35s promoter was used. A transfection without Cas9 (mock) served as a negative editing control, and negative transfection controls were cultivated directly without any treatment. Due to variability in protoplast yield across isolation attempts, not all treatments were performed for both genotypes. Table 2.2 lists the sgRNAs, combination, and control treatments used in the transfection experiments, along with the cultivar(s) each was performed on.

Table 2.2: List of transfection treatments. Mock control indicates transfections carried out with only the sgRNA, in absence of the Cas9 protein. x marks the treatments that were carried out

Single target	Chardonnay	Zweigelt
sgRNA_DMR6-1_1	x	x
sgRNA_DMR6-1_2	x	x
sgRNA_DMR6-1_3	x	x
sgRNA_DMR6-1_5	x	x
sgRNA_DMR6-1_47	x	x
sgRNA_DMR6-1_95	x	x
sgRNA_DMR6-1_193	x	x
sgRNA_DLO1_1	x	x
sgRNA_DLO1_2	x	x
sgRNA_DLO1_3	x	x
sgRNA_DLO1_4	x	x
sgRNA_DLO1_5	x	x
Combination treatment	**Chardonnay**	**Zweigelt**
sgRNA_DMR6-1_47+sgRNA_DLO1_1	x	
sgRNA_DMR6-1_47+sgRNA_DLO1_2	x	
sgRNA_DMR6-1_47+sgRNA_DLO1_3	x	
sgRNA_DMR6-1_47+sgRNA_DLO1_4	x	
sgRNA_DMR6-1_47+sgRNA_DLO1_5	x	
sgRNA_DMR6-1_1+sgRNA_DLO1_1	x	
sgRNA_DMR6-1_1+sgRNA_DLO1_2	x	
sgRNA_DMR6-1_1+sgRNA_DLO1_3	x	
sgRNA_DMR6-1_1+sgRNA_DLO1_4	x	
sgRNA_DMR6-1_5+sgRNA_DLO1_4		x
sgRNA_DMR6-1_95+sgRNA_DLO1_4		x
sgRNA_DMR6-1_193+sgRNA_DLO1_4		x

Control type	Treatment	Chardonnay	Zweigelt
Positive transfection control	pB7WGF2	x	x
Negative transfection control	/	x	x
mock	sgRNA_DMR6-1_1		x
mock	sgRNA_DMR6-1_2		x
mock	sgRNA_DMR6-1_3	x	x
mock	sgRNA_DMR6-1_47		x
mock	sgRNA_DMR6-1_5	x	
mock	sgRNA_DMR6-1_95	x	
mock	sgRNA_DMR6-1_193	x	
mock	sgRNA_DLO1_1	x	

Table 2.2 (Continued)

Control type	Treatment	Chardonnay	Zweigelt
mock	sgRNA_DLO1_2	x	
mock	sgRNA_DLO1_3	x	x
mock	sgRNA_DLO1_4	x	
mock	sgRNA_DLO1_5	x	

2.4.5 Plant regeneration

Protoplasts obtained after transfection were resuspended in 50 °C solid protoplast cultivation medium (Nitsch medium [171], sucrose 30 g/l, glucose 54 g/l, 1-naphthaleneacetic acid (NAA) 2 mg/l, BAP 0.5 mg/l, gellan gum 2 g/l). The medium was left to completely solidify before adding the liquid protoplast cultivation medium (Nitsch medium [171], sucrose 30 g/l, glucose 54 g/l, 1-naphtaleneacetic acid (NAA) 2 mg/l, BAP 0.5 mg/l, activated charcoal 3 g/l). Thereafter, protoplasts were cultivated in the dark at a constant 27 °C and monitored for embryo development for up to six months. The liquid medium was replaced every week. Three days after transfection, the positive transfection control treatments were checked for GFP fluorescence. Microscopy was performed with the Stellaris 8 confocal microscope using a HC PL FLUOTAR 10×/0.30 DRY objective (Leica Microsystems, Wetzlar, Germany).

As visible embryos developed, they were transferred for germination to Nitsch medium [171] with sucrose 30 g/l, and gellan gum 2 g/l, and cultivated in the dark at a constant 27 °C and regularly examined for germination. Germinated embryos were transferred to light conditions (16 h photoperiod, light intensity 60 µmol m^{-2} s^{-1}, day temperature 22 °C, night temperature 20 °C, relative humidity of 40–60%) on C2D shooting medium (C2D medium [172], sucrose 30 g/l, and tissue culture agar 7 g/l) with or without the addition of 6-benzylaminopurine (BAP) at a final concentration of 5 µM. The embryos were kept on shooting media for the first three months, then transferred to ¾ strength MS media, and transferred to fresh MS media every two to three months after that. Successfully developed shoots were transferred to Murashige and Skoog medium and maintained in growth chamber conditions. A shoot regenerated from one embryo and successfully clonally propagated was considered an independently regenerated line and is referred to as regenerated plant.

2.4.6 Editing confirmation

Leaf samples were collected from the independent lines produced in Methods Section 2.4.5. Total DNA was extracted using the DNeasy Plant Mini Kit (Qiagen) according to the manufacturer's instructions. The concentration and purity (260/280 and 260/230 absorbance ratios) of the DNA samples were assessed using a NanoDrop ND-1000 spectrophotometer (Nanodrop Technologies).

To examine the presence of editing events in the regenerated plants, the *VviDMR6-1* and *VviDLO1* regions targeted by the sgRNAs were amplified using Phusion® High-Fidelity PCR kit (New England Biolabs), with the reaction composition following the manufacturer's instructions. Table 2.3 lists the primers and Tm conditions used to investigate each target. The PCR products were run on an agarose gel, and appropriately sized fragments were excised and purified using Wizard® SV Gel and PCR Clean-Up System (Promega). Purified PCR products were then Sanger sequenced (Eurofins Genomics) using primers listed in Table 2.4. None of the plants were tested for the presence of exogenous DNA.

The precise sequence of positive samples was further investigated. Purified PCR products were cloned into the pJET1.2 blunt cloning vector (Thermo Fisher Scientific) according to the manufacturer's instructions, and the resulting plasmids were transformed into One Shot™ TOP10 chemically competent *Escherichia coli* cells (Invitrogen). Plasmids were isolated from 6-12 colonies per transformation using GenElute™ Plasmid Miniprep Kit (Sigma) and Sanger sequenced (Eurofins Genomics). The regenerated plants for which genome editing was confirmed are referred to as edited lines.

Table 2.3: Primers for amplification of editing target regions.

PCR primer name	Sequence	Phusion-adjusted Tm	PCR product size [bp]	Detects sgRNA target edit
DMR6.1-1F	TTTTAGTGCAAGTGATCAGAC			
DMR6.1-1R	ACAACACCTATGATGGAGAAA	60	873	DMR6-1_1, DMR6-1_2, sgRNA_DMR6-1_3, DMR6-1_47, DMR6-1_193
DMR6.1-5F	TTCTCGAACAAATCCTAATTCA			
DMR6.1-5R	CAACAATAATCAAGGAAAGTTCA	59	866	DMR6-1_95, DMR6-1_5
DLO1 AF	TCTTCCTCCTGAACAGGCC			
DLO1 PAR	GAAAGATGGAGGGTTGGAGG	68	1107	DLO1_1, DLO1_2, DLO1_3, DLO1_4, DLO1_5

Table 2.4: Sequencing primers

Sanger sequencing primers	Sequence	Detects sgRNA target edit
DMR6.1-1F	TTTTAGTGCAAGTGATCAGAC	DMR6-1_1, DMR6-1_2, DMR6-1_47, DMR6-1_193
DMR6_e2r	AGGAAGGAGGATTGGAAGGC	DMR6-1_3
DMR6.1 P2 F	TCGAAAACTAGACAGGAAAGGC	DMR6-1_95
DMR6_v2E3r	TGATAGCGAGCCAAGTACCA	DMR6-1_5
DLO1 PA1 F	GGCCATCCCTCAGTACAAAG	
DLO1 PA1 R	GAAAGATGGAGGGTTGGAGG	DLO1_1, DLO1_2
Sanger sequencing primers	Sequence	Detects sgRNA target edit
DLO1 PA2 F	GAAGAACTACTCCGACGACC	DLO1_4, DLO1_5
DLO1 PA2 R	GTGAGGGCATTAGGATCAGC	DLO1_4, DLO1_5

Chapter 3

Results

3.1 Water Deficit Response in Cabernet Volos and Fleurtai

The sequencing results of water deficit experiments have been published by Strah et al. [146] and are summarized in this section. Raw reads obtained from sequencing are available at https://www.ebi.ac.uk/ena under the study accession PRJEB44212 and following accession numbers: ERS6293633, ERS6293634, ERS6293635, ERS6293636, ERS6293637, ERS6293638, ERS6293639, ERS6293640, ERS6293641, ERS6293642, ERS6293643, ERS6293644, ERS6293645, ERS6293646, ERS6293647, ERS6293648, ERS6293649, ERS6293650, ERS6293651, ERS6293652, ERS6293653, ERS6293654, ERS6293655, ERS6293656, ERS6293657, ERS6293658, ERS6293659, ERS6293660, ERS6293661, ERS6293662, ERS6293663, ERS6293664, ERS6293665, ERS6293666, ERS6293667, ERS6293668, ERS6293669, ERS6293670, ERS6293671, ERS6293672, ERS6293673, ERS6293674, ERS6293675, ERS6293676, ERS6293677, ERS6293678, ERS6293679, ERS6293680, ERS6293681, ERS6293682, ERS6293683, ERS6293684, ERS6293685, ERS6293686, ERS6293687, ERS6293688, ERS6293689, ERS6293690, ERS6293691, ERS6293692, ERS6293693, ERS6293694, ERS6293695, ERS6293696, ERS6293697, ERS6293698, ERS6293699, ERS6293700, ERS6293701, ERS6293702, ERS6293703, ERS6293704, ERS6293705, ERS6293706, ERS6293707, ERS6293708, ERS6293709, ERS6293710, ERS6293711, ERS6293712. Normalized counts are available as supplementary material in the article at https://www.frontiersin.org/articles/10.3389/fpls.2026.1818883/full#supplementary-material.

Of the 42,413 genes annotated in the grapevine genome, expression was detected in mature leaves for 16,005 genes in 2018 and 15,562 genes in 2019. Of these, 15,242 genes were expressed in both seasons, while 763 and 320 genes were detected exclusively in 2018 and 2019, respectively.

Thirty-two of the 55 identified metabolites changed in abundance under water stress conditions in grapevine leaves. These metabolites are associated with several biological processes, including photosynthesis; major and minor carbohydrate (CHO) metabolism; the TCA cycle; cell wall composition; lipid, nitrogen, amino acid, nucleotide, and secondary metabolism; and redox reactions.

Principal Component Analysis (PCA) showed that both transcripts and metabolites were separated primarily by year of experiment (PC1), followed by genotype and water stress level, measured as Ψ_s (PC2) (Figure 3.1). Separation by water stress level was more pronounced for transcripts than for metabolites.

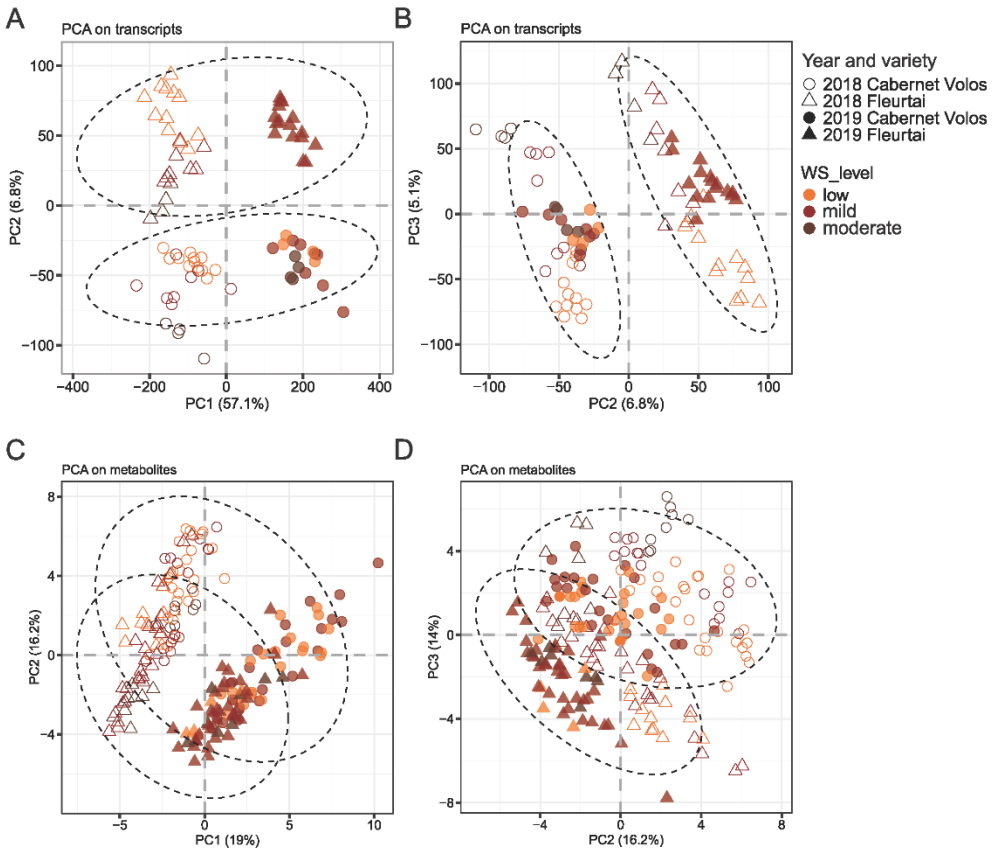


Figure 3.1: Principal Component Analysis (PCA) of transcripts and metabolites in water deficit experiment. PCA scatter plots show sample distribution based on transcript reads (A, B) and metabolite concentrations (C, D) in leaves of Cabernet Volos (circles) and Fleurtai (triangles), collected in 2018 (empty symbols) and 2019 (filled symbols). Samples are colored by stress severity: low stress (orange), mild stress (red), and moderate stress (brown). Stress categories were defined based on Ψ_s as follows: low stress, $\Psi_s > -0.5$ MPa (Cabernet Volos) or $\Psi_s > -0.4$ MPa (Fleurtai); mild stress, -1.3 MPa $\leq \Psi_s \leq -0.5$ MPa (Cabernet Volos) or -1.15 MPa $\leq \Psi_s \leq -0.4$ MPa (Fleurtai); moderate stress, $\Psi_s \leq -1.3$ MPa (Cabernet Volos) or $\Psi_s \leq -1.15$ MPa (Fleurtai). Republished from Combined omics data reveal multilevel response to water deficit in grapevine disease-resistant varieties, Strah et al. 2026, Frontiers in Plant Science, 17:1818883, 10.3389/fpls.2026.1818883, according to Creative Common Attribution ("CC BY") license.

To identify genes whose expression patterns were consistent with the observed drops in Ψ_s, we analyzed the transcriptomic and metabolomic data using a multifactor linear model incorporating genotype and Ψ_s interactions. Based on gene expression profiles and metabolite abundance relative to decreasing Ψ_s, three categories emerged (Type 1, Type 2, Type 3), as detailed in Methods Section 2.3.1 and Figure 2.1. In short, Type 1 represents genes and metabolites responsive to water deficit in both cultivars, Type 2 represents genes and metabolites responsive only in Cabernet Volos, and Type 3 represents genes and metabolites responsive only in Fleurtai.

3.1.1 Type 1

The 689 genes assigned to Type 1 belonged to 22 different GoMapMan gene sets based on predicted function, with minor carbohydrate metabolism and amino acid metabolism among the most represented functional groups. Moreover, a significant positive correlation was found between raffinose abundance and the expression of raffinose synthase genes (*Vitvi14g01717*, *Vitvi11g00513*, *Vitvi17g00885*), and between galactinol abundance and the expression of several galactinol synthase genes (*Vitvi07g00457*, *Vitvi07g02242*, *Vitvi14g02461*, *Vitvi05g00170*, *Vitvi14g00063*, *Vitvi01g00714*). The minor carbohydrate synthesis pathway mapped with gene expression and metabolites is visualized in Figure 3.2.

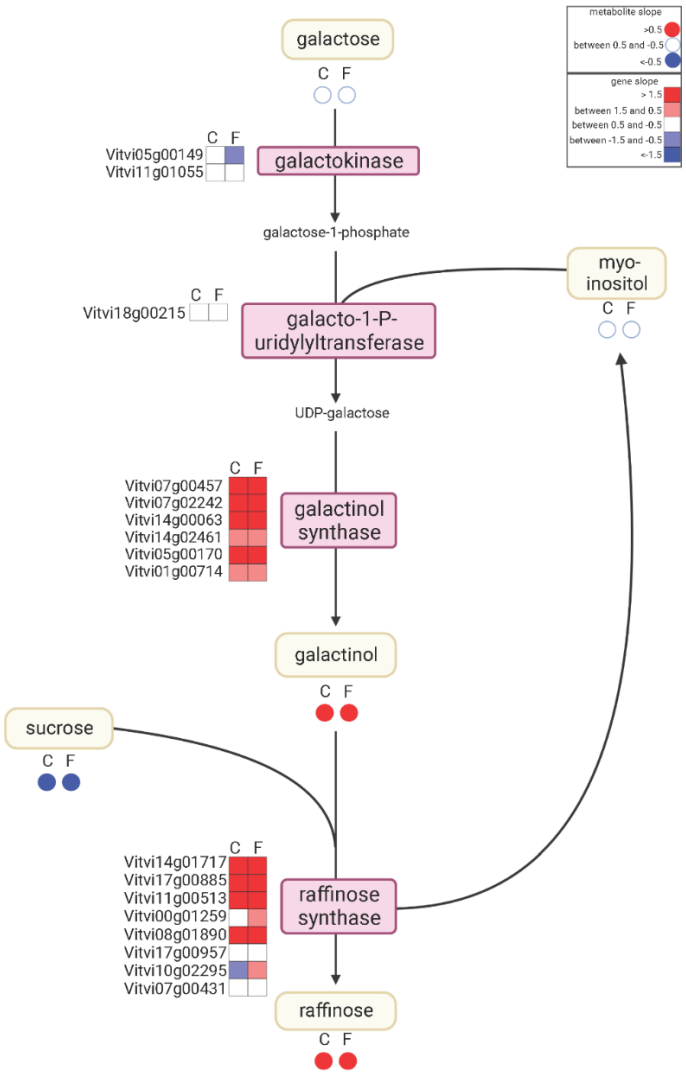


Figure 3.2: Raffinose synthesis pathway with transcript and metabolite measurements in water deficit experiment. Slopes of the regression lines relating metabolite abundance to Ψ_s (metabolite slope) and gene expression to Ψ_s (gene slope) are shown as color-coded scales for Cabernet Volos (C) and Fleurtai (F). Red indicates increased abundance with increasing Ψ_s; blue indicates decreased abundance with increasing Ψ_s. Metabolites are represented as circles and transcripts as squares. Republished from Combined omics data reveal multilevel response to water deficit in grapevine disease-resistant varieties, Strah

et al. 2026, Frontiers in Plant Science, 17:1818883, 10.3389/fpls.2026.1818883, according to Creative Common Attribution ("CC BY") license.

Amino acids also showed correlations with genes related to their biosynthesis. For instance, we found a positive correlation between proline and delta-1-pyrroline-5-carboxylate synthase 2 (*Vitvi13g00355*), and between GABA and a glutamate decarboxylase (*Vitvi04g00870*), in both genotypes.

Several upregulated Type 1 genes were related to abscisic acid synthesis, including NCED and aldehyde oxidase (*Vitvi19g01356*, *Vitvi02g01288*, and *Vitvi18g02167*), as well as ABA-inducible genes (*Vitvi03g01727* and *Vitvi17g00085*). Conversely, genes downregulated with decreasing Ψ_s were related to auxin, ethylene, and gibberellin signal transduction (*Vitvi14g01899*, *Vitvi09g00050*, *Vitvi01g02286*, *Vitvi16g00349*, *Vitvi07g02064*, *Vitvi16g00350*, and *Vitvi17g00601*), and to gibberellin, cytokinin, and salicylic acid metabolism (*Vitvi16g00890*, *Vitvi19g02230*, *Vitvi14g03084*, *Vitvi18g01019,* and *Vitvi04g02118*).

The change in Ψ_s also affected the expression of genes involved in transcriptional regulation. Fifteen transcription factors were upregulated as Ψ_s decreased, including genes from the MYB, NAC, and bZIP families, while twenty-eight genes were repressed with decreasing Ψ_s, including genes from the WRKY, basic helix-loop-helix (bHLH), and MYB families. Several genes related to protein synthesis and modification were also modulated, most of them upregulated. We also observed considerable downregulation in functional groups related to cell wall metabolism, primarily genes associated with cell wall degradation and modification.

Genes encoding biotic stress receptors, such as osmotins (*Vitvi02g01408* and *Vitvi02g01409*), and other abiotic stress-response proteins, such as small HSPs, were upregulated in both varieties. By contrast, several biotic stress-associated genes were downregulated in response to water deficit; the majority were PR proteins, with PR5 being the most represented (*Vitvi02g00391*, *Vitvi02g01404*, and *Vitvi17g00217*).

Finally, Type 1 also contained a large group of 48 kinase and receptor kinase genes, all but four of which were downregulated as Ψ_s decreased.

3.1.2 Type 2

Type 2 contained 63 genes responsive to Ψ_s in Cabernet Volos but not in Fleurtai. Kinases and receptor kinases were the most represented functional group in this category, accounting for 27 of the 63 genes.

3.1.3 Type 3

Type 3 contained 41 genes that were significantly responsive to decreasing Ψ_s in Fleurtai, but not in Cabernet Volos. Among these, 26 genes were upregulated and 15 downregulated with decreasing Ψ_s. Genes related to secondary metabolism represented the largest upregulated group, comprising three terpene synthase genes (*Vitvi19g00391*, *Vitvi18g02446*, *Vitvi12g00574*) and two UDP-glycosyltransferase genes (*Vitvi15g01075* and *Vitvi15g01643*). Additionally, a GCR2-like 1 gene involved in ABA signaling (*Vitvi00g02022*) and a gene encoding a disease resistance protein (TIR-NBS-LRR class) (*Vitvi18g01877*) were upregulated. Transport-related genes were also represented in this category, including an ABC transporter, a cation efflux protein, and sulfate transporters (*Vitvi09g00303*, *Vitvi19g01715*, *Vitvi07g01779*).

The abundance of shikimate, a precursor of phenylalanine and polyphenols, decreased over the experimental period, while several genes involved in shikimate biosynthesis—such

as 3-deoxy-D-arabino-heptulosonic acid 7-phosphate synthase (DAHPS, *Vitvi07g03049*, *Vitvi02g01749*) and 3-dehydroquinate synthase (DHQS, *Vitvi14g01919*)—showed increased transcript levels in both genotypes. These results suggest rapid turnover of the shikimate pool toward the biosynthesis of phenylalanine and downstream metabolites.

Consistently, several genes involved in the chorismate pathway and phenylalanine synthesis were upregulated with decreasing Ψ_s, e.g., shikimate kinase (*Vitvi14g01497*), 5-enolpyruvylshikimate 3-phosphate synthase (EPSPS) (*Vitvi15g01490*), and chorismate synthase (*Vitvi13g00597*). Quinate abundance remained unchanged regardless of Ψ_s in both Fleurtai and Cabernet Volos, while caffeoylquinate abundance increased considerably in Fleurtai as Ψ_s dropped. Combined with the negative correlation found between DHQS and quinate, this suggests an increase in caffeoylquinate biosynthesis. The caffeoylquinic acid synthesis pathway mapped with gene expression and metabolites is visualized in Figure 3.3.

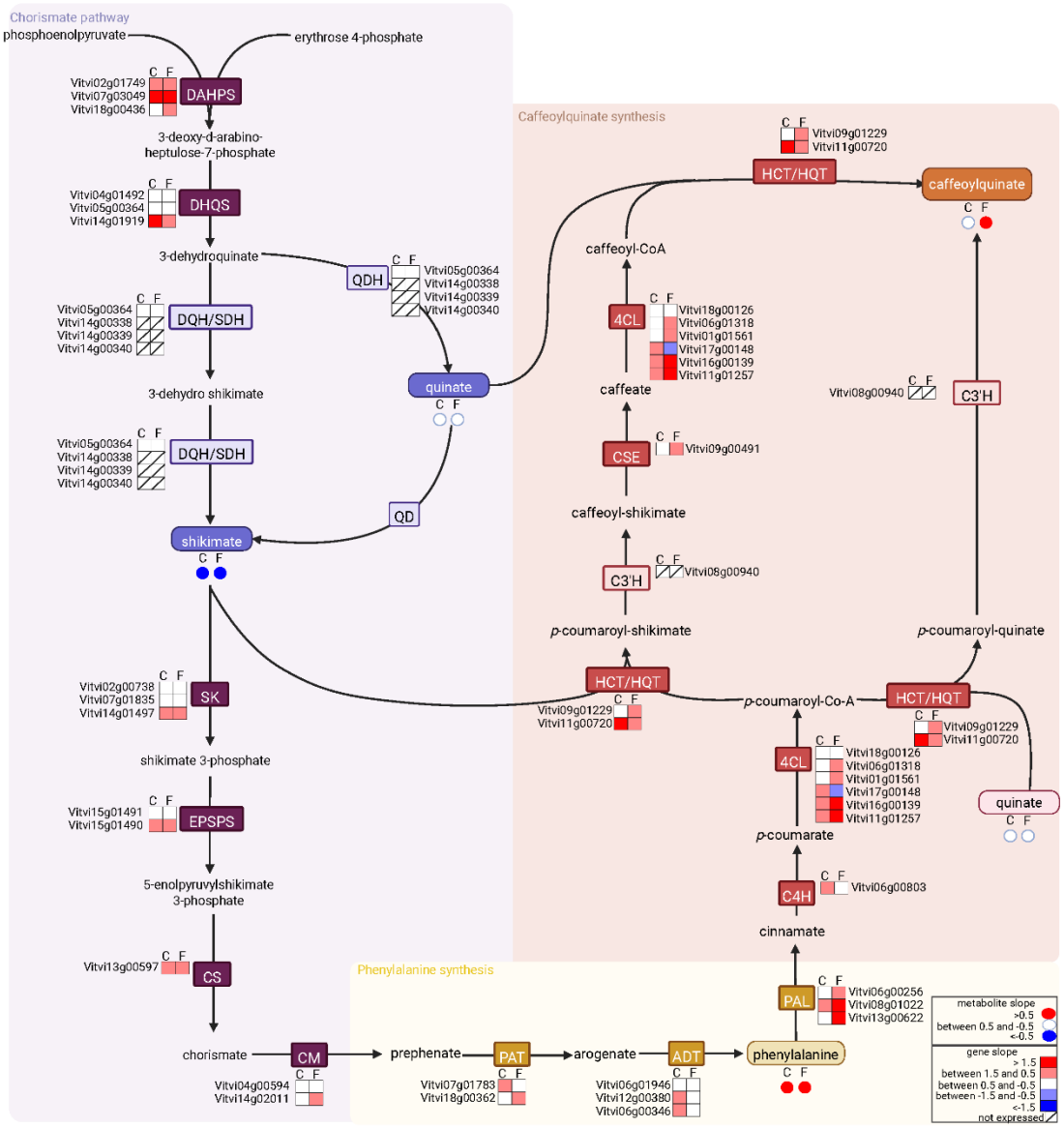


Figure 3.3: Response of caffeoylquinate synthesis pathway with transcript and metabolite measurements in water deficit experiment. Slopes of the regression lines relating metabolite abundance to Ψ_s (metabolite slope) and gene expression to Ψ_s (gene slope) are shown as color-coded scales for Cabernet Volos (C) and Fleurtai (F). Red indicates increased abundance with increasing Ψ_s; blue indicates decreased abundance with increasing Ψ_s. Metabolites are represented as circles and transcripts as squares. Republished from Combined omics data reveal multilevel response to water deficit in grapevine disease-resistant varieties, Strah et al. 2026, Frontiers in Plant Science, 17:1818883, 10.3389/fpls.2026.1818883, according to Creative Common Attribution ("CC BY") license.

3.2 High Salinity Responses in M1, M4 and 1103 Paulsen Rootstocks

The sequencing results of high salinity experiments have been published by Buesa et al. [147] and are summarized in this section. Raw reads obtained from sequencing are available at https://www.ebi.ac.uk/ena under the study accession PRJEB44658 and following accession numbers: ERS6409479, ERS6409480, ERS6409481, ERS6409482, ERS6409483, ERS6409484, ERS6409485, ERS6409486, ERS6409487, ERS6409488, ERS6409489, ERS6409490, ERS6409491, ERS6409492, ERS6409493, ERS6409494, ERS6409495, ERS6409496, ERS6409497, ERS6409498, ERS6409499, ERS6409500, ERS6409501, ERS6409502, ERS6409503, ERS6409504, ERS6409505, ERS6409506, ERS6409507, ERS6409508, ERS6409509, ERS6409510, ERS6409511, ERS6409512, ERS6409513. Normalized counts are available as supplementary material in the article at https://www.frontiersin.org/articles/10.3389/fpls.2022.866053/full#supplementary-material.

The sequencing was performed on whole leaf and berry skin samples from cv. Tempranillo grafted onto three different rootstocks and exposed to salinity stress. On average, 41,326,458 reads were mapped in pairs to the grapevine genome. Of the 42,413 genes annotated in the grapevine genome, 16,790 were expressed at sufficient levels for statistical analysis.

Although hierarchical clustering analysis and PCA of leaf and berry skin samples showed no apparent correlation in gene expression with either water quality or rootstock, and no clear clustering was observed on PCA for either tissue (Figure 3.4, Figure 3.5), GSEA identified several processes that were significantly differentially expressed (FDR q < 0.25) due to water quality in leaves and berries of scions grafted onto the three rootstocks (Figure 3.6). The number of significantly differentially expressed bins was higher in leaves and berries of scions grafted onto M4 and M1 than onto 1103 Paulsen. The strongest enrichment was detected for flavonoid synthesis gene sets in berry skins across all three rootstocks, with chalcone synthase genes contributing predominantly.

When examining the expression of individual genes involved in this pathway, up to fourfold differences in average values were observed. A uniformly dominant upregulation pattern was observed, although no statistically significant differences in gene expression were found between control and saline treatments. The largest differences in average expression between salt-stressed and control vines were observed for chalcone synthase (*CHS*) and phenylalanine ammonia-lyase (*PAL*) genes. This was most apparent in berry skins, where most *PAL* and *CHS* genes showed an upregulation pattern due to water quality (Figure 3.7); these differences were greatest in vines grafted onto 1103 Paulsen compared to M4 and M1. However, several flavanone 3-hydroxylase genes showed a downregulation pattern in these same samples. Leaf samples, by contrast, showed smaller differences, observed in *CHS* genes in M1-rooted samples, and in *F3H*, *F3'H*, and *F3'5'H* genes in M4-rooted samples (Figure 3.8).

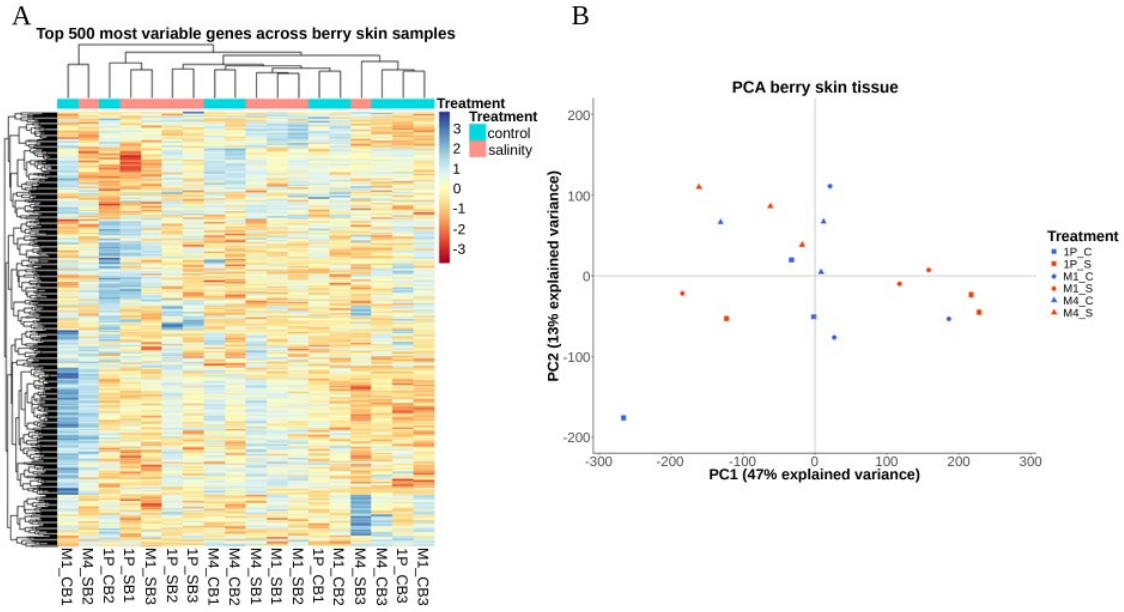


Figure 3.4: Gene expression overview in berry skin samples of grapevine cv. Tempranillo grafted onto three different rootstocks and exposed to salinity stress. (A) Hierarchical clustering analysis of the 500 most variable genes in berry skin samples. (B) Principal component analysis of the berry skin samples. PC, principal component; 1P, 1103 Paulsen; C, control; S, salinity. Republished from Physiological and Transcriptional Responses to Saline Irrigation of Young 'Tempranillo' Vines Grafted Onto Different Rootstocks, Buesa et al. 2022, Frontiers in Plant Science, 13:866053., 10.3389/fpls.2022.866053, according to Creative Common Attribution ("CC BY") license.

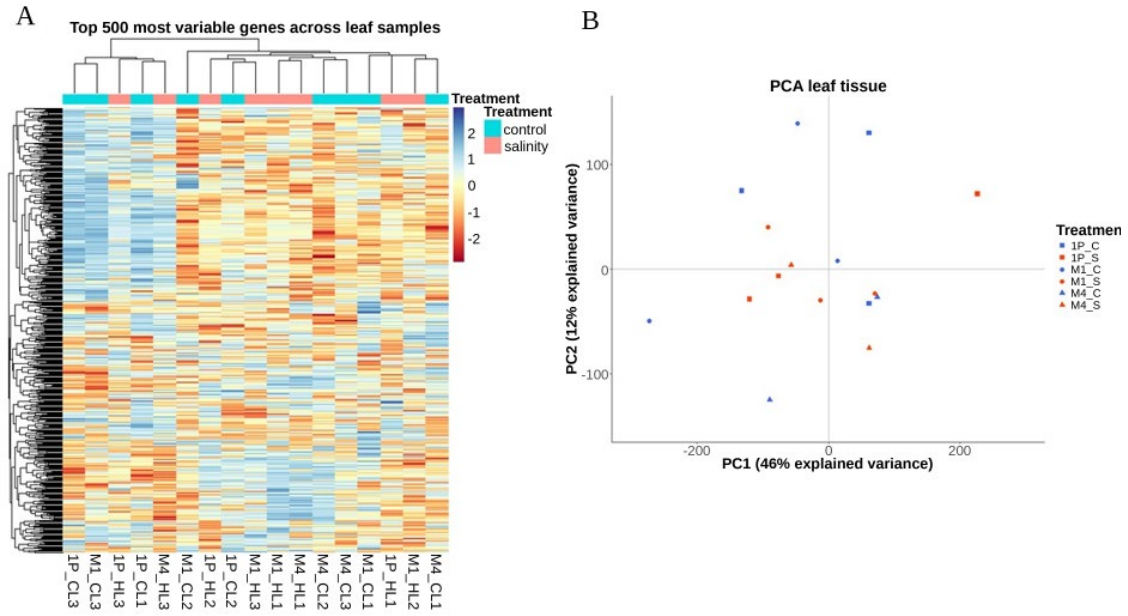
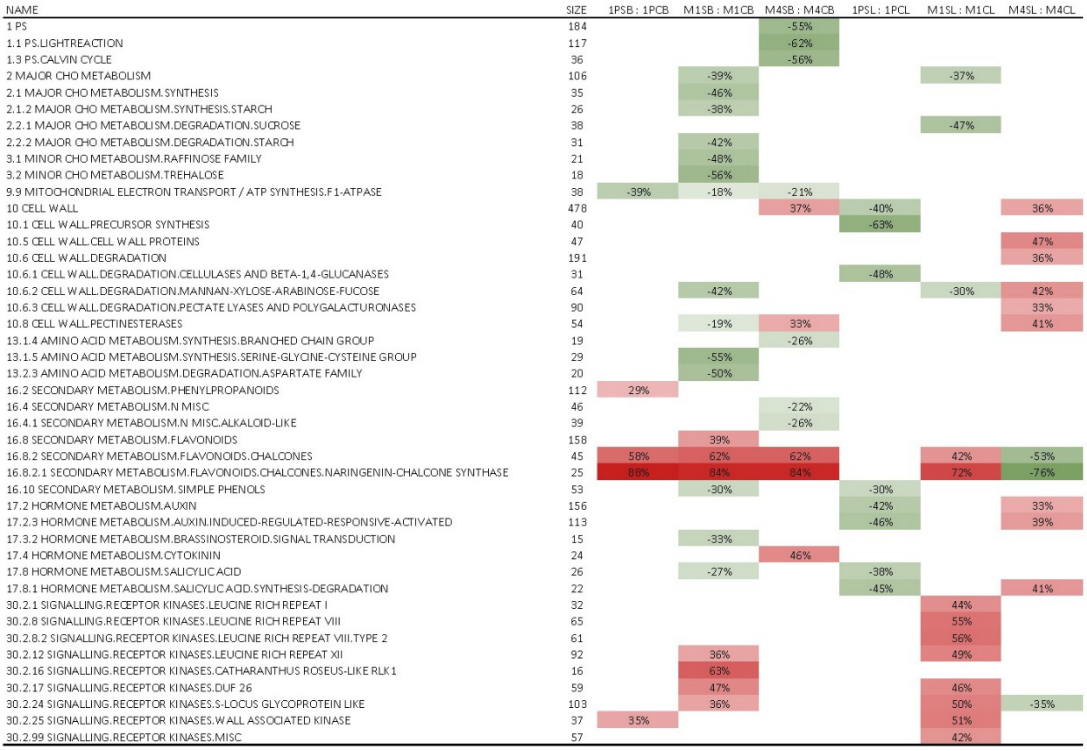


Figure 3.5: Gene expression overview in leaf samples of grapevine cv. Tempranillo grafted onto three different rootstocks and exposed to salinity stress. (A) Hierarchical clustering analysis of the 500 most variable genes in leaf samples. (B) Principal component analysis of the leaf samples. PC, principal component; 1P, 1103 Paulsen; C, control; S, salinity. Republished from Physiological and Transcriptional Responses to Saline Irrigation of Young 'Tempranillo' Vines Grafted Onto Different Rootstocks, Buesa et al. 2022, Frontiers in Plant Science, 13:866053., 10.3389/fpls.2022.866053, according to Creative Common Attribution ("CC BY") license.



NAME	SIZE	1PSB : 1PCB	M1SB : M1CB	M4SB : M4CB	1PSL : 1PCL	M1SL : M1CL	M4SL : M4CL
1 PS	184			-55%			
1.1 PS.LIGHTREACTION	117			-62%			
1.3 PS.CALVIN CYCLE	36			-56%			
2 MAJOR CHO METABOLISM	106		-39%			-37%	
2.1 MAJOR CHO METABOLISM.SYNTHESIS	35		-46%				
2.1.2 MAJOR CHO METABOLISM.SYNTHESIS.STARCH	26		-38%				
2.2.1 MAJOR CHO METABOLISM.DEGRADATION.SUCROSE	38					-47%	
2.2.2 MAJOR CHO METABOLISM.DEGRADATION.STARCH	31		-42%				
3.1 MINOR CHO METABOLISM.RAFFINOSE FAMILY	21		-48%				
3.2 MINOR CHO METABOLISM.TREHALOSE	18		-56%				
9.9 MITOCHONDRIAL ELECTRON TRANSPORT / ATP SYNTHESIS.F1-ATPASE	38	-39%	-18%	-21%			
10 CELL WALL	478			37%	-40%		36%
10.1 CELL WALL.PRECURSOR SYNTHESIS	40				-63%		
10.5 CELL WALL.CELL WALL PROTEINS	47						47%
10.6 CELL WALL.DEGRADATION	191						36%
10.6.1 CELL WALL.DEGRADATION.CELLULASES AND BETA-1,4-GLUCANASES	31				-48%		
10.6.2 CELL WALL.DEGRADATION.MANNAN-XYLOSE-ARABINOSE-FUCOSE	64		-42%			-30%	42%
10.6.3 CELL WALL.DEGRADATION.PECTATE LYASES AND POLYGALACTURONASES	90						33%
10.8 CELL WALL.PECTINESTERASES	54		-19%	33%			41%
13.1.4 AMINO ACID METABOLISM.SYNTHESIS.BRANCHED CHAIN GROUP	19			-26%			
13.1.5 AMINO ACID METABOLISM.SYNTHESIS.SERINE-GLYCINE-CYSTEINE GROUP	29		-55%				
13.2.3 AMINO ACID METABOLISM.DEGRADATION.ASPARTATE FAMILY	20		-50%				
16.2 SECONDARY METABOLISM.PHENYLPROPANOIDS	112	29%					
16.4 SECONDARY METABOLISM.N MISC	46			-22%			
16.4.1 SECONDARY METABOLISM.N MISC.ALKALOID-LIKE	39			-26%			
16.8 SECONDARY METABOLISM.FLAVONOIDS	158		39%				
16.8.2 SECONDARY METABOLISM.FLAVONOIDS.CHALCONES	45	58%	62%	62%		42%	-53%
16.8.2.1 SECONDARY METABOLISM.FLAVONOIDS.CHALCONES.NARINGENIN-CHALCONE SYNTHASE	25	88%	84%	84%		72%	-76%
16.10 SECONDARY METABOLISM.SIMPLE PHENOLS	53		-30%		-30%		
17.2 HORMONE METABOLISM.AUXIN	156				-42%		33%
17.2.3 HORMONE METABOLISM.AUXIN.INDUCED-REGULATED-RESPONSIVE-ACTIVATED	113				-46%		39%
17.3.2 HORMONE METABOLISM.BRASSINOSTEROID.SIGNAL TRANSDUCTION	15		-33%				
17.4 HORMONE METABOLISM.CYTOKININ	24			46%			
17.8 HORMONE METABOLISM.SALICYLIC ACID	26		-27%		-38%		
17.8.1 HORMONE METABOLISM.SALICYLIC ACID.SYNTHESIS-DEGRADATION	22				-45%		41%
30.2.1 SIGNALLING.RECEPTOR KINASES.LEUCINE RICH REPEAT I	32					44%	
30.2.8 SIGNALLING.RECEPTOR KINASES.LEUCINE RICH REPEAT VIII	65					55%	
30.2.8.2 SIGNALLING.RECEPTOR KINASES.LEUCINE RICH REPEAT VIII.TYPE 2	61					56%	
30.2.12 SIGNALLING.RECEPTOR KINASES.LEUCINE RICH REPEAT XII	92		36%			49%	
30.2.16 SIGNALLING.RECEPTOR KINASES.CATHARANTHUS ROSEUS-LIKE RLK1	16		63%				
30.2.17 SIGNALLING.RECEPTOR KINASES.DUF 26	59		47%			46%	
30.2.24 SIGNALLING.RECEPTOR KINASES.S-LOCUS GLYCOPROTEIN LIKE	103		36%			50%	-35%
30.2.25 SIGNALLING.RECEPTOR KINASES.WALL ASSOCIATED KINASE	37	35%				51%	
30.2.99 SIGNALLING.RECEPTOR KINASES.MISC	57					42%	

Figure 3.6: Subset of significantly enriched gene sets identified by GSEA of grapevine cv. Tempranillo grafted onto three different rootstocks and exposed to salinity stress. Values represent the percentage of genes positively (red) or negatively (green) regulated within a given set, in leaves and berries of cv. Tempranillo vines grafted onto 1103 Paulsen, M1, or M4 rootstocks and subjected to salinity irrigation. Only statistically significant values (FDR q $<$ 0.25) are shown. Red denotes positive enrichment/upregulation; green denotes negative enrichment/downregulation. C, control; S, salinity; 1P, 1103 Paulsen rootstock; M1, M1 rootstock; M4, M4 rootstock; L, leaves; B, berries. Republished from Physiological and Transcriptional Responses to Saline Irrigation of Young 'Tempranillo' Vines Grafted Onto Different Rootstocks, Buesa et al. 2022, Frontiers in Plant Science, 13:866053., 10.3389/fpls.2022.866053, according to Creative Common Attribution ("CC BY") license.

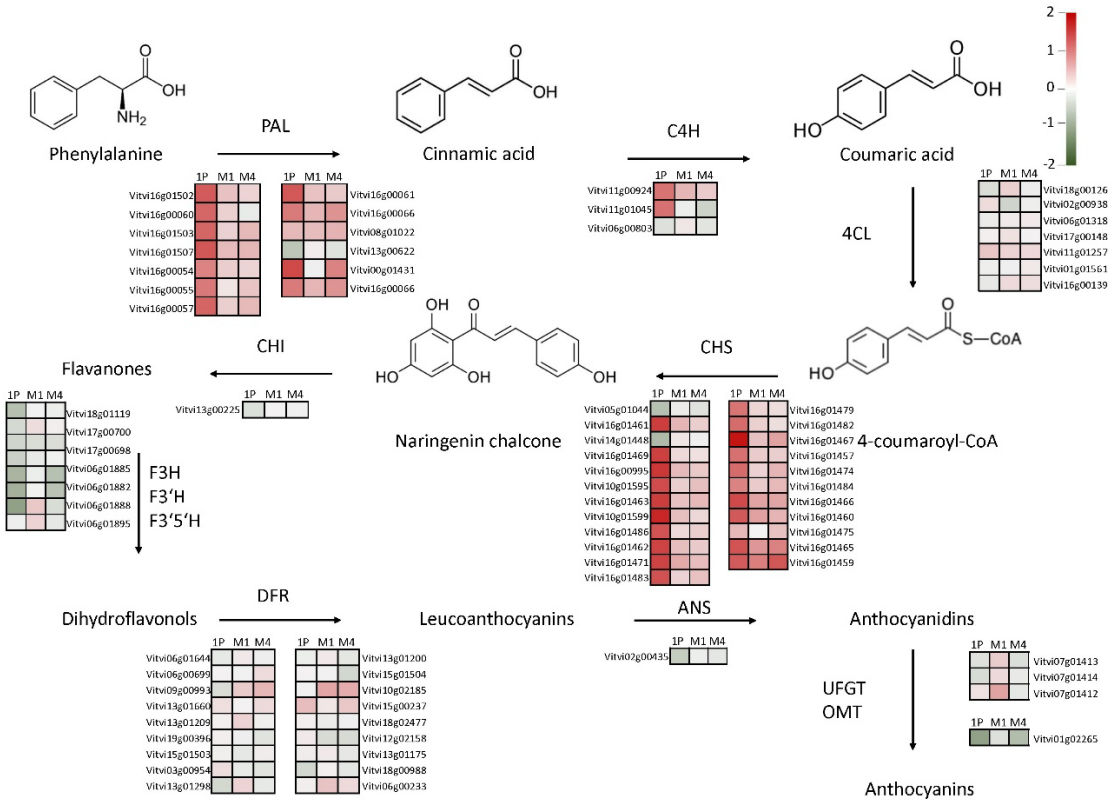


Figure 3.7: Expression of genes involved in anthocyanin synthesis in berry skins of grapevine cv. Tempranillo grafted onto three different rootstocks and exposed to salinity stress. Squares represent Log_2FC values comparing salinity treated and control vines grafted onto 1103 Paulsen, M1, and M4. Color represents the value of Log_2FC, red denoting upregulation; green denoting downregulation. PAL – phenylalanine ammonia-lyase; C4H, cinnamate-4-hydroxylase; 4CL, 4-coumarate: CoA ligase; CHS, chalcone synthase; CHI, chalcone-flavanone isomerase; F3H, flavanone 3-hydroxylase; F3'H, flavonoid 3'-hydroxylase; F3'5'H, flavonoid 3'5'-hydroxylase; DFR, dihydroflavonol 4-reductase; ANS, anthocyanin synthase; UFGT, anthocyanidin 3-O-glucosyltransferase; OMT, O-methyltransferase; 1P, 1103 Paulsen rootstock; M1, M1 rootstock; M4, M4 rootstock. Republished from Physiological and Transcriptional Responses to Saline Irrigation of Young 'Tempranillo' Vines Grafted Onto Different Rootstocks, Buesa et al. 2022, Frontiers in Plant Science, 13:866053., 10.3389/fpls.2022.866053, according to Creative Common Attribution ("CC BY") license.

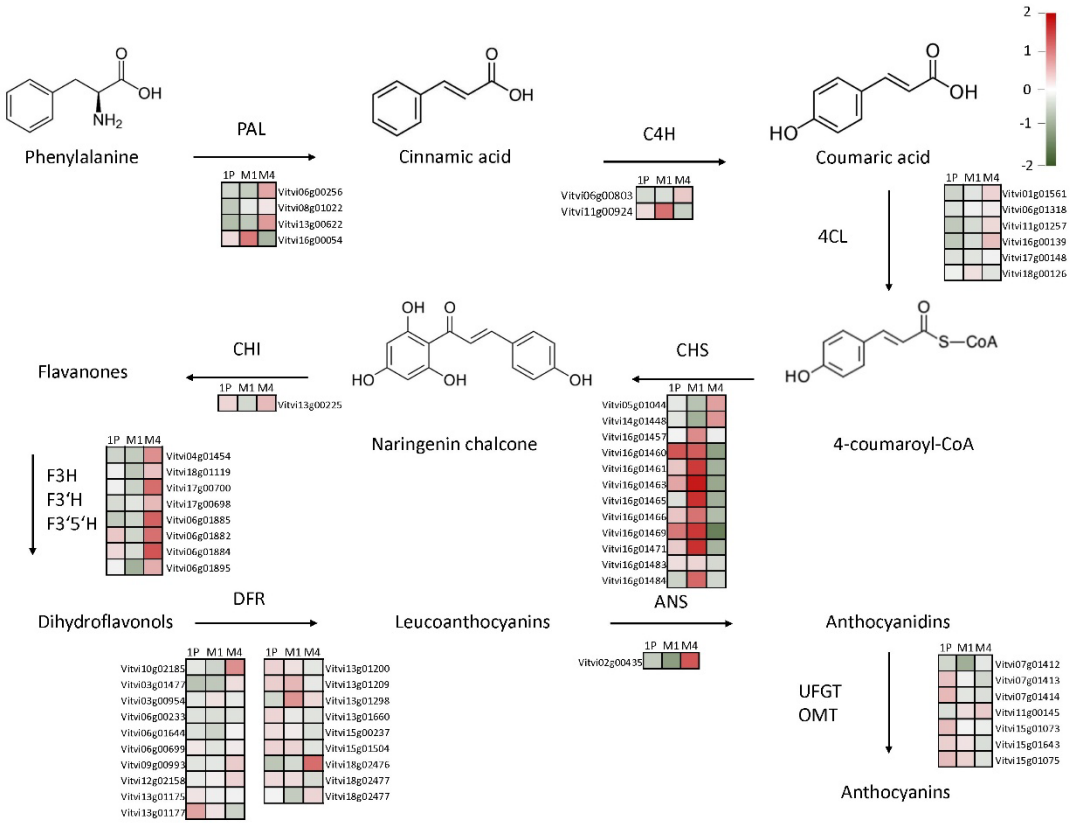


Figure 3.8: Expression of genes involved in anthocyanin synthesis in cv. Tempranillo in salinity-treated leaves. Squares represent Log_2FC values comparing salinity treated and control vines grafted onto 1103 Paulsen, M1, and M4. Color represents the value of Log_2FC, red denoting upregulation; green denoting downregulation. PAL – phenylalanine ammonia-lyase; C4H, cinnamate-4-hydroxylase; 4CL, 4-coumarate: CoA ligase; CHS, chalcone synthase; CHI, chalcone-flavanone isomerase; F3H, flavanone 3-hydroxylase; F3'H, flavonoid 3'-hydroxylase; F3'5'H, flavonoid 3'5'-hydroxylase; DFR, dihydroflavonol 4-reductase; ANS, anthocyanin synthase; UFGT, anthocyanidin 3-O-glucosyltransferase; OMT, O-methyltransferase; 1P, 1103 Paulsen rootstock; M1, M1 rootstock; M4, M4 rootstock. Republished from Physiological and Transcriptional Responses to Saline Irrigation of Young 'Tempranillo' Vines Grafted Onto Different Rootstocks, Buesa et al. 2022, Frontiers in Plant Science, 13:866053., 10.3389/fpls.2022.866053, according to Creative Common Attribution ("CC BY") license.

3.3 Iron Deficit in Fercal and 3309 C

3.3.1 Nitrogen source and iron availability

Our collaborators at BOKU University showed that nitrogen source had a considerable effect on iron deficiency symptoms. Treatments with nitrate as the sole nitrogen source (N1A0/–Fe) showed stronger chlorosis symptoms, especially in the more sensitive 3309 C rootstock. This more severe response was also reflected in a greater decrease in biomass

and photosynthetic capacity. N1A0/–Fe-treated vines likewise had higher organic acid contents in root exudates, again most pronounced in 3309 C, while ferric chelate reductase activity was highest in N1A0/–Fe-treated Fercal vines. PCA clearly separated samples by treatment and rootstock genotype in terms of gene expression, and the number of differentially expressed genes was higher in N1A0/+Fe treatments. In our work, we focused on the expression of core iron deficiency response genes and the response of genes involved in ABA and auxin signaling.

The sequencing results of nitrogen source iron deficit response experiments have been published in Khalil et al. [148] and are summarized in this section. Raw reads obtained from sequencing are available at https://www.ebi.ac.uk/ena under the study accession PRJNA1068036 and following accession numbers: SAMN39593695, SAMN39593699, SAMN39593693, SAMN39593696, SAMN39593713, SAMN39593711, SAMN39593710, SAMN39593709, SAMN39593692, SAMN39593707, SAMN39593704, SAMN39593702, SAMN39593701, SAMN39593698, SAMN39593697, SAMN39593694, SAMN39593712, SAMN39593708, SAMN39593706, SAMN39593705, SAMN39593703, SAMN39593700, SAMN39593691, SAMN39593690. Normalized counts are available as supplementary material in the online article version at https://doi.org/10.1186/s12870-024-04906-y.

We first examined the expression of twelve core genes involved in iron deficit response, nitrogen transport, and root development: Fe uptake (*FRO2, IRT1, AHA2*); Fe transport (*IREG3, OPT3, VIT1, YSL6*); transcription factor involved in the regulation of uptake genes (*bHLH38/39*); Fe storage (*FER1*); N uptake and transport (*NR2, NRT1:2*); and genes involved in the regulation of root development (*ZAT11*). Their expression is presented as Log_2FC in Table 3.1.

Table 3.1: Expression of iron deficiency- and nitrogen-responsive genes in Fercal and 3309 C. Log_2FC values (logFC) are derived from comparing treatment to control. In the N1A0 treatment, nitrate is the sole nitrogen source; in the N1A1 treatment, nitrogen is supplied as a mixture of nitrate and ammonium. Red represents upregulation, blue represents downregulation. Bolded values are statistically significant ($p < 0.05$).

			N1A0		N1A1	
Function	Gene ID	Gene name	Fercal logFC	3309 C logFC	Fercal logFC	3309 C logFC
Fe uptake	*Vitvi16g01090*	*VviFRO2*	**2.47**	1.68	**7.26**	-0.50
	Vitvi11g01208	*VviAHA2*	0.27	**1.03**	0.08	-0.15
	Vitvi10g01358	*VviIRT1*	**7.35**	**7.54**	NA	NA
Fe transport	*Vitvi08g02084*	*VviIREG3*	-0.10	-0.40	-0.37	**-0.74**
	Vitvi10g00247	*VviOPT3*	**1.61**	**1.63**	0.29	**0.94**
	Vitvi01g00512	*VviVIT1*	0.35	0.17	**0.96**	-0.08
	Vitvi14g01520	*VviYSL6*	0.25	-0.26	**0.92**	0.27
Fe regulation	*Vitvi13g01037*	*VvibHLH38/39*	**8.54**	**6.72**	**4.31**	**2.81**
Fe storage	*Vitvi06g01761*	*VviFER1*	**-2.18**	-1.76	1.30	1.08
N uptake and transport	*Vitvi18g00326*	*VviNR2*	-0.43	-0.25	**4.31**	**2.34**
	Vitvi01g00921	*VviNRT 1:2*	**1.13**	-0.05	**1.53**	**0.80**
Root development	*Vitvi06g01682*	*VviZAT11*	1.26	0.82	**4.67**	**-1.18**

N1A0 treatment caused very similar expression patterns in both genotypes. The iron deficiency-related transcription factor *bHLH38/39* was induced, as were iron uptake-related genes and the *OPT3* iron transporter. The iron storage-related *FER1* was downregulated, while root development-related genes were upregulated. The N1A1 treatment with mixed nitrogen sources displayed a different pattern of iron deficiency response and accentuated the differences between the two genotypes. Most notably, 3309 C did not induce the iron uptake-related genes under this treatment; nitrogen transport and root development genes were more strongly induced in both genotypes, and iron storage-associated *FER1* was upregulated.

We then examined the expression of a selection of ABA- and auxin-related genes, as these two phytohormones modulate responses to iron deficiency (Figure 3.9). Among the auxin-related genes, six encoding Aux/IAA family transcription factors were highly upregulated by Fe deficiency in both rootstocks, and an additional three genes were upregulated only in 3309 C when supplied with both N forms, while they were not upregulated when supplied with nitrate alone. In 3309 C an additional 12 genes encoding SAUR family transcription factors were highly upregulated by Fe deficiency when supplied with both N forms, while they were not upregulated when supplied with nitrate alone. Among these, only two genes were also significantly upregulated by Fe deficiency in Fercal when supplied with both N forms. In addition, some genes upregulated by Fe deficiency were also found in the auxin synthesis pathway; these genes, too, were upregulated only when supplied with both N forms.

Similarly, in the ABA signaling pathway, most of the genes belonging to the RCAR, PYL, PP2C, and SnRK2 families were upregulated only when both forms of N were provided. Of these, three genes were highly upregulated in both rootstocks, four genes only in Fercal, and four other genes only in 3309 C. Likewise, in the ABA synthesis pathway and among transcription factors involved in ABA metabolism, the majority of upregulated genes belonged to 3309 C supplied with both N forms.

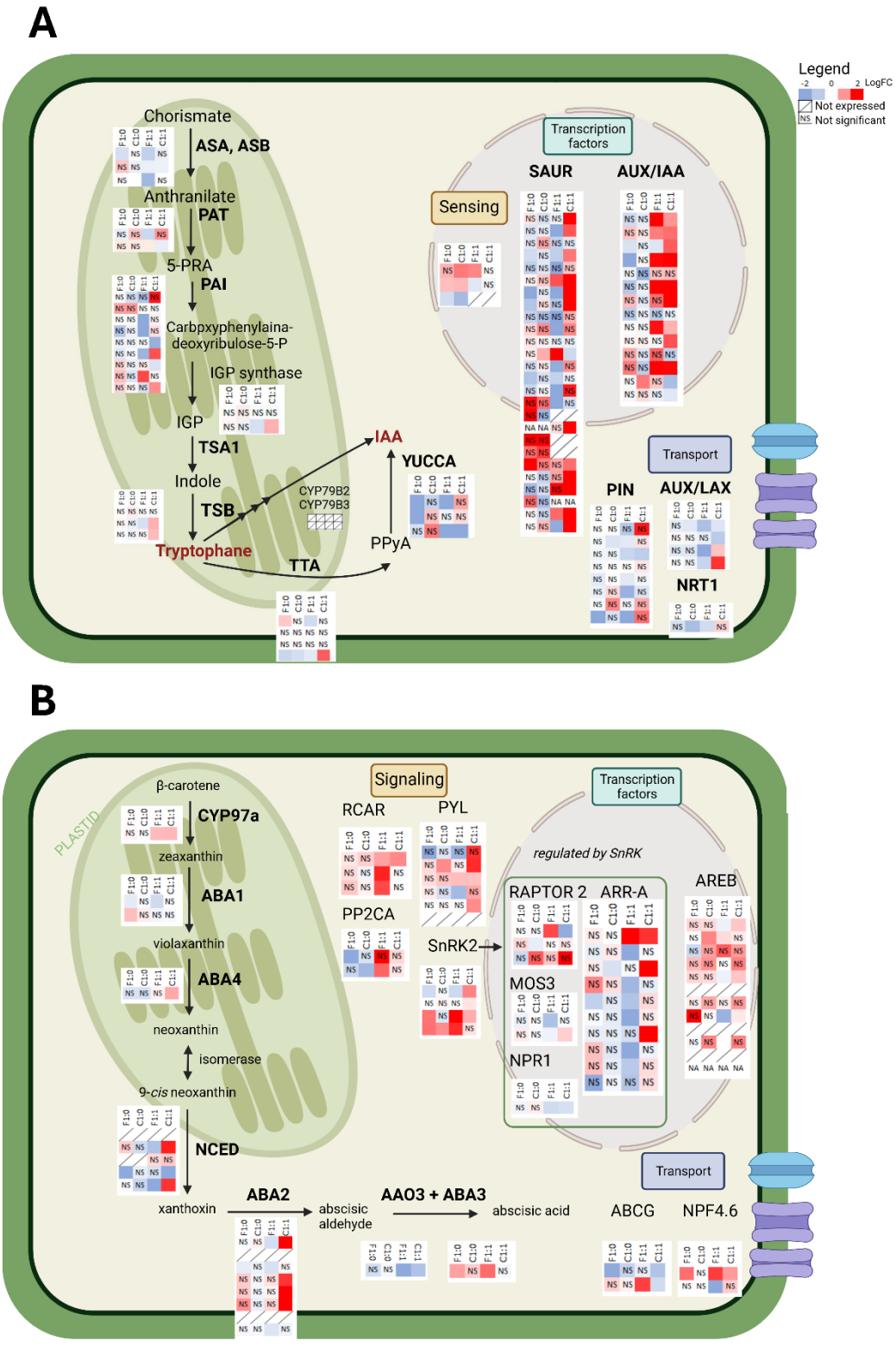


Figure 3.9: Expression response of auxin- and ABA-responsive genes in Fercal and 3309 C in iron deficiency.Squares represent Log_2FC values. (A) Auxin synthesis, transport, sensing, and transcription factors pathway, and (B) Abscisic acid synthesis, transport, signaling, and transcription factors pathway. Box color indicates up (red) and down (blue)-regulated genes. / - not expressed; NS - not statistically significant; F1:0 - Fercal N1A0 (-Fe vs. + Fe); C1:0–3309 C N1A0 (-Fe vs. + Fe); F1:1 - Fercal N1A1 (-Fe vs. +

Fe); C1:1–3309 C N1A1 (-Fe vs. + Fe). Republished from The activation of iron deficiency responses of grapevine rootstocks is dependent to the availability of the nitrogen forms, Khalil et al. 2024, BMC Plant Biology, 24:218., 10.1186/s12870-024-04906-y, according to Creative Common Attribution ("CC BY") license.

3.3.2 Direct and induced iron deficiency

Our collaborators at BOKU University showed that in both conditions of low Fe availability, there were noticeable reductions in various growth parameters, as well as leaf chlorosis and reduced chlorophyll content. These effects were stronger in the more sensitive 3309 C rootstock. Fercal increased root biomass under the bicarbonate treatment (+Fe+BIC) and was able to maintain high FCR activity in root tips under direct Fe deficiency (–Fe), while 3309 C showed a severe decrease in FCR activity under both conditions. Organic acid content in root tips increased especially strongly under +Fe+BIC in both rootstocks. In 3309 C root exudates, –Fe caused a strong increase in malic acid, while +Fe+BIC increased citric acid. In Fercal root exudates, the increases in organic acid abundance were smaller and more prominent under –Fe. Transcriptomic analysis showed that +Fe+BIC induced a higher number of differentially expressed genes than –Fe, and PCA clustered the samples mostly according to rootstock genotype, with the +Fe+BIC samples also clustering very distinctly apart from –Fe and control samples. In our work, we focused on the expression of core iron deficiency response genes and the response of genes involved in organic acid metabolism.

The sequencing results of iron deficiency response experiments have been published in Khalil et al. [149] and are summarized in this section. Raw reads obtained from sequencing are available at https://www.ebi.ac.uk/ena under the study accession PRJNA1122387 and following accession numbers: SAMN42050796, SAMN42050794, SAMN42050790, SAMN42050797, SAMN42050805, SAMN42050801, SAMN42050792, SAMN42050791, SAMN42050806, SAMN42050804, SAMN42050800, SAMN42050798, SAMN42050795, SAMN42050793, SAMN42050803, SAMN42050799, SAMN42050789, SAMN42050802. Normalized counts are available as supplementary material in the online article version at https://doi.org/10.1016/j.stress.2025.100841.

First, we investigated the expression patterns of genes known to be involved in Fe uptake, transport, storage, homeostasis, root development, and organic acid metabolism (Table 3.2). Notably, while Log_2FC values were high for some of the selected genes, only two reached statistical significance. Genes involved in Fe acquisition were not strongly affected, with the exception of Iron-Regulated Transporter 1 (*IRT1*), which was strongly upregulated in 3309 C and slightly upregulated in Fercal. Fe homeostasis regulators (*bHLH38*, *bHLH38/39*) were induced in both rootstocks, with stronger activation in 3309 C under +Fe+BIC and in Fercal under –Fe. For Fe transport and translocation, most genes (*VIT*1, *IREG3*, *OPT3*, *NRAMP1*, *YSL6*) showed limited expression changes, though levels were generally lower in 3309 C. *FRD3* is the exception, as it was highly expressed under both stress conditions, with 3309 C showing higher expression under +Fe+BIC and Fercal under –Fe. In addition, *ZIF1* expression increased under –Fe in both rootstocks but only in Fercal under +Fe+BIC. The expression of *FERRITIN1* (*FER1*) drastically decreased under both treatments in 3309 C, while Fercal showed only modest changes.

Table 3.2: Expression of direct and indirect iron deficiency-responsive genes in Fercal and 3309 C. Log_2FC values (logFC) are derived from comparing treatment to control. –Fe –direct iron deficiency; +Fe+BIC – indirect iron deficiency induced by bicarbonate. Red represents upregulation, blue represents downregulation. Bolded values are statistically significant ($p < 0.05$).

			3309 C		Fercal	
Function	Gene ID	Gene name	–Fe Log2FC	+Fe+BIC Log2FC	–Fe Log2FC	+Fe+BIC Log2FC
Fe uptake	*Vitvi16g01090*	*VviFRO2*	-1.24	0.23	0.95	1.14
	Vitvi11g01208	*VviAHA2*	0.12	-0.09	0.02	0.54
	Vitvi10g01358	*VviIRT1*	2.50	4.80	1.40	1.20
Fe transport	*Vitvi08g02084*	*VviIREG3*	0.20	0.50	0.30	0.60
	Vitvi10g00247	*VviOPT3*	0.41	0.09	1.38	1.05
	Vitvi01g00512	*VviVIT1*	-1.00	-0.08	0.50	-0.80
	Vitvi14g01520	*VviYSL6*	0.00	0.26	0.30	0.56
	Vitvi18g00242	*VviNRAMP1*	-0.44	-0.66	0.63	0.79
	Vitvi13g01734	*VviFRD3*	2.02	3.45	6.57	3.59
	Vitvi13g01095	*VviZIF1*	1.26	0.11	0.91	1.09
Fe regulation	*Vitvi13g01037*	*VvibHLH38/39*	1.70	**2.90**	3.10	1.20
	Vitvi13g01164	*VvibHLH38*	1.78	4.60	2.97	1.92
Fe storage	*Vitvi06g01761*	*VviFER1*	-1.06	-1.28	0.24	-0.23
Root development	*Vitvi06g01682*	*VviZAT11*	-0.13	1.00	0.12	0.62
	Vitvi03g01471	*VviSAUR*	0.00	4.47	2.83	5.17
	Vitvi03g01458	*VviSAUR66*	0.00	3.54	4.42	4.42
Organic acid metabolism	*Vitvi12g00185*	*VviPEPC3*	0.66	0.31	0.92	0.33
	Vitvi05g00736	*VviPPCK1*	0.67	**2.29**	0.30	1.05

To understand the changes leading to the differences in malate and citrate contents in root tips and exudates, we examined changes in the expression of genes involved in the TCA (tricarboxylic acid) cycle in roots (Figure 3.10). Overall, the fold changes were not large, and few of the changes were statistically significant. Furthermore, both rootstocks appeared to respond similarly to both treatments. The most noticeable changes were in genes coding for pyruvate dehydrogenase, aconitase, isocitrate dehydrogenase, α-ketoglutarate dehydrogenase, fumarase, and malate dehydrogenase. –Fe induced downregulation in both rootstocks, while +Fe+BIC induced upregulation. These changes were largest for α-ketoglutarate dehydrogenase and malate dehydrogenase, both enzymes that provide reducing equivalents for the cell in the form of NADH. The changes in gene expression could not be directly correlated with the changes in organic acids observed in

roots and root exudates; however, the accumulation of malate in roots exhibited a similar pattern of change, increasing significantly under bicarbonate treatment +Fe+BIC.

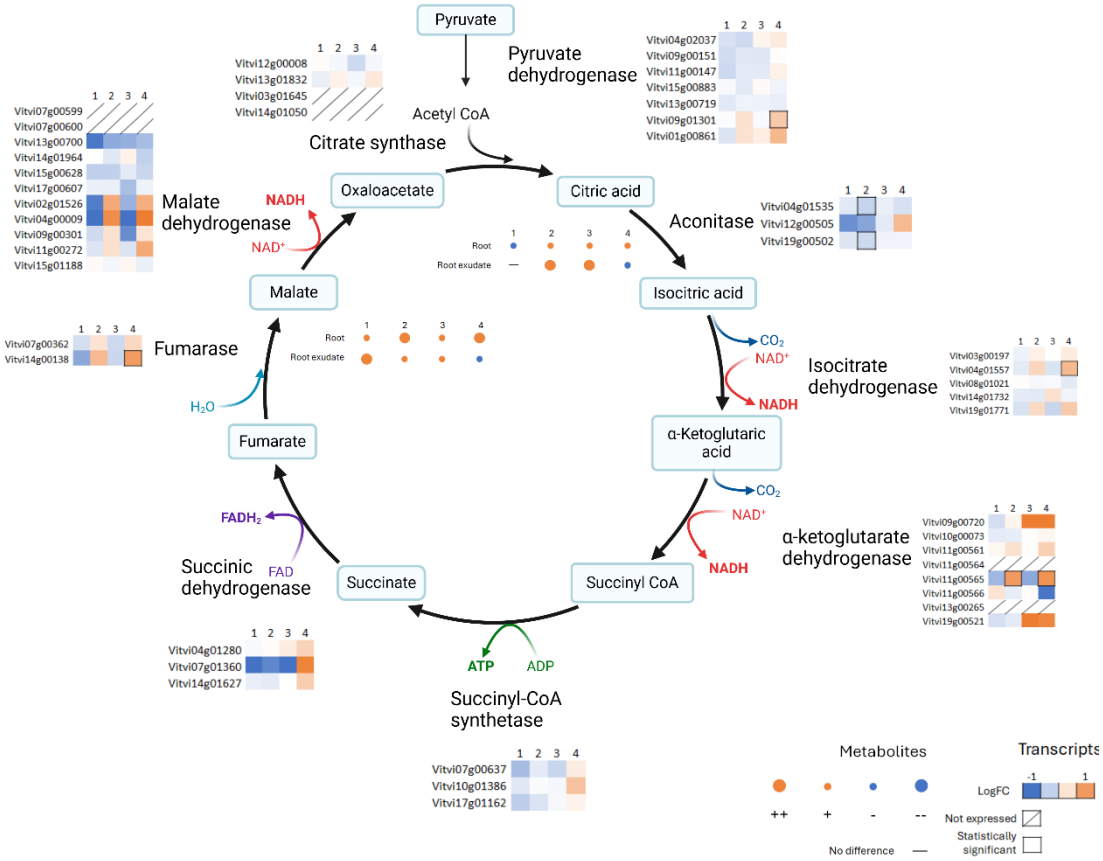


Figure 3.10: Changes in expression of genes involved in TCA cycle and abundance of organic acids in Fercal and 3309 C in iron deficiency.Treatments: 1: 3309 C direct Fe deficit vs control (–Fe vs +Fe); 2: 3309 C indirect Fe deficit vs control (+Fe+BIC vs +Fe); 3: Fercal direct Fe deficit vs control (–Fe vs +Fe); 4: Fercal indirect Fe deficit vs control (+Fe+BIC vs +Fe). Orange represents upregulation, blue represents downregulation. Squares represent gene Log_2FC values, circles represent metabolite abundance. / - not expressed; NS - not statistically significant. Republished from Lime-induced iron deficiency stimulates a stronger response in tolerant grapevine rootstocks compared to low iron availability, Khalil et al. 2025, Plant Stress, 16: 100841., 10.1016/j.stress.2025.100841, according to Creative Common Attribution ("CC BY") license.

3.4 '*Candidatus* Phytoplasma solani' Infection in cv. Zweigelt

The sequencing results of '*Candidatus* Phytoplasma solani' infection response experiments have been published in Dermastia et al. [150] and are summarized in this section. Raw reads obtained from sequencing are available at https://www.ebi.ac.uk/ena under the project accession PRJEB42777 and following accession numbers: ERS5673290, ERS5673291, ERS5673292, ERS5673293, ERS5673294, ERS5673295, ERS5673296,

ERS5673297, ERS5673298, ERS5673299, ERS5673300, ERS5673301, ERS5673302, ERS5673303, ERS5673304, ERS5673305, ERS5673306, ERS5673307, ERS5673308, ERS5673309, ERS5673310, ERS5673311. Normalized counts are available as supplementary material in the online article version at https://www.mdpi.com/article/10.3390/ijms22073531/s1.

High-throughput RNA-Seq was performed on leaf vein samples collected during the early and late growing seasons of 2017. RNA-Seq analysis yielded an average of 82,335,298 reads per sample, which were aligned to the grapevine reference genome. Of the 42,413 annotated genes, 24,279 were removed by filtering out those that did not have raw counts above 50 in at least four samples. Of the remaining 18,134 genes, 15,319 were significantly differentially expressed in at least one comparison, corresponding to 84% of the 18,134 expressed genes and 36% of the 42,413 annotated genes.

PCA of normalized log-transformed expression data clustered the samples clearly according to sanitary status and season (Figure 3.11). Growing season had the largest effect on sample clustering. It corresponded to the first principal component and explained 35.3% of sample variance. Sanitary status corresponded to the second principal component and explained 18.5% of sample variance.

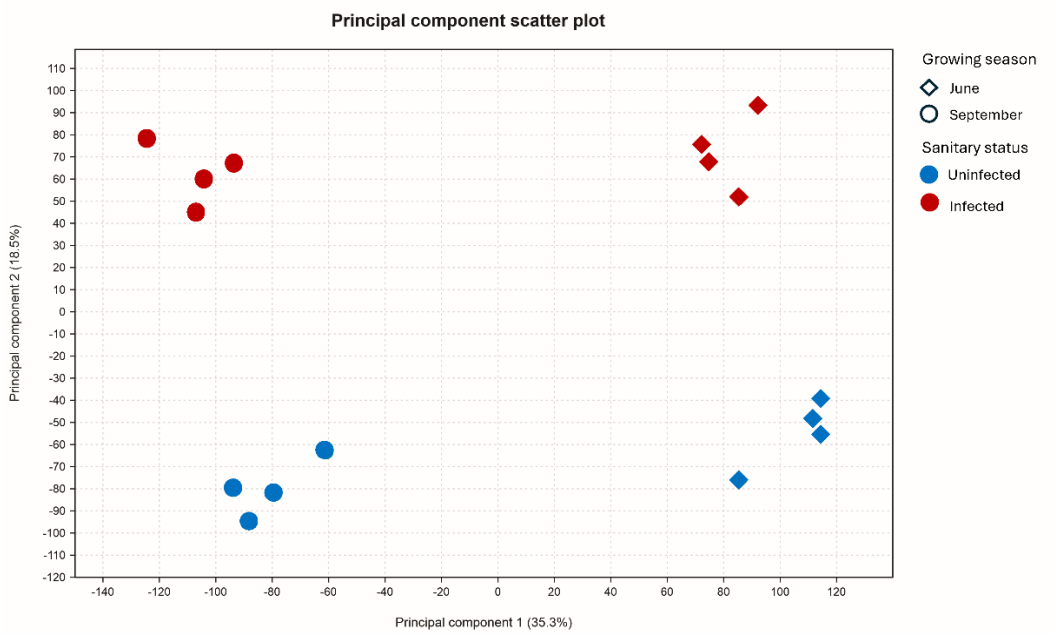


Figure 3.11: Principal component scatterplot of gene expression in '*Ca.* P. solani'-infected grapevine samples.

GSEA identified 261 changed biological processes according to GoMapMan gene ontology and 137 of those were statistically significant (FDR<0.25). Selected results are presented in Table 3.3 and the full table is presented in Supplementary Table 1.

Table 3.3: Subset of significantly enriched processes in '*Ca.* P. solani'-infected grapevine identified by GSEA. The samples are leaf-vein-enriched tissue collected in early (June) and late (September) growing season. Statistically significantly enriched (FDR<0.25) processes are marked with percent number and color. Positive enrichment is represented in red; negative enrichment is represented in blue. Blank cells represent processes with changes not reaching statistical significance.

Process	June	September
PHOTOSYNTHESIS	-70%	-72%
LIGHT REACTION	-67%	-82%
CALVIN CYCLE	-78%	-75%
SUCROSE DEGRADATION	54%	42%
STARCH DEGRADATION	-38%	
RAFFINOSE METABOLISM	-31%	-38%
FERMENTATION	48%	43%
TCA	53%	
MITOCHONDRIAL ELECTRON TRANSPORT AND ATP SYNTHESIS	53%	
CELL WALL	38%	35%
AMINO ACID METABOLISM	41%	
ISOPRENOID METABOLISM		-50%
PHENYLPROPANOID METABOLISM	44%	25%
FLAVONOID METABOLISM	38%	27%
JASMONIC ACID METABOLISM		32%
BIOTIC STRESS	27%	
BIOTIC STRESS RECEPTORS	25%	25%
PR PROTEINS	49%	49%
REDOX		-33%
TRANSCRIPTION REGULATION		-31%
CHLOROPLAST RIBOSOME SYNTHESIS	-67%	-65%
PLANT RIBOSOME SYNTHESIS	76%	-76%
PROTEIN DEGRADATION	85%	
LRR RECEPTOR KINASES	63%	

Gene expression of several biological processes responded strongly to infection with '*Ca.* P. solani' early in the growing season, before symptom development. Both in the early and late growing season, photosynthesis, raffinose metabolism, transport regulation and chloroplast ribosome synthesis were downregulated, and sucrose degradation, fermentation, cell wall-related processes, phenylpropanoid and flavonoid metabolism and biotic stress response were all upregulated. Early season responses were characterized by upregulation of tricarboxylic acid cycle, mitochondrial electron transport, amino acid metabolism, biotic

stress response, LRR receptor kinases and protein degradation. Downregulation of redox processes and isoprenoids was detected in the late growing season, along with an upregulation of jasmonic acid-related processes.

Processes with the largest proportions of enriched genes were associated with protein amino acid activation; synthesis of ribosomal proteins; and synthesis initiation, elongation, targeting, degradation, folding, glycosylation, assembly, and cofactor ligation. Early in the growing season, the majority of genes in these processes were up-regulated; late in the growing season, the majority were down-regulated. One notable exception was genes related to chloroplast ribosome synthesis, which were already strongly down-regulated early in the growing season.

Based on the GSEA results, we selected several processes for closer examination and highlighted genes with significant changes in expression; these are presented in Table 3.4. We observed a predominant downregulation of glycolysis- and sucrose-synthesis-related genes. Genes involved in starch synthesis were also mostly down-regulated, with the exception of an ADP-glucose pyrophosphorylase (*Vitvi08g01815*) and an α-amylase-like gene (*Vitvi03g01571*). Ascorbate peroxidases and dehydroascorbate reductase were mostly downregulated. Laccase expression trended toward up-regulation early in the season and down-regulation late in the season, while genes involved in flavonoid synthesis were strongly up-regulated in both periods. Genes involved in jasmonic acid synthesis (lipoxygenase, *Vitvi06g00155*; 12-oxophytodienoate reductase, *Vitvi18g02138*), as well as several jasmonic acid response marker genes, were up-regulated. Finally, although several salicylic acid response marker genes (*PR1*s) were up-regulated, expression of the *NPR1 (Vitvi10g01335)* receptor remained largely unchanged, and expression of the SA hydroxylase *DMR6 (Vitvi16g01336)* was strongly induced.

Table 3.4: Expression changes of selected genes from '*Ca.* P. solani'-infected grapevine. Gene expression change is represented as Log_2FC values comparing infected and uninfected samples in early (June) and late (September) growing season. Orange represents upregulation, green represents downregulation. Bolded values are statistically significant ($p < 0.05$)

Process	Gene ID	Gene name	June	September
Starch	*Vitvi08g01815*	*ADP-glucose-pyrophosphorylase*	**0.51**	**0.49**
	Vitvi03g00500	*alpha amylase like*	**-2.08**	-0.39
	Vitvi03g01571	*alpha amylase like*	**1.78**	0.38
	Vitvi01g00932	*alpha amylase*	**-0.75**	-0.41
	Vitvi10g00739	*starch synthase*	**-0.86**	**-1.12**
Sucrose	*Vitvi04g00831*	*sucrose synthase*	**2.12**	**2.20**
Glycolysis	*Vitvi01g00360*	*aldolase*	**0.67**	**1.10**
Lignification	*Vitvi18g01438*	*laccase*	**2.77**	-0.96
	Vitvi18g02906	*laccase*	1.96	**-2.27**
	Vitvi08g01031	*laccase*	-1.45	**-2.52**
Flavonoid	*Vitvi02g00435*	*leucoanthocyanidin reductase*	**2.96**	**4.05**
synthesis	*Vitvi13g00225*	*chalcone isomerase*	**2.10**	**2.58**
	Vitvi10g02185	*dihydroflavonol 4-reductase*	**1.68**	**2.37**
	Vitvi18g01119	*flavanone 3-hydroxylase*	**1.58**	**1.67**
	Vitvi01g00234	*isoflavone reductase*	**3.20**	**4.66**
	Vitvi18g02538	*flavonol synthase*	1.62	**3.41**
SA response	*Vitvi16g01336*	*DMR6*	**5.26**	**3.33**
	Vitvi04g02118	*SAMT*	**3.23**	1.68
	Vitvi10g01335	*NPR1*	**0.05**	**-0.55**
	Vitvi03g01651	*PR1*	**3.03**	1.03
	Vitvi03g00752	*PR1*	**5.97**	**6.39**
	Vitvi07g01266	*PR1*	**-2.00**	-2.07
	Vitvi02g00391	*PR5*	**5.25**	**3.51**
	Vitvi04g01471	*PR5*	**-1.20**	**-1.39**
	Vitvi13g00330	*PR5*	**2.37**	**1.42**
JA response	*Vitvi06g00155*	*LOX*	**1.33**	**4.62**
	Vitvi18g00886	*ALLENE OXIDASE*	-0.39	**1.68**
	Vitvi18g02762	*JAMT*	**-1.93**	**-1.82**
	Vitvi18g02138	*12-oxophytodienoate reductase*	**5.37**	**1.89**
	Vitvi15g01035	*chitinase A*	**3.71**	**2.12**
Redox	*Vitvi04g02166*	*ascorbate peroxidase*	**2.00**	**2.51**
	Vitvi18g00445	*ascorbate peroxidase*	**-1.28**	**-1.64**
	Vitvi13g00241	*dehydroascorbate reductase*	0.05	**0.59**

3.5 DNA-Free Genome Editing of *DMR6* Genes in cv. Chardonnay and cv. Zweigelt

3.5.1 Embryogenic callus induction

Embryogenic callus was induced from stamens and pistils of Chardonnay and Zweigelt flowers obtained as described in Methods Section 2.4.1. Chardonnay explants generally produced beige or browning callus (Figure 3.12), while Zweigelt callus commonly presented pink or purple tissue (Figure 3.13). The proembryogenic masses were very similar in both cultivars, consisting of compact, white or light-yellow globular tissue.

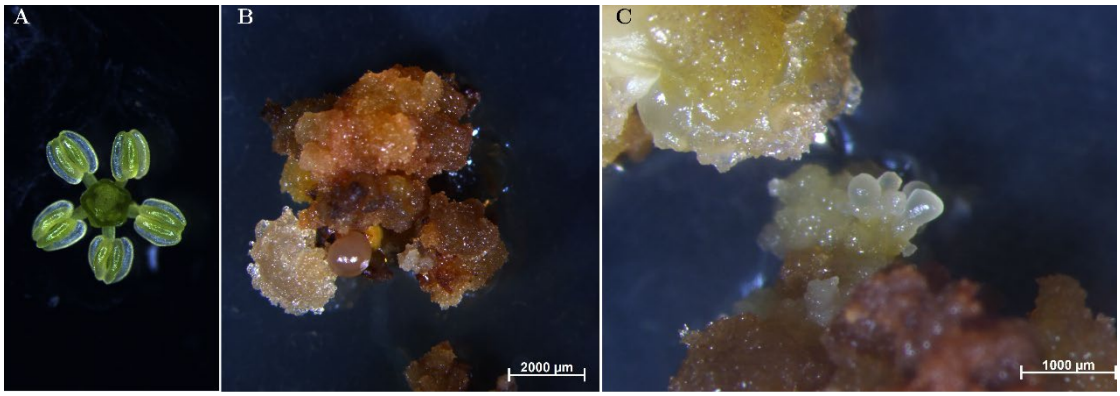


Figure 3.12: Chardonnay embryogenic callus induction.(A) Stamens and pistil; (B) Non-embryogenic callus; (C) Embryogenic callus.

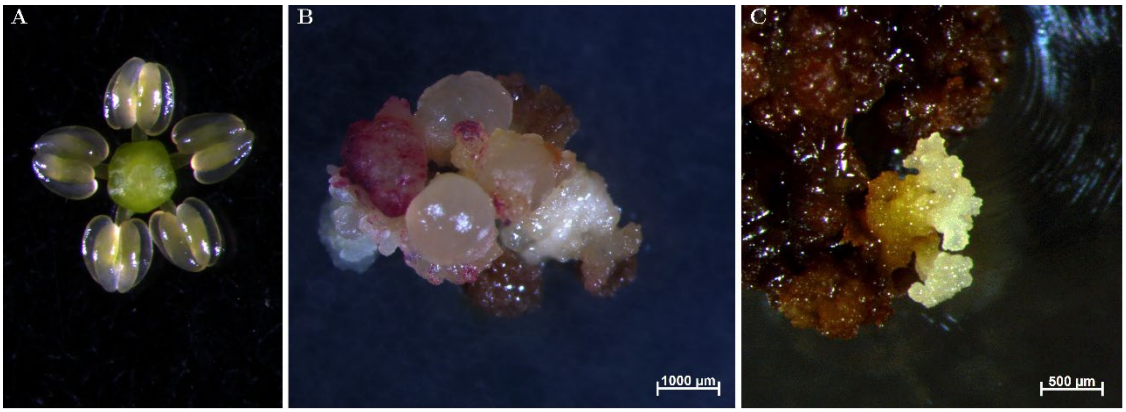


Figure 3.13: Zweigelt embryogenic callus induction.(A) Stamens and pistil; (B) Non-embryogenic callus; (C) Embryogenic callus.

3.5.2 Protoplast isolation and cultivation

Protoplasts were isolated from embryogenic callus of Chardonnay and Zweigelt cultivars in three separate extractions. The average protoplast yield was 3.6×10^6 cells per extraction and did not vary considerably between replicates. A total of 32 different treatments were performed on Chardonnay and 22 on Zweigelt (Table 2.2). Protoplasts were transfected on the same day of isolation, with positive and negative controls included

in each individual experiment. This brought the total number of observations to 36 for Chardonnay and 26 for Zweigelt.

Three days after transfection, GFP fluorescence was detected in protoplasts from positive control treatments (Figure 3.14). All but one Zweigelt positive transfection control was subsequently discarded. The remaining protoplasts were cultivated on solid medium for six months and monitored for embryo development. Embryos that formed were transferred to germination medium. After the negative transfection controls developed embryos, they were discarded as well, excepting two Zweigelt replicates. Of the 29 Chardonnay cultures retained, only 15 developed embryos, while 14 out of the 24 retained Zweigelt cultures produced embryos. Notably, no mock treatments were regenerated from Chardonnay. The different steps of the regeneration process are shown in Figure 3.15.

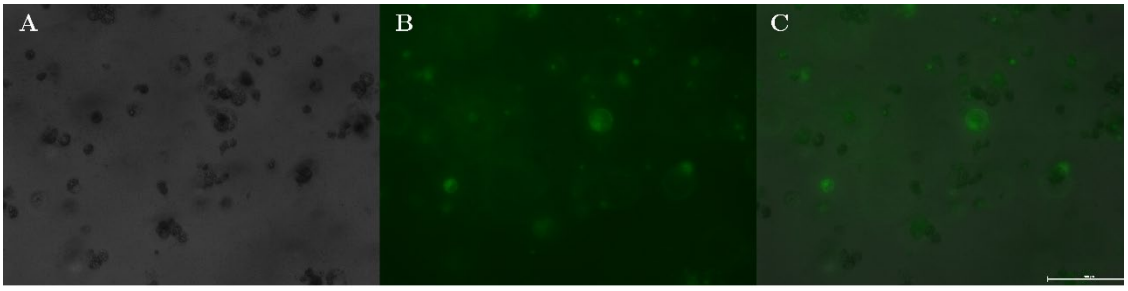


Figure 3.14: Protoplasts in solid culture expressing GFP. (A) Brightfield; (B) GFP; (C) Merged image. Scale bar represents 100 µm.

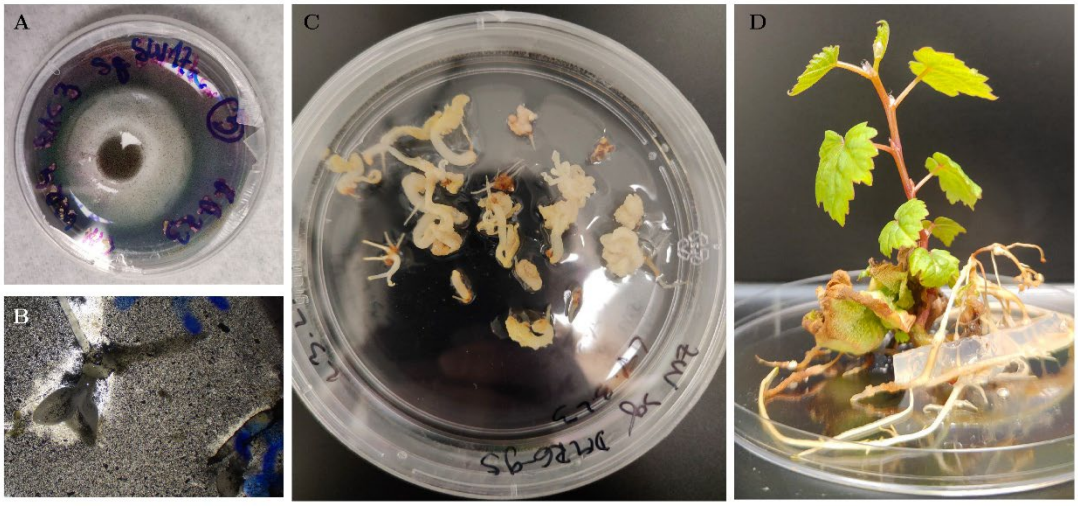


Figure 3.15: Plant regeneration from protoplasts. (A) Protoplasts in solid culture; (B) Embryo in solid culture; (C) Germinated embryos; (D) Regenerated plant.

3.5.3 Plant regeneration

A total of 10,704 embryos developed and were transferred for germination: 5,298 from Chardonnay and 5,406 from Zweigelt. During germination, 1,587 embryos were discarded due to tissue browning and mortality. Germinated embryos were transferred to shooting medium supplemented with or without BAP and incubated in growth chambers until shoots developed. Overall, 538 embryos were regenerated to plantlets. The effects of genotype and BAP treatment on regeneration efficiency are presented in Table 3.5.

In the absence of BAP, Zweigelt showed considerably higher regeneration efficiency (7.2%) compared to Chardonnay (1.3%). BAP treatment doubled the regeneration efficiency in Zweigelt but had minimal effect on Chardonnay.

Table 3.5: BAP effect on plant germination and regeneration in Chardonnay and Zweigelt. Count of germinated embryos and regenerated plants are separated by genotype and the presence (C2D+B) or absence (C2D) of BAP in the shooting medium.

Shooting medium	Cultivar	Germinated embryos	Regenerated plants	Regeneration efficiency (%)
C2D	Zweigelt	3189	229	7.2
	Chardonnay	2884	38	1.3
	Combined	6073	267	4.4
C2D+B	Zweigelt	1666	237	14.2
	Chardonnay	1369	25	1.8
	Combined	3035	262	8.6
Unrecorded	Zweigelt	5	5	
	Chardonnay	4	4	
	Combined	9	9	
Not transferred to shooting medium	Zweigelt	546	0	
	Chardonnay	1041	0	
	Combined	1587	0	

We next evaluated how genotype impacts the number of germinated embryos, number of regenerated plants, and regeneration efficiency. In both Chardonnay (N=15) and Zweigelt (N=14), there was large variability in the number of germinated embryos between individual treatment replicates, ranging from 1 to 2,585 for the former and from 3 to 2014 for the latter. The average number of germinated embryos obtained per sample was similar between the two genotypes. However, the number of regenerated plants and the regeneration efficiency differed considerably between genotypes (Figure 3.16). Chardonnay samples regenerated 4.5 plants on average, with an average regeneration efficiency of 1.9% (Table 3.6), while Zweigelt samples regenerated 33.6 plants on average, with an average regeneration efficiency of 20.6% (Table 3.7). We evaluated the statistical significance of these observations using the Mann-Whitney U test. Since the negative and positive controls were discarded for Chardonnay before the germination step, we excluded the negative transformation control Zweigelt samples from this comparison and included the positive transfection control to the mock group, bringing the final sample number for the Mann-Whitney U test to 15 in Chardonnay and 12 in Zweigelt. The number of germinated embryos was confirmed not to differ significantly between genotypes ($p=0.467$), whereas the differences in the number of regenerated plants ($p=0.001$) and in regeneration efficiency ($p=0.001$) were both statistically significant.

Table 3.6: Embryo germination and plant regeneration in Chardonnay.

Treatment	Germinated embryos	Regenerated plants	Regeneration efficiency (%)
sgDMR6-1_1	53	0	0.0
sgDMR6-1_2	66	1	1.5
sgDMR6-1_3	299	3	1.0
sgDMR6-1_5	140	7	5.0
sgDMR6-1_47	126	0	0.0
sgDMR6-1_193	33	0	0.0
sgDLO1_1	55	5	9.1
sgDLO1_2	1815	18	1.0
sgDLO1_3	34	0	0.0
sgDLO1_4	1	0	0.0
sgDLO1_5	1	0	0.0
sgDMR6-1_1+sgDLO1_3	2585	25	1.0
sgDMR6-1_1+sgDLO1_2	6	0	0.0
sgDMR6-1_1+sgDLO1_4	4	0	0.0
sgDMR6-1-47+sgDLO1_1	80	8	10.0
Mean	353.2	4.5	1.9
Median	55	0	0
Standard deviation	741.6	7.3	3.3

Table 3.7: Embryo germination and plant regeneration in Zweigelt.

Treatment	Germinated embryos	Regenerated plants	Regeneration efficiency (%)
sgDMR6-1_1	57	18	31.6
sgDMR6-1_2	610	64	10.5
sgDMR6-1_3	1325	87	6.6
sgDMR6-1_5	10	2	20.0
sgDMR6-1_95	932	48	5.2
sgDLO1_1	2014	137	6.8
sgDLO1_2	3	0	0.0
sgDLO1_3	11	0	0.0
mock sgDMR6-1_1	200	49	24.5
mock sgDMR6-1_2	50	12	24.0
mock sgDMR6-1_47	57	13	22.8
Negative control 1	113	30	26.5
Negative control 2	3	2	66.7
Positive control	21	9	42.9
Mean	386.1	33.6	20.6
Median	57.0	15.5	21.4
Standard deviation	599.3	38.7	17.7

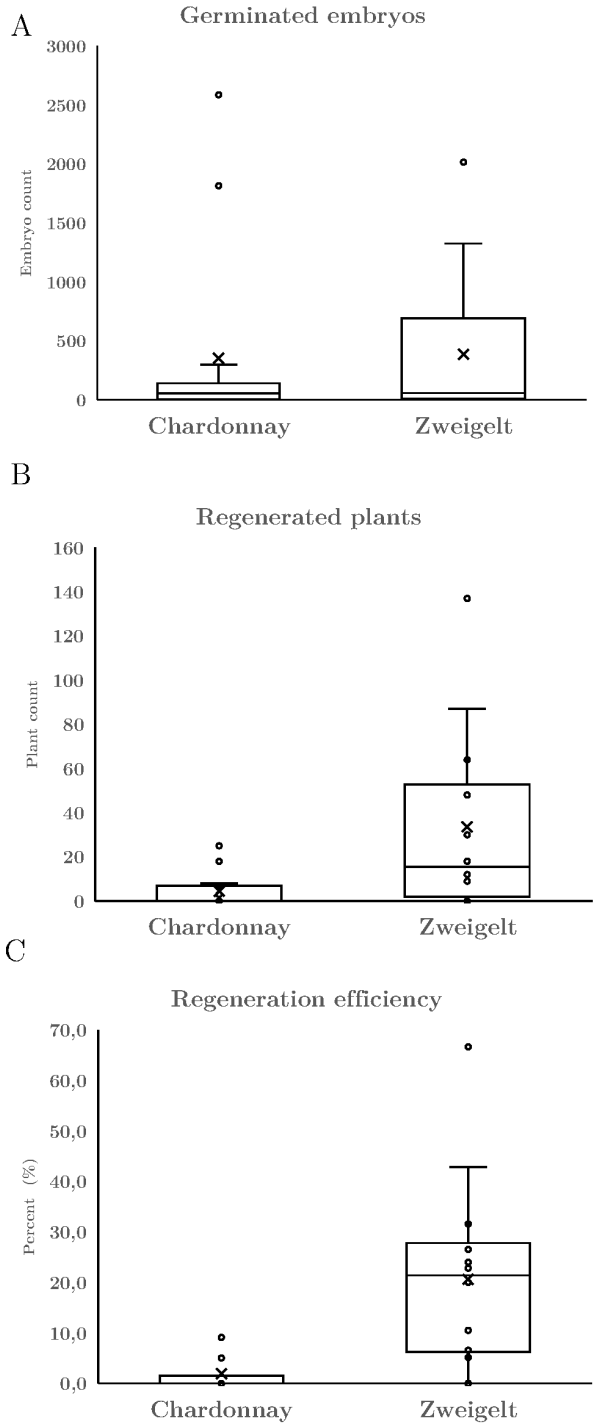


Figure 3.16: Boxplots of embryo germination (A), plant regeneration (B) and regeneration efficiency (C) in Chardonnay and Zweigelt.

Because mock treatments were successfully regenerated in Zweigelt samples, we were able to evaluate the effects of different treatment types: RNP (N=8), mock (N=4), and negative control (N=2). The average number of germinated embryos differed substantially between treatments, with mock and negative control samples germinating an order of magnitude fewer embryos than RNP samples (Table 3.8, Figure 3.17). However, these differences were less pronounced for the average number of regenerated plants and

regeneration efficiency. The average number of regenerated plants was highest in RNP samples, and less than half as high in the mock and negative control samples. RNP samples had the lowest average regeneration efficiency (10%). Although the differences between treatments were noticeable, the small sample sizes for the mock and negative control treatments, combined with high variability, precluded these comparisons from reaching statistical significance. Negative transfection controls are shown for comparison but were excluded from the Mann-Whitney U test.

Table 3.8: Effect of transfection treatment type on germination, regeneration, and regeneration efficiency in Zweigelt. The mock group includes the positive transfection control.

		Germinated embryos	Regenerated plants	Regeneration efficiency (%)
RNP	mean	620.3	44.5	10.1
	median	333.5	33.0	6.7
	standard deviation	705.2	46.4	10.1
Mock	mean	82.0	20.8	28.5
	median	53.5	12.5	24.3
	standard deviation	69.5	16.4	8.3
Negative control	mean	58.0	16.0	46.6
	median	58.0	16.0	46.6
	standard deviation	55.0	14.0	20.1

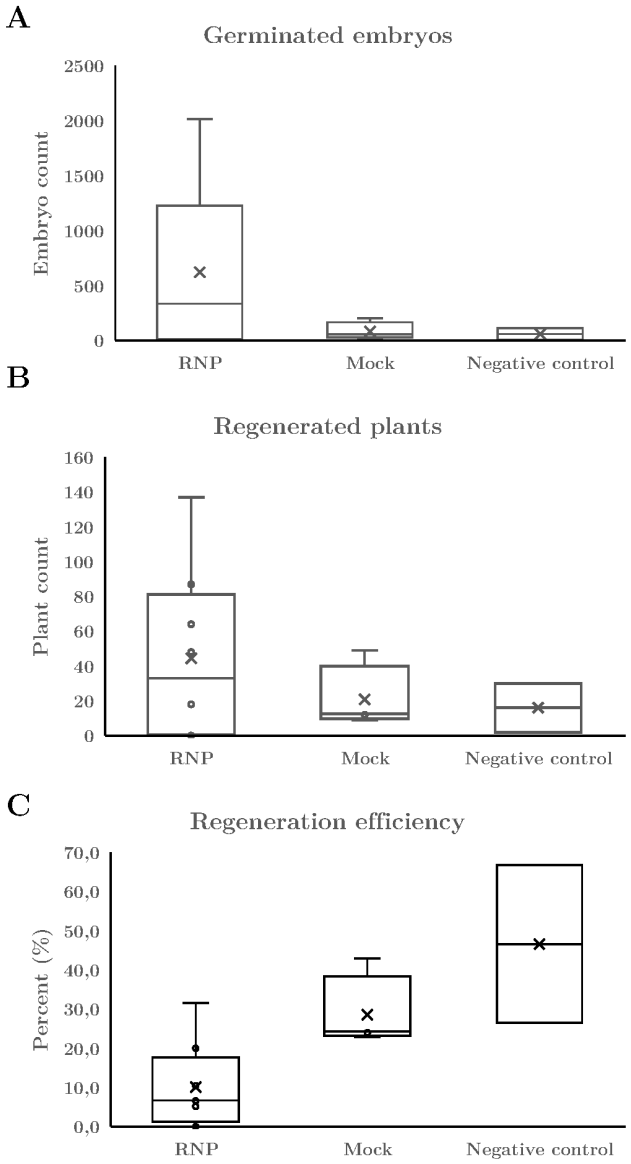


Figure 3.17: Boxplots of transfection treatment effects on embryo germination (A), plant regeneration (B) and regeneration efficiency (C) in Zweigelt.

3.5.4 Genome editing confirmation

All successfully regenerated plants of both genotypes were checked for editing success. First, the segments corresponding to the target regions of the RNP treatments were amplified and sequenced. A characteristic phenomenon was observed in positive samples: Sanger chromatogram quality decreased three nucleotides upstream of the PAM site, consistent with the Cas9 predicted cleavage site (Figure 3.18). This decrease in quality indicates diverging sequences between the two chromosomes, likely due to the occurrence of indel mutations. In total, seven edited lines were confirmed for Chardonnay and one for Zweigelt. The target treatments for each successfully edited line are listed in Table 3.9. No edits were detected in the mock-treated lines.



Figure 3.18: Example alignment of sequencing chromatograms of a successfully edited line. The gRNA position and its orientation are marked with a purple arrow. The PAM region is marked with a green box on the original sequence.

Table 3.9: A list of successfully edited recovered lines and their corresponding editing targets.

Line name	Editing targets
Chardonnay L11	sgRNA_DMR6-1_2
Chardonnay L22	sgRNA_DMR6-1_5
Chardonnay L23	sgRNA_DMR6-1_5
Chardonnay L24	sgRNA_DLO1_2
Chardonnay L25	sgRNA_DLO1_2
Chardonnay L44	sgRNA_DMR6-1_1+sgRNA_DLO1_3
Chardonnay L50	sgRNA_DMR6-1_1+sgRNA_DLO1_3
Zweigelt L308	sgRNA_DMR6-1_2

To resolve the sequences of gene edits on individual chromosomes, the corresponding amplicons were cloned into *E. coli* plasmids, and individual colonies were selected for plasmid isolation and sequencing. Representative results for each mutation type are shown in Figure 3.19. Plasmid sequencing showed that all positive lines carried one edited and one non-edited allele, and that all edits detected within a given line were identical.

Successfully edited lines targeted with sgRNA_DMR6-1_2 all had an adenine insertion at position 143 in the first exon of *DMR6-1*, resulting in a frameshift and a premature stop codon. Lines targeted with sgRNA_DMR6-1_5 had a 3-bp deletion at positions 2891–2893, resulting in the loss of a cysteine residue in the third exon of *DMR6-1*. In Chardonnay, a silent natural variant (T/C SNP) is also present at position 2893. The lines targeted with sgRNA_DLO1_2 had an adenine insertion after position 132 in the first

exon of *DLO1*, causing a frameshift and a premature stop codon. Finally, in lines treated with the sgRNA_DMR6-1_1 + sgRNA_DLO1_3 combination, *DMR6-1* was successfully edited, producing the same result as sgRNA_DMR6-1_2, while no edits were observed at *DLO1*.

The edited lines were grown in tissue culture and eventually transferred into soil. No phenotypic differences could be observed between edited lines and the unedited Chardonnay and Zweigelt controls.

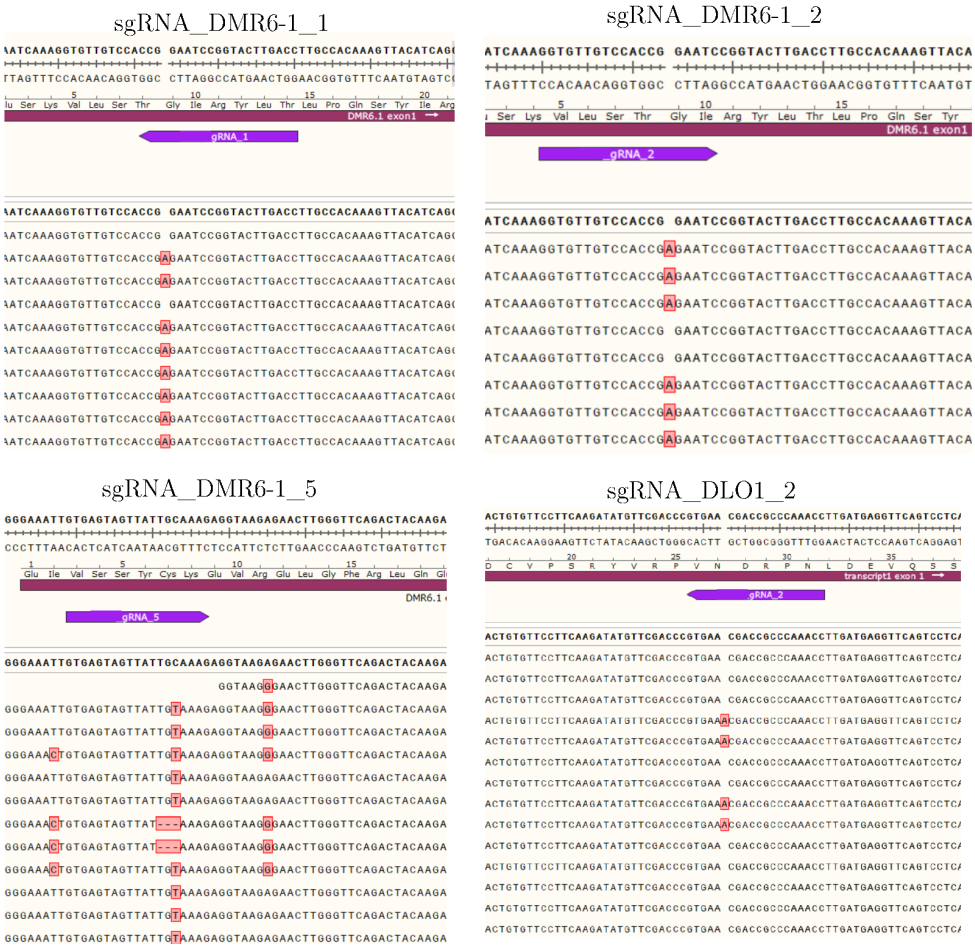


Figure 3.19: Representative results of each successful mutation detected in the edited lines. The gRNA positions and their orientation are marked with a purple arrow.

Chapter 4

Discussion

4.1 Water Deficit Induces a Metabolic Shift and Transcriptional Reprogramming

Grapevine adopts several strategies to cope with water shortage, ranging from limited growth to stomatal closure and, ultimately, leaf shedding [173, 174, 175, 176]. Nonetheless, large differences in water stress tolerance occur among grapevine genotypes under field conditions. Moreover, the impact of water scarcity on grapevine growth is expected to intensify with climate change, affecting viticultural practices such as cultivar choice and the selection of locations suited to viticulture [1, 177].

Reduced water availability affects plant physiology through both morphological and transcriptional modifications [178, 179, 180]. Deloire et al. [181] indicated that stem water potential (Ψ_s) values below -1.4 MPa are critical for grape production, as they can cause physiological damage and atypical berry maturation; for white or more sensitive varieties, this threshold is raised to -1.2 MPa to preserve the aromatic profile. For these reasons, our water deficit treatment consisted of non-irrigated plots, with water added only when the above-mentioned thresholds were reached. As expected, water stress caused a consistent reduction in Ψ_s, demonstrating similar trends in both cultivars.

Limited knowledge exists about the water stress tolerance of newly developed grapevine hybrids resistant to biotic stresses, derived from only a few recent studies. Braidotti et al. [152] investigated how two fungus-resistant varieties (Sauvignon Kretos and Merlot Kanthus) responded to water deficits and found that, under moderate stress, each cultivar exhibited notable differences in stomatal conductance that were more cultivar- than stress-dependent. The same was true for the leaf metabolite profile. By measuring ABA and the expression of genes involved in its perception, they showed that ABA was water deficit-responsive, but each genotype displayed different levels of ABA sensitivity. In contrast to the findings of this study, they observed an increase in salicylic and jasmonic acid. de Almeida et al. [182] also demonstrated that water deficit responses are highly cultivar-specific. They measured indicators of primary metabolism and thiol precursors in berries of Syrah and six different disease-resistant varieties, showing that water deficit negatively affected primary metabolism and thiol precursor accumulation in a similar manner across most genotypes. The exception was 3159-B, which preferentially accumulated thiol precursors under water deficit. In this study, we set out to broaden the knowledge of how disease-resistant varieties respond to water deficit by capturing a bigger picture of the transcriptome and metabolome state of stressed plants.

We used both transcriptomic and metabolomic approaches to unveil the molecular pathways of the water deficit responses in two disease-resistant grapevine varieties, Fleurtai and Cabernet Volos, which had not previously been investigated for this trait. The factorial

design of the analyses implemented here took advantage of the availability of gene expression, metabolite accumulation, and Ψ_s data from the same vines. This approach identified three response types: genes and metabolites shared between both genotypes (Type 1), and genotype-specific responses unique to Cabernet Volos (Type 2) or Fleurtai (Type 3), discussed below.

4.1.1 Shared responses to water deficit (Type 1)

In Type 1, where transcript and metabolite accumulation patterns behaved the same in both genotypes, we identified 19 metabolites and 689 genes as important in the grapevine response to water stress. It is not surprising that this group included several upregulated sugars and amino acids, as well as transcripts involved in carbohydrate metabolism, cell wall synthesis, modification and degradation, lipid metabolism, amino acid metabolism, secondary metabolism, and hormone metabolism, as it is well known that resource reallocation is part of the plant's strategy to adapt to water stress [183]. Furthermore, the highest Pearson correlation values between transcripts and metabolites were found for raffinose family oligosaccharides, a group of sugars involved in the response to drought and desiccation in different plant organs [184, 185, 186]. Several studies in grapevine have shown that these metabolic pathways change in response to drought stress [187, 188, 189, 190].

It is very likely that conserved metabolic pathways related to central metabolism — including sugars and their derivatives, and amino and organic acids involved in major C-N and energy metabolism, as measured by the GC-MS protocol used — respond similarly between species, and even more so between varieties [191]. Urano et al. [192] showed metabolite accumulation in *Arabidopsis* leaves exposed to water stress that resembles the results found in the current study, including the accumulation of raffinose family oligosaccharides, GABA, and proline. Urano et al. proposed an ABA-dependent transcriptional regulation of metabolite accumulation in response to drought, which is consistent with the many upregulated ABA-related genes found in our data. This universal metabolic response of central metabolism and the accumulation of metabolites under stress is, at least in part, a result of reduced growth, i.e., an accumulation driven by decreased consumption of C-N backbones [193].

Notably, both Fleurtai and Cabernet Volos showed modulation of genes related to osmotic stress response (galactinol and raffinose synthesis, GABA and proline metabolism, osmotins), to abscisic acid hormone synthesis or ABA-inducible genes (i.e., *HVA22*), and to the transport of ABA and amino acids, confirming the common tissue-specific adaptation mechanisms acting in the primary response to drought stress [189]. Metabolomic analysis further revealed an accumulation of osmoprotectants (i.e., sugars and amino acids) in the drought stress response of both genotypes, in agreement with previous reports for grapevine and other plant species [193, 194, 195]. Compatible solutes such as sugar alcohols (e.g., galactinol) and amino acids function in osmotic adjustment, preserving cell turgor under stress conditions. Proline has a well-known function as a compatible solute, and increasing its accumulation through overexpression of its main biosynthesis gene (*P5CR*) has been shown to increase drought resistance in both transgenic Arabidopsis and grapevine [196, 197]. Several studies have reported the increased importance of both proline and ABA in the grapevine response to combined heat and drought stress [198, 199]. Moreover, these compatible solutes, especially galactinol and proline, can also act as reactive oxygen species (ROS) scavengers [200]. Similarly, GABA, a non-protein amino acid, accumulates in plants under stress to mitigate drought-depressed cell elongation and wax biosynthesis [200, 201, 202].

Members of the bZIP, MYB, and NAC transcription factor families were found to be upregulated in both Fleurtai and Cabernet Volos in this study, confirming their role in the regulation of plant drought responses [203]. Interestingly, among them we found *VviNAC26* (*Vitvi01g01038*), a transcription factor that has been cloned from *V. amurensis* (a cold- and drought-hardy *Vitis* species) and shown to improve drought tolerance in transgenic Arabidopsis [204]. The same gene was upregulated in both root and shoot in response to water deficit in *V. riparia* [205].

Downregulated transcripts common to both genotypes (Type 1) were mostly related to cell wall degradation and modification. Several studies are consistent with this finding, reporting that cellulose biosynthesis can be altered in response to water deficit, as shown by declining synthesis and a clear shift in cell wall composition in grape leaves under drought conditions [206, 207].

In addition, several biotic stress-associated genes, mostly PR proteins (with PR5 and PR5-like receptor kinases being the most represented), showed downregulation in response to water deficit. Haider et al. [195] reported similar results, finding that, in contrast to heat shock proteins, most PR proteins showed downregulation in grapevine leaves under drought stress, suggesting that water deficit has a negative effect on the defense response. Increasing evidence suggests that leucine-rich repeat kinases could regulate abiotic and biotic stress responses and play a major role in integrating environmental and plant hormone signaling, with variable regulation depending on genotype and timing [207, 208]. In our study, we observed some upregulation of these kinases; however, downregulation predominated, indicating a trade-off between abiotic and biotic stress responses.

4.1.2 Cabernet Volos-specific responses (Type 2)

Downregulation of biotic defense-related genes was a marked feature of the Type 2 gene category, which contains genes responsive in Cabernet Volos but not in Fleurtai. Out of the 63 genes found in Type 2, 24 were annotated as LRR and PR5-like receptor kinases. Most of the other genes in this category were downregulated as well, with one particularly interesting exception being an upregulated GDSL-motif lipase (*Vitvi09g00038*). The same gene was identified by transcriptomic network analyses of leaf dehydration responses in Cabernet Sauvignon, Riparia Gloire, and Ramsey genotypes [209]. Although the exact role of GDSL lipases has not been clarified in grapevine, several studies link them to plant stress adaptation and leaf water retention, as they are involved in cutin biosynthesis [210, 211].

4.1.3 Fleurtai-specific responses (Type 3)

Fleurtai-specific transcriptomic and metabolomic changes in response to water stress (41 Type 3 genes) occurred mainly in hormone signal transduction and secondary metabolism. Cabernet Volos had a high but constant level of caffeoylquinate regardless of treatment. At the same time, Fleurtai increased its accumulation of caffeoylquinate in response to water deficit, but never reached the levels recorded in Cabernet Volos. Caffeoylquinate is a plant phenolic compound believed to be an intermediate in lignin biosynthesis. Due to its antioxidative properties, it is an important protective molecule for plants under many different environmental stresses, including low temperature, drought, and high light [212]. Hochberg et al. [191] showed that caffeoylquinate was specifically associated with drought in the Syrah metabolic network; in conjunction, an accumulation of suberin in the vascular bundles was also reported. Similarly, in this study, the phenylpropanoid pathway was strongly induced, suggesting that vascular remodeling may be a large part of the adaptation strategy in both Fleurtai and Cabernet Volos. Moreover, in both genotypes, strong

upregulation of *CYP98A3* (*Vitvi06g00605*), involved in precursor synthesis for lignin and related compounds [213], was observed.

The accumulation of flavonoid compounds in response to water deficit is a commonly noted phenomenon, although it appears to depend strongly on stress duration and plant developmental phase. For example, Tan et al. [199] found that Cabernet Sauvignon exposed to a combination of heat and drought stress showed transcript-level responses very similar to those observed in our experiments; however, they reported a marked decrease in the expression of genes related to the phenylpropanoid synthesis pathway. This could be related to the duration of stress, as well as to the use of self-rooted, one-year-old cuttings in their experiments.

We found several terpene synthase-encoding genes that were uniquely upregulated in Fleurtai, which is not surprising given the role of terpenes in mitigating drought stress in plants [214]. This is consistent with the idea that, in white cultivars, terpenes and carotenoids take over the protective function that anthocyanins play in red varieties during the stress response.

A GCR2-like 1-encoding gene (*Vitvi00g02022*) was also upregulated in Fleurtai. This gene is involved in the ABA signaling pathway, central to drought stress perception, and has a recognized role in drought tolerance [215, 216, 217, 218]. Although belonging to the Type 1 category, *CYP707A4* (*Vitvi18g00792*), crucial for ABA catabolism [219], exhibited a much higher degree of induction in Fleurtai. Gaiotti et al. [220] reported that Moscato Giallo controlled its stomata more tightly in response to drought and had higher ABA sensitivity compared to more anisohydric varieties.

4.2 Tolerant Rootstocks Limit Major Salinity-Induced Transcriptomic Disturbances in the Scion

The effects of water quality and rootstock on the transcriptomics of cv. Tempranillo vines were assessed indirectly, as all determinations were carried out on the scion rather than on the rootstock, which is the barrier against soil salinity. However, the scion cultivar is the genotype that ultimately bears and ripens the fruit, thereby conferring economic value on the crop [34]. Thus, the scion is considered an integrator of the effects induced by the rootstock. This is important when interpreting the results of the transcriptome analyses, because although two *Vitis* spp. genotypes were involved in a biological replicate, only *Vitis vinifera* was directly evaluated. Most grapevine transcriptomic responses reported in the literature have been assessed on a single genotype, i.e., either directly in own-rooted *Vitis vinifera* [43, 198, 221, 222] or in the rootstock without grafting [63, 68, 78, 223, 224, 225, 226]. Where both the scion and the rootstock have been studied together, this has been done under highly controlled conditions [222, 227, 228, 229], i.e., not under real field-grown conditions.

The physiological responses in leaves and berries (measured by our collaborators and described in more detail in Buesa et al. [147]) revealed several differences between the rootstock genotypes. As already described elsewhere [68, 230], 1103 Paulsen had the highest capacity to exclude Cl^- from leaves among the tested rootstocks. However, the higher Cl^- concentration in M1- and M4-rooted samples did not cause any significant changes in gene expression in either leaves or berry skins. Henderson et al. [63] found that the salinity tolerance of different rootstocks originates from constitutively higher expression of the relevant transporters, rather than from a stress-induced response. Since this study measured only the scion response, this hypothesis could not be evaluated.

Salinity treatments decreased stomatal conductance and photosynthetic assimilation, likely due to a salinity-induced water deficit, but this did not strongly affect water use

efficiency, suggesting that the treatments did not cause damage to the photosynthetic apparatus. This mild effect is also consistent with the negligible differences between treatments observed at the transcriptomic level, where the differences were mainly observed by GSEA, indicating that all three rootstocks limit the effect of salinity on the scion.

Although no statistically significant differentially expressed genes could be identified by Log_2FC comparisons, GSEA was able to detect changes in functionally related groups of genes. It indicated changes in the expression of genes involved in flavonoid synthesis, which we then mapped onto a metabolic pathway, shown for berries in Figure 3.7 and leaves in Figure 3.8. 1103 Paulsen- and M1-rooted leaves trended towards increased expression of *CHS* and decreased expression of *F3H*, *F3'H*, and *F3'5'H*. This pattern was reversed in M4-rooted samples, where the trend was decreased expression of *CHS* and increased expression of *F3H*, *F3'H*, and *F3'5'H*, suggesting higher anthocyanin content. This is consistent with previous findings showing that M4 has a lower capacity for Cl^- exclusion but maintains high salinity tolerance through its higher antioxidant capacity [68, 224, 231, 232].

In berry skins, we observed a trend of increased expression of *PAL* and *CHS,* and decreased expression of *F3H*, *F3'H*, and *F3'5'H* in salinity treatments. This pattern was strongest in 1103 Paulsen-rooted samples. The decreased expression of *F3H*, *F3'H*, and *F3'5'H* may explain the decreased abundance of anthocyanins and polyphenols observed in 1103 Paulsen- and M1-rooted samples. Flavonoids can play a role in drought and osmotic adjustment in grape berries and leaves, and their response can be genotype-dependent [227, 233], although these changes in berries fade as the fruit reaches final maturity [234].

4.3 Iron Deficiency Responses Vary Between Genotypes

Nitrogen and iron are growth-limiting factors in many fruit crops, given their involvement in vital plant processes such as chlorophyll synthesis, electron transport, and photosynthesis. Accordingly, Fe deficiency is a major constraint for vineyards grown on soils with low Fe availability.

4.3.1 Nitrogen source impacts the response to Fe deficiency

Nitrogen source can influence soil pH and change Fe availability for plants. We sought to better understand how N form and Fe acquisition interact to shape the physiological, biochemical, and molecular responses of two grapevine rootstocks differing in their susceptibility to Fe chlorosis, thereby shedding further light on the mechanisms underlying Fe homeostasis in this species.

In this experiment, N form significantly affected Fe deficiency symptoms. Using nitrate as the sole N form raised the nutrient solution pH, which reduced Fe availability and impaired its translocation from roots to leaves. Consequently, N1A0-treated plants developed more severe chlorosis symptoms than those supplied with both N forms. The two rootstock genotypes differed markedly in their susceptibility, with Fercal showing consistently milder responses than 3309 C regardless of N form. Indeed, Fercal induced Fe acquisition-related genes more efficiently under Fe deficiency in both N treatments, correlating with increased ferric chelate reductase (FCR) activity; this is a common grapevine response to lack of Fe [235]. 3309 C, by contrast, activated neither Fe acquisition genes nor FCR enzyme activity when both N forms were supplied together, suggesting it relies on an alternative strategy. Still, it remained capable of acidifying the rhizosphere when necessary.

Unlike 3309 C, Fercal was also able to increase root biomass under Fe deficit when both nitrogen forms were present, which is associated with improved resilience against nutrient deficiency [236]. Consistent with this, expression of the transcription factor ZAT11, which is linked to root development [237, 238] and metal homeostasis, was strongly enhanced in Fercal under treatment N1A1/-Fe.

Several plant hormones have been reported to regulate responses to Fe deficiency. Auxin has been suggested to induce modifications in root architecture as an adaptive strategy to facilitate Fe acquisition. These modifications include increased root branching, and greater density and length of lateral roots [235, 239]. Low Fe availability has also been associated with greater reductions of aboveground biomass compared to root biomass [235]. However, we did not observe a corresponding shift in the root-shoot ratio in this study. Nonetheless, we did observe significantly downregulated genes of the auxin metabolic pathway, especially in Fercal, but an increased expression of several auxin-responsive genes in both genotypes, especially in the N1A1 treatments. The overexpression of auxin primary response genes of the Aux/IAA and SAUR families in plants grown under Fe deficiency with both N forms present is consistent with the observed increase in root biomass, including an apparent enhancement in branching, which was more evident in Fercal.

Although Fe has traditionally been considered to have limited mobility towards young leaves, recent work has shown that under Fe deprivation, Fe can be partially remobilized from the root cell wall to sink organs [235, 240]. Abscisic acid (ABA) has similarly been reported to have a positive impact on Fe deficiency symptoms by promoting Fe transport and translocation [240]. In this work, Fe deficiency induced the expression of genes involved in the ABA signaling pathway (PYR/PYL, PP2C, SnRK2) in both rootstocks when supplied with both N forms. Low nitrate levels have been shown to increase plant ABA content, which in turn promotes Fe remobilization from cell walls and its translocation from root to shoot [240]. Taken together, these results suggest that a balanced supply of N forms could support the stress response of grapevine rootstocks under Fe deficiency.

FERRITIN1 (*FER1*) has been characterized as playing a role in Fe storage in several plant species, with stored Fe released when needed [239]. When nitrate was the sole N form, both rootstocks showed *FER1* downregulation under Fe-deficient conditions, together with strong induction of *OPT3*. The latter result was surprising, given that OPT3 is known to load Fe into the leaf phloem but has no reported function in roots [88]. When both N forms were supplied, *FER1* expression increased, indicating higher Fe storage, accompanied by a trend towards increased expression of *OPT3*, as well as *IREG3*, *VIT1*, and *YSL6* — genes associated with Fe transport and mobilization [87, 239, 240].

4.3.2 Bicarbonate-induced iron deficiency elicits a stronger response

Both Fe deficiency treatments used in this study caused a decrease in growth of aerial parts and chlorosis symptoms especially in the younger leaves, which were all a result of decreased Fe availability. Induced Fe deficiency caused more severe symptoms compared to direct Fe deficiency in both cultivars, but the more sensitive 3309 C exhibited the most severe symptoms.

Fe homeostasis depends on uptake, transport, and storage, and our expression results highlight several genotype-specific differences between the susceptible and tolerant rootstocks. FCR enzyme activity was reduced in 3309 C under both applied stresses, whereas no change was observed in the root tips of Fercal. Previous studies have reported increased FCR activity in tolerant grapevine rootstocks such as 140Ru, which shows a high capacity to increase Fe reduction under Fe-limited conditions [241]. *VviFRO2* expression increased non-significantly in Fercal under both Fe deficiency conditions, while 3309 C showed only a slight increase in expression under +Fe+BIC treatment. Furthermore, these

transcriptional differences did not correspond directly to changes in FCR enzyme activity. It is also worth noting that the larger root system observed under +Fe+BIC treatment could itself influence FCR activity calculations.

Fe transport from the soil into root cells is facilitated by the IRT1 transporter, and its upregulation, together with that of FRO2, is a well-established marker of Fe deficiency in many plants, including grapevine [78, 242, 243, 244, 245]. Interestingly, *VviIRT1* expression was strongly enhanced in the susceptible rootstock 3309 C under both stress conditions, and particularly under bicarbonate stress, where induction was much higher than in the tolerant rootstock Fercal. We showed enhanced expression of the bHLH genes *VvibHLH38* and *VvibHLH38/39* in both rootstocks and under both Fe deficiency conditions. Similarly, Vannozzi et al. [78] reported enhanced expression of *VvibHLH38* in both a tolerant (M1) and a susceptible (101.14) grapevine rootstock. This evidence supports the conclusion that, as in other species, the upregulation of *VviIRT1*, *VviFRO2*, and *VviAHA2* in grapevine may be driven by transcriptional regulation via bHLH transcription factors.

There was a trend of upregulation of *VviIREG3*, and *VviZIF1* under both Fe deficiency treatments, with Fercal showing slightly higher expression under bicarbonate stress. These genes are involved in Fe transport and mobilization [246, 247]. Like in the previous section, there was a trend of increased gene expression for *VviOPT3*, this time more so in Fercal. Expression of *VviVIT1* appeared to be inhibited by bicarbonate stress in both rootstocks. *FRD3* encodes a MATE family transporter required for Fe(III)-citrate complex transport in the xylem sap and for Fe translocation to the shoot [248], while *YSL* (*Yellow Stripe-Like*) genes encode transporters involved in the transport and translocation of Fe(II)-nicotianamine complexes within the plant [249]. In our study, *VviFRD3* was among the most highly expressed genes, although this was not statistically significant, increasing under both Fe deficiency conditions in both rootstocks (more markedly in Fercal, especially under -Fe treatment), while *VviYSL6* showed a trend of higher expression under bicarbonate stress in Fercal compared to 3309 C.

When we combine these expression observations with the different Fe concentrations in roots and leaves measured by our collaborators, we can speculate that both rootstocks were able to translocate Fe towards young leaves under -Fe treatment. However, only the tolerant Fercal was able to translocate Fe to young leaves under +Fe+BIC treatment, whereas this was not possible for the susceptible 3309 C.

Both Fe deficiency treatments induced changes in the content of malate and citrate in roots and root exudates. To better understand the changes underlying this outcome, we examined the expression of genes involved in the TCA (tricarboxylic acid) cycle in root tips. Overall, fold changes were modest and few reached statistical significance, consistent with the strong post-transcriptional regulation typical of TCA cycle enzymes. Furthermore, both rootstocks responded similarly to both treatments. The most notable changes were observed in genes encoding pyruvate dehydrogenase, aconitase, isocitrate dehydrogenase, α-ketoglutarate dehydrogenase, fumarase, and malate dehydrogenase. Direct Fe deficiency induced downregulation of these genes in both rootstocks, while indirect Fe deficiency induced upregulation. These changes were largest for α-ketoglutarate dehydrogenase and malate dehydrogenase, both of which provide reducing equivalents to the cell in the form of NADH. Although these changes in gene expression could not be directly correlated with the changes in organic acid content observed in roots and root exudates, the accumulation of malate in roots followed a similar pattern, increasing significantly under indirect Fe deficiency (+Fe+BIC). We suspect that the observed change in malate and citrate accumulation is caused mostly by post-transcriptional regulation.

4.4 '*Ca.* P. solani' Induces Significant Responses Before Symptom Appearance

'*Ca.* P. solani' infection caused significant changes in gene expression in infected grapevines that were apparent already in the early growing season, before any symptoms were visible. Several processes already known to be involved in, or altered by, infection were affected.

Decreased photosynthesis is a common occurrence in phytoplasma-infected plants and was also observed in this study [250]. At the same time, expression of genes encoding chloroplast ribosomal proteins also decreased. This phenomenon is typically correlated with the source-to-sink transition of leaves in phytoplasma-infected plants and has several plausible explanations. One possibility is feedback inhibition of photosynthesis due to blocked phloem flow and accumulation of photosynthesis products. Another possibility is the influence of phytoplasma effectors, which are known to cause developmental changes and deformations of plant organs. While neither possibility has been systematically investigated to date, the feedback inhibition hypothesis is supported by the starch accumulation observed in leaves of infected plants, which is likewise a common occurrence in phytoplasma-infected plants [126, 251, 252]. The origin of this starch remains unclear. In our study, starch-related genes as a group were found to be slightly down-regulated in the early season in the GSEA analysis. Expression of the rate-limiting synthesis gene ADP-glucose pyrophosphorylase was only mildly increased, and α-amylases showed mixed regulation patterns [253]. This is consistent with findings in mulberry, which indicated that the increase in starch content results from decreased degradation [252].

Tricarboxylic acid cycle genes were positively enriched in the early growing season, along with genes involved in mitochondrial respiratory chain and ATP synthesis. These findings point to increased energy production in infected plants in the early growing season. Phytoplasma infection increases the accumulation of hexose-6-phosphates in the middle leaf veins of infected grapevines [130] and some findings point to the possibility that this phenomenon could be related to putative effector proteins [254]. However, it is highly likely that the increased energy production observed in our study is related to energy needs due to increased protein turnover in the early growing season, as indicated by the very prominent increase in expression of amino acid synthesis, eukaryotic ribosomal protein and protein degradation genes. Interestingly, the apparent increase in protein production was accompanied by a global downturn in expression of various transcription factors, which was not previously reported for phytoplasma-infected grapevine.

Increased protein turnover can occur due to oxidative damage, which is common during infection. Phytoplasma-infected grapevines have been shown to exhibit increased expression and activity of enzymes involved in ROS detoxification, including those of the ascorbate-glutathione cycle. GSEA analysis indicated a general decrease in ROS-protective gene expression, particularly pronounced in the late growing season, while some individual genes, like ascorbate peroxidase and dehydroascorbate reductase, still showed positive expression. Indeed, enzyme activity measurements of ascorbate peroxidase and dehydroascorbate reductase (reported in Dermastia et al. [150]) showed that these enzymes were induced in infected samples in both growing seasons. This suggests that their activity levels are governed by post-transcriptional mechanisms.

Incomplete lignification is another common symptom in phytoplasma-infected grapevine and is thought to be related to the developmental disturbances mentioned above. Monolignols, the monomers bound together by laccase enzymes to form lignin, are synthesized from precursors obtained via the phenylpropanoid pathway. In our study, we found a strong increase in gene expression along the phenylpropanoid pathway; however, expression of laccases was considerably downregulated, suggesting that lignin formation

was also dysregulated in our samples. Phenylpropanoids, however, are also precursors for flavonoids, and many flavonoid synthesis-related genes were strongly up-regulated in infected samples in both growing seasons. Indeed, increased anthocyanin production is a characteristic phenomenon in red grapevine varieties infected with phytoplasma [150]. This phenomenon is not yet mechanistically explained, but is believed to represent another sink for carbon accumulating in the infected leaves.

SA and JA are the two phytohormones predominantly involved in plant-pathogen responses. Phytoplasmas are similar to biotrophic pathogens in that they inhabit living phloem cells; one would therefore expect plants to respond to phytoplasma infection via the SA-mediated pathway. In reality, the hormonal disturbances caused by phytoplasma are much more complex. A large meta-analysis showed SA accumulation and strong SA-mediated responses during FD phytoplasma infection [250]; however, grapevine cultivars that successfully induce a JA-mediated response are much more likely to recover naturally. Moreover, phytoplasmas possess effector proteins that directly interfere with the JA-mediated response. The effector protein SAP11, first identified in '*Candidatus* Phytoplasma asteris' and later found in several other species, has been shown to destabilize TCP transcription factors, which are involved in the JA signaling pathway [255, 256]. Arabidopsis plants overexpressing SAP11 show decreased JA production and, consequently, a reduced response to herbivory [135]. Indeed, both phytoplasma-infected and SAP11-overexpressing *Arabidopsis* plants have been shown to be favored by phytoplasma-carrying insects compared to healthy plants, leading to the proposal that suppressing JA-mediated responses increases phytoplasma fitness by promoting its spread, rather than being essential to the direct interaction between phytoplasma and host plant. In our study, we observed increased expression of JA synthesis and marker genes persisting across both growing seasons, indicating that a similar response is at play in our samples.

One common feature of phytoplasma-infected grapevines is increased expression of *DMR6,* an SA hydroxylase crucial for modulating the SA-mediated response during infection. Because of its role, *DMR6* is targeted as a susceptibility gene by several different pathogens across multiple species, including grapevine. Increased *DMR6* expression was also observed in our study. However, since *DMR6* expression is increased by SA presence as part of a negative feedback loop, it is unclear whether the observed response is induced specifically by phytoplasma or reflects a normal part of the SA-mediated response. In our study, we observed mixed modulation of *PR1* (SA-response marker) genes with a trend toward upregulation. *NPR1*, the master regulator of SA response which induces transcription of *PR1* genes, was not particularly responsive in our study. This is unsurprising, as *NPR1* regulation is known to occur mostly post-transcriptionally [257, 258]. NPR1 has a double role as an SA sensor and a transcription activator in the first steps of the signaling cascade, consequently small changes in expression lead to large responses in downstream genes.

4.5 Genome Editing of Grapevine Protoplasts Depends on the Genotype

Regeneration of protoplasts into whole plants is crucial for RNP-mediated genome editing and is usually the most challenging part of applying this approach in grapevine. The first RNP-mediated genome editing in grapevine was reported in Chardonnay; however, protoplasts were not regenerated into plants in that study [259]. RNP-mediated genome editing followed by successful regeneration has since been reported in only a handful of publications. Bertini et al. [167] reported efficient regeneration of grapevine protoplasts in cvs. Garganega and Sangiovese using a disc culture method. Soon after, Najafi et al. [168]

were the first to report RNP-mediated editing and plant regeneration in cv. Thompson Seedless using this approach. Since then, reports of successful editing and regeneration in grapevine have multiplied. Tricoli et al. regenerated several wine, table, and rootstock genotypes using alginate beads and feeder suspensions [260], and reported successful regeneration of the genome-edited rootstock 1103 Paulsen. Gambino et al. edited the very recalcitrant cv. Nebbiolo using lipofectamine-mediated transfection [261]. Most recently, Böttcher et al. reported success with Chardonnay, Cabernet Sauvignon, Shiraz, and Sauvignon Blanc [262].

In our study, Zweigelt had a higher capacity to regenerate into whole plants than Chardonnay, which is often considered one of the cultivars more amenable to embryogenesis [263]. In fact, compared to Böttcher et al. [262], who regenerated protoplasts of several wine varieties, including Chardonnay, using the calcium alginate bead method, our regeneration rates were surprisingly low for Chardonnay, while our Zweigelt rates were comparable to their reports. Najafi et al. [168], who used a solid disc cultivation method similar to the one used in this study, reported a 33% regeneration efficiency in cv. Thompson Seedless, considerably higher than our findings for both Chardonnay and Zweigelt. They also reported a positive effect of BAP on plant regeneration; consistent with this, we found that adding BAP to the shooting medium doubled the regeneration efficiency of Zweigelt, while it had barely any effect on Chardonnay.

We observed high variability in success or failure, germination, and regeneration efficiency between individual transfections, likely due to the delicate nature of protoplast isolation and handling. Additionally, polyethylene glycol (PEG), our transfection chemical of choice, is known to be toxic and has previously been reported to impair embryo development in sensitive cultivars [261]. We found similar rates of embryo formation in both genotypes, indicating that they respond similarly to PEG treatment.

We were able to regenerate some mock treatments from Zweigelt and compare them to RNP treatments. Surprisingly, we observed a trend toward lower germination in both mock and negative control treatments. However, of the embryos that did germinate, a greater proportion developed into whole plants in the mock and negative control treatments, resulting in higher regeneration efficiency. The low editing efficiency of RNP treatments, combined with the small sample size and high variability, suggests that biological and technical variability are a likely cause of these differences.

While a large proportion of Zweigelt protoplasts regenerated into plants, only one line was successfully edited. Conversely, seven of the 67 regenerated Chardonnay plants were successfully edited. The editing rate observed in Chardonnay is similar to the rates reported by Najafi et al. [168] and Gambino et al. [261], but low compared to that reported by Böttcher et al. [262]. The editing rate in Zweigelt is remarkably low by comparison. Since regeneration capacity is not a limiting factor in Zweigelt, the difference likely arises from the editing process itself. Reduced chromatin accessibility can impair genome editing; alternatively, Zweigelt may have a higher capacity to repair the double-stranded breaks induced by Cas9 compared to Chardonnay.

Another consequence of the relatively low editing efficiency in our experiments is the partial editing of target sites, producing heterozygous plants. Since this was observed in all edited lines, it is unlikely to be a random occurrence and could also result from lower chromatin accessibility on one of the two chromosomes. Differential editing is rarely reported with RNP-mediated delivery and is instead more common in plants produced via Agrobacterium-mediated delivery of Cas9 and sgRNA, where editing occurs constitutively and regenerated plants are commonly chimeric [114]. In our case, the regenerated lines are presumed to have arisen from single cells, so chimerism is unlikely. However, we cannot completely exclude the possibility of individual lines merging during the regeneration process.

Resistance conferred by S gene knockout usually behaves in a recessive manner. Furthermore, studies of *dmr6* gene knockout in grapevine have indicated that targeting only one gene in the *DMR6* family may not be sufficient to confer resistance. Both Giacomelli et al. and Gambino et al. [114, 261] found that only grapevines with both *dmr6-1* and *dmr6-2* knocked out exhibited increased resistance to *Plasmopara viticola*. Still, the effect of *DMR6* editing appears to be highly cultivar-dependent: Sugraone susceptibility remained unchanged regardless of gene knockout [114], whereas Holm et al. [116] reported that *dmr6-1* knockout alone was sufficient to increase resistance to *Plasmopara viticola* in the rootstock Richter 110. Since the edited lines in our study retained an unedited allele, a complete loss-of-function resistance phenotype may be less likely; however, susceptibility to '*Candidatus* Phytoplasma solani' remains to be experimentally evaluated.

Chapter 5

Conclusions

In this dissertation, we evaluated grapevine transcriptomic responses to four different types of environmental challenges and employed a state-of-the-art method to obtain genome edited grapevine.

Cabernet Volos and Fleurtai showed a common response to water deficit, largely consisting of increased osmoprotectant accumulation and downregulation of biotic defense. As hypothesized, we also observed differences between genotypes. Cabernet Volos invested in constitutive protection by accumulating more protective compounds, such as caffeoylquinate, while Fleurtai mounted the defense dynamically and synthesized these compounds in later stress stages. Moreover, Cabernet Volos decreased the expression of biotic response-related genes more vigorously than Fleurtai, while the latter more strongly induced the expression of genes involved in terpene synthesis and ABA signaling. These findings will help inform cultivar selection as viticulture adapts to increasing water scarcity under climate change.

We did not detect any significantly differentially expressed genes in leaves or berries of salinity-challenged Tempranillo vines grafted onto M1, M4 and 1103 Paulsen rootstocks, and therefore could not find conclusive support for our second hypothesis. At the level of gene expression, none of the three rootstocks were associated with major salinity-induced disturbances in the scion under our experimental conditions. However, 1103 Paulsen was able to exclude Cl^- from leaves more efficiently than the other rootstocks, and M4-rooted berries accumulated more polyphenols. These observations suggest divergent underlying tolerance strategies.

3309 C and Fercal, the two rootstocks subjected to different iron deficit conditions, had considerable differences in gene expression to these challenges, confirming our third hypothesis. When iron deficit was combined with different nitrogen sources, the more tolerant Fercal was able to more efficiently induce genes involved in Fe acquisition and root growth, while the more sensitive 3309 C discriminated between the conditions of nitrogen supply and did not induce rhizosphere acidification-related genes when both ammonium and nitrate were present. When presented with direct iron deficit or deficit induced by the presence of bicarbonate, both rootstocks responded more vigorously to the induced deficiency, with minor but interesting differences between them. The results of this dissertation have indicated new avenues for investigations of iron deficiency mechanisms in grapevine.

We detected significant changes in gene expression of '*Candidatus* Phytoplasma solani' infected grapevines in the early growing season and therefore confirmed our fourth hypothesis. Photosynthesis-related genes were strongly decreased, energy metabolism and protein production-related genes were increased, and genes involved in the phenylpropanoid pathway and lignification were disturbed. For the most part, the changes persisted also

into the later growing season as symptoms emerged. The results we report in this dissertation shed light on grapevine-phytoplasma interactions and indicate promising response networks to target for improvement of grapevine resistance to this pathogen.

Finally, we selected promising phytoplasma susceptibility genes *VviDMR6-1* and *VviDLO1* and were able to target them using DNA-free genome editing in Chardonnay and Zweigelt protoplasts, obtaining partially edited plants. The obtained partial mutants have yet to be evaluated for susceptibility. With this, we confirmed the feasibility of DNA-free genome editing approaches in Chardonnay and Zweigelt, which can now be expanded to target any other gene of choice.

The knowledge obtained in this dissertation can be further used to investigate the mechanisms involved in water deficit, salinity, iron deficit, and phytoplasma infection responses in grapevine, as well as the search for new targets in both conventional and modern breeding approaches. Moreover, the reported genome editing method can be implemented to edit any newly identified targets, and expanded to other grapevine cultivars.

Appendix A

Supplementary Material

A.1 Supplementary Material for Section 3.4

■

Supplementary Table 1: Complete table of enriched biological processes in '*Candidatus* phytoplasma solani'-infected grapevine during early and late growing season identified by gene set enrichment analysis.Enrichment is represented as proportions (%) of genes upregulated (red) or downregulated (blue) in the particular GoMapMan process (bin) in grapevines infected with '*Ca.* P. solani' compared to uninfected grapevines. Processes not reaching statistical significance have blank cells.

BIN NAME	Early	Late
1 PS	-70%	-72%
1.1 PS.LIGHTREACTION	-67%	-82%
1.1.1 PS.LIGHTREACTION.PHOTOSYSTEM II	-92%	-89%
1.1.1.2 PS.LIGHTREACTION.PHOTOSYSTEM II.PSII POLYPEPTIDE SUBUNITS	-88%	-92%
1.1.2 PS.LIGHTREACTION.PHOTOSYSTEM I	-89%	-94%
1.2 PS.PHOTORESPIRATION	-52%	-52%
1.3 PS.CALVIN CYCLE	-78%	-75%
2 MAJOR CHO METABOLISM	-	-
2.1 MAJOR CHO METABOLISM.SYNTHESIS	-	-
2.1.2 MAJOR CHO METABOLISM.SYNTHESIS.STARCH	-	-
2.2 MAJOR CHO METABOLISM.DEGRADATION	-	-
2.2.1 MAJOR CHO METABOLISM.DEGRADATION.SUCROSE	54%	42%
2.2.2 MAJOR CHO METABOLISM.DEGRADATION.STARCH	-38%	-
3 MINOR CHO METABOLISM	-	-
3.1 MINOR CHO METABOLISM.RAFFINOSE FAMILY	-31%	-38%
3.5 MINOR CHO METABOLISM.OTHERS	-	-
4 GLYCOLYSIS	51%	-
4.1 GLYCOLYSIS.CYTOSOLIC BRANCH	45%	-
5 FERMENTATION	48%	43%
7 OPP	-	-

Supplementary Table 1 (Continued)

BIN NAME	Early	Late
8 TCA / ORGANIC TRANSFORMATION	53%	-
8.1 TCA / ORGANIC TRANSFORMATION.TCA	72%	31%
8.2 TCA / ORGANIC TRANSFORMATION.OTHER ORGANIC ACID TRANSFORMATIONS	-	-
9 MITOCHONDRIAL ELECTRON TRANSPORT / ATP SYNTHESIS	53%	-
9.1 MITOCHONDRIAL ELECTRON TRANSPORT / ATP SYNTHESIS.NADH-DH (TYPE I)	75%	-
9.7 MITOCHONDRIAL ELECTRON TRANSPORT / ATP SYNTHESIS.CYTOCHROME C OXIDASE	-	-
9.9 MITOCHONDRIAL ELECTRON TRANSPORT / ATP SYNTHESIS.F1-ATPASE	60%	-30%
10 CELL WALL	38%	35%
10.1 CELL WALL.PRECURSOR SYNTHESIS	56%	53%
10.2 CELL WALL.CELLULOSE SYNTHESIS	-	43%
10.2.1 CELL WALL.CELLULOSE SYNTHESIS.CELLULOSE SYNTHASE	-	41%
10.5 CELL WALL.CELL WALL PROTEINS	27%	40%
10.6 CELL WALL.DEGRADATION	35%	34%
10.6.1 CELL WALL.DEGRADATION.CELLULASES AND BETA-1,4-GLUCANASES	47%	-
10.6.2 CELL WALL.DEGRADATION.MANNAN-XYLOSE-ARABINOSE-FUCOSE	30%	61%
10.6.3 CELL WALL.DEGRADATION.PECTATE LYASES AND POLYGALACTURONASES	-	-
10.7 CELL WALL.MODIFICATION	-	-
10.8 CELL WALL.PECTINESTERASES	43%	26%
10.8.1 CELL WALL.PECTINESTERASES.PME	41%	24%
11 LIPID METABOLISM	-	-
11.1 LIPID METABOLISM.FA SYNTHESIS AND FA ELONGATION	-	-
11.3 LIPID METABOLISM.PHOSPHOLIPID SYNTHESIS	-	-
11.8 LIPID METABOLISM.EXOTICS (STEROIDS, SQUALENE ETC)	-	-
11.8.1 LIPID METABOLISM.EXOTICS (STEROIDS, SQUALENE ETC).SPHINGOLIPIDS	-	-
11.9 LIPID METABOLISM.LIPID DEGRADATION	48%	-
11.9.2 LIPID METABOLISM.LIPID DEGRADATION.LIPASES	-	-
11.9.2.1 LIPID METABOLISM.LIPID DEGRADATION.LIPASES.TRIACYLGLYCEROL LIPASE	-	-
11.9.3 LIPID METABOLISM.LIPID DEGRADATION.LYSOPHOSPHOLIPASES	-	16%
11.9.4 LIPID METABOLISM.LIPID DEGRADATION.BETA-OXIDATION	50%	-
12 N-METABOLISM	-	-36%
13 AMINO ACID METABOLISM	41%	-
13.1 AMINO ACID METABOLISM.SYNTHESIS	42%	-

Supplementary Table 1 (Continued)

BIN NAME	Early	Late
13.1.1 AMINO ACID METABOLISM.SYNTHESIS.CENTRAL AMINO ACID METABOLISM	61%	50%
13.1.3 AMINO ACID METABOLISM.SYNTHESIS.ASPARTATE FAMILY	-	-
13.1.5 AMINO ACID METABOLISM.SYNTHESIS.SERINE-GLYCINE-CYSTEINE GROUP	46%	-
13.1.5.3 AMINO ACID METABOLISM.SYNTHESIS.SERINE-GLYCINE-CYSTEINE GROUP.CYSTEINE	45%	-
13.1.6 AMINO ACID METABOLISM.SYNTHESIS.AROMATIC AA	37%	-
13.1.6.5 AMINO ACID METABOLISM.SYNTHESIS.AROMATIC AA.TRYPTOPHAN	33%	-
13.2 AMINO ACID METABOLISM.DEGRADATION	-	-
13.2.3 AMINO ACID METABOLISM.DEGRADATION.ASPARTATE FAMILY	-	-
15 METAL HANDLING	-	-
15.2 METAL HANDLING.BINDING, CHELATION AND STORAGE	-	-
16 SECONDARY METABOLISM	28%	-
16.1 SECONDARY METABOLISM.ISOPRENOIDS	-	-50%
16.1.1 SECONDARY METABOLISM.ISOPRENOIDS.NON-MEVALONATE PATHWAY	-	-59%
16.1.2 SECONDARY METABOLISM.ISOPRENOIDS.MEVALONATE PATHWAY	-	-
16.10 SECONDARY METABOLISM.SIMPLE PHENOLS	-	18%
16.2 SECONDARY METABOLISM.PHENYLPROPANOIDS	44%	25%
16.2.1 SECONDARY METABOLISM.PHENYLPROPANOIDS.LIGNIN BIOSYNTHESIS	50%	28%
16.4 SECONDARY METABOLISM.N MISC	-	-
16.5 SECONDARY METABOLISM.SULFUR-CONTAINING	-	-
16.5.1 SECONDARY METABOLISM.SULFUR-CONTAINING.GLUCOSINOLATES	-	-
16.5.1.1 SECONDARY METABOLISM.SULFUR-CONTAINING.GLUCOSINOLATES.SYNTHESIS	-	-
16.5.1.1.1 SECONDARY METABOLISM.SULFUR-CONTAINING.GLUCOSINOLATES.SYNTHESIS.ALIPHATIC	-	-
16.8 SECONDARY METABOLISM.FLAVONOIDS	38%	27%
16.8.3 SECONDARY METABOLISM.FLAVONOIDS.DIHYDROFLAVONOLS	37%	33%
16.8.3.1 SECONDARY METABOLISM.FLAVONOIDS.DIHYDROFLAVONOLS.DIHYDROFLAVONOL 4-REDUCTASE	-	-
17 HORMONE METABOLISM	-	-
17.1 HORMONE METABOLISM.ABSCISIC ACID	-	24%
17.1.2 HORMONE METABOLISM.ABSCISIC ACID.SIGNAL TRANSDUCTION	-	-
17.1.3 HORMONE METABOLISM.ABSCISIC ACID.INDUCED-REGULATED-RESPONSIVE-ACTIVATED	-	40%
17.2 HORMONE METABOLISM.AUXIN	-	-

Supplementary Table 1 (Continued)

BIN NAME	Early	Late
17.2.2 HORMONE METABOLISM.AUXIN.SIGNAL TRANSDUCTION	-	-32%
17.2.3 HORMONE METABOLISM.AUXIN.INDUCED-REGULATED-RESPONSIVE-ACTIVATED	-	-
17.3 HORMONE METABOLISM.BRASSINOSTEROID	-	-
17.3.1 HORMONE METABOLISM.BRASSINOSTEROID.SYNTHESIS-DEGRADATION	-	-
17.5 HORMONE METABOLISM.ETHYLENE	-	-
17.5.1 HORMONE METABOLISM.ETHYLENE.SYNTHESIS-DEGRADATION	-	-52%
17.5.2 HORMONE METABOLISM.ETHYLENE.SIGNAL TRANSDUCTION	-52%	-
17.6 HORMONE METABOLISM.GIBBERELIN	-	-43%
17.7 HORMONE METABOLISM.JASMONATE	-	-
17.7.1 HORMONE METABOLISM.JASMONATE.SYNTHESIS-DEGRADATION	-	32%
18 CO-FACTOR AND VITAMINE METABOLISM	-	-50%
19 TETRAPYRROLE SYNTHESIS	-68%	-54%
20.1 STRESS.BIOTIC	27%	-
20.1.2 STRESS.BIOTIC.RECEPTORS	25%	25%
20.1.2.1 STRESS.BIOTIC.RECEPTORS.CC-NBS-LRR	-	-
20.1.2.2 STRESS.BIOTIC.RECEPTORS.TIR-NBS-LRR	-	33%
20.1.3 STRESS.BIOTIC.SIGNALLING	-	-
20.1.7 STRESS.BIOTIC.PR-PROTEINS	49%	49%
20.1.7.3 STRESS.BIOTIC.PR-PROTEINS.PR3/4/8/11 (CHITINASES AND CHITIN BINDING PROTEINS)	47%	-
20.1.7.5 STRESS.BIOTIC.PR-PROTEINS.PR5 (THAUMATIN-LIKE PROTEINS)	67%	56%
20.2 STRESS.ABIOTIC	-	-
20.2.1 STRESS.ABIOTIC.HEAT	-	-
20.2.3 STRESS.ABIOTIC.DROUGHT/SALT	-	-
21 REDOX	-	-33%
21.1 REDOX.THIOREDOXIN	-	-46%
21.2 REDOX.ASCORBATE AND GLUTATHIONE	-	-
21.2.1 REDOX.ASCORBATE AND GLUTATHIONE.ASCORBATE	-	-
23 NUCLEOTIDE METABOLISM	-	-
23.1 NUCLEOTIDE METABOLISM.SYNTHESIS	-	-38%
23.2 NUCLEOTIDE METABOLISM.DEGRADATION	-	-
23.3 NUCLEOTIDE METABOLISM.SALVAGE	-15%	-
23.3.3 NUCLEOTIDE METABOLISM.SALVAGE.NUDIX HYDROLASES	-40%	-
23.4 NUCLEOTIDE METABOLISM.PHOSPHOTRANSFER AND PYROPHOSPHATASES	-	-
24 BIODEGRADATION OF XENOBIOTICS	-	35%
25 C1-METABOLISM	-	-
26.10 MISC.CYTOCHROME P450	-	-33%

Supplementary Table 1 (Continued)

BIN NAME	Early	Late
26.11 MISC.ALCOHOL DEHYDROGENASES	-	-
26.11.1 MISC.ALCOHOL DEHYDROGENASES.CINNAMYL ALCOHOL DEHYDROGENASE	-	-
26.12 MISC.PEROXIDASES	61%	39%
26.13 MISC.ACID AND OTHER PHOSPHATASES	-	-
26.2 MISC.UDP GLUCOSYL AND GLUCORONYL TRANSFERASES	-	-
26.22 MISC.SHORT CHAIN DEHYDROGENASE/REDUCTASE (SDR)	-	-
26.24 MISC.GCN5-RELATED N-ACETYLTRANSFERASE	-	-47%
26.27 MISC.CALCINEURIN-LIKE PHOSPHOESTERASE FAMILY PROTEIN	35%	-
26.28 MISC.GDSL-MOTIF LIPASE	-	-
26.3 MISC.GLUCO-, GALACTO- AND MANNOSIDASES	29%	-
26.3.5 MISC.GLUCO-, GALACTO- AND MANNOSIDASES.GLYCOSYL HYDROLASE FAMILY 5	-	-
26.4 MISC.BETA 1,3 GLUCAN HYDROLASES	55%	50%
26.4.1 MISC.BETA 1,3 GLUCAN HYDROLASES.GLUCAN ENDO-1,3-BETA-GLUCOSIDASE	50%	47%
26.6 MISC.O-METHYL TRANSFERASES	52%	-
26.7 MISC.OXIDASES - COPPER, FLAVONE ETC	-	-
26.8 MISC.NITRILASES, NITRILE LYASES, BERBERINE BRIDGE ENZYMES, RETICULINE OXIDASES, TROPONINE REDUCTASES	-	-
26.9 MISC.GLUTATHIONE S TRANSFERASES	53%	-
27.1 RNA.PROCESSING	-	-
27.1.1 RNA.PROCESSING.SPLICING	-	-
27.1.19 RNA.PROCESSING.RIBONUCLEASES	-	-
27.1.2 RNA.PROCESSING.RNA HELICASE	-	-
27.1.3 RNA.PROCESSING.3' END PROCESSING	-	-
27.2 RNA.TRANSCRIPTION	-	-
27.3.11 RNA.REGULATION OF TRANSCRIPTION.C2H2 ZINC FINGER FAMILY	-	-
27.3.12 RNA.REGULATION OF TRANSCRIPTION.C3H ZINC FINGER FAMILY	-	-
27.3.22 RNA.REGULATION OF TRANSCRIPTION.HOMEOBOX TRANSCRIPTION FACTOR FAMILY (HB)	-	-24%
27.3.23 RNA.REGULATION OF TRANSCRIPTION.HEAT-SHOCK TRANSCRIPTION FACTOR FAMILY (HSF)	-	-
27.3.25 RNA.REGULATION OF TRANSCRIPTION.MYB DOMAIN TRANSCRIPTION FACTOR FAMILY	-	-31%
27.3.26 RNA.REGULATION OF TRANSCRIPTION.MYB-RELATED TRANSCRIPTION FACTOR FAMILY	-	-67%
27.3.27 RNA.REGULATION OF TRANSCRIPTION.NAC DOMAIN TRANSCRIPTION FACTOR FAMILY	-	-
27.3.3 RNA.REGULATION OF TRANSCRIPTION.AP2/EREBP, APETALA2/ETHYLENE-RESPONSIVE ELEMENT BINDING PROTEIN FAMILY	-26%	-

Supplementary Table 1 (Continued)

BIN NAME	Early	Late
27.3.30 RNA.REGULATION OF TRANSCRIPTION.TRIPLE-HELIX TRANSCRIPTION FACTOR FAMILY (TRIHELIX)	-	-
27.3.32 RNA.REGULATION OF TRANSCRIPTION.WRKY DOMAIN TRANSCRIPTION FACTOR FAMILY	-	-
27.3.35 RNA.REGULATION OF TRANSCRIPTION.BZIP TRANSCRIPTION FACTOR FAMILY	-	-
27.3.4 RNA.REGULATION OF TRANSCRIPTION.AUXIN RESPONSE TRANSCRIPTION FACTOR FAMILY (ARF)	-72%	-61%
27.3.40 RNA.REGULATION OF TRANSCRIPTION.AUX/IAA FAMILY	-75%	-85%
27.3.44 RNA.REGULATION OF TRANSCRIPTION.CHROMATIN REMODELING FACTORS	-	-
27.3.5 RNA.REGULATION OF TRANSCRIPTION.ARR	-	-44%
27.3.50 RNA.REGULATION OF TRANSCRIPTION.GENERAL TRANSCRIPTION	-	-
27.3.57 RNA.REGULATION OF TRANSCRIPTION.JUMONJI FAMILY	-	-
27.3.6 RNA.REGULATION OF TRANSCRIPTION.BASIC HELIX-LOOP-HELIX FAMILY (BHLH)	-28%	-32%
27.3.67 RNA.REGULATION OF TRANSCRIPTION.PUTATIVE TRANSCRIPTION REGULATOR	-	-
27.3.69 RNA.REGULATION OF TRANSCRIPTION.SET-DOMAIN TRANSCRIPTIONAL REGULATOR FAMILY	-	-
27.3.7 RNA.REGULATION OF TRANSCRIPTION.C2C2(ZN) CONSTANS-LIKE ZINC FINGER FAMILY (CO-LIKE)	-55%	-80%
27.3.8 RNA.REGULATION OF TRANSCRIPTION.C2C2(ZN) DOF ZINC FINGER FAMILY	45%	-
27.3.99 RNA.REGULATION OF TRANSCRIPTION.UNCLASSIFIED	-	-
27.4 RNA.RNA BINDING	-	-
28 DNA	39%	-
28.1 DNA.SYNTHESIS/CHROMATIN STRUCTURE	33%	-
28.1.3 DNA.SYNTHESIS/CHROMATIN STRUCTURE.HISTONE	56%	-
28.1.3.2 DNA.SYNTHESIS/CHROMATIN STRUCTURE.HISTONE.CORE	66%	-
28.2 DNA.REPAIR	-	-
28.99 DNA.UNSPECIFIED	-	-
29.1 PROTEIN.AA ACTIVATION	-	-67%
29.2.1 PROTEIN.SYNTHESIS.RIBOSOMAL PROTEIN	61%	-65%
29.2.1.1 PROTEIN.SYNTHESIS.RIBOSOMAL PROTEIN.PROKARYOTIC	-35%	-41%
29.2.1.1.1 PROTEIN.SYNTHESIS.RIBOSOMAL PROTEIN.PROKARYOTIC.CHLOROPLAST	-67%	-65%
29.2.1.1.1.2 PROTEIN.SYNTHESIS.RIBOSOMAL PROTEIN.PROKARYOTIC.CHLOROPLAST.50S SUBUNIT	-63%	-59%
29.2.1.1.3 PROTEIN.SYNTHESIS.RIBOSOMAL PROTEIN.PROKARYOTIC.UNKNOWN ORGANELLAR	-	-
29.2.1.1.3.2 PROTEIN.SYNTHESIS.RIBOSOMAL PROTEIN.PROKARYOTIC.UNKNOWN ORGANELLAR.50S SUBUNIT	-	-

Supplementary Table 1 (Continued)

BIN NAME	Early	Late
29.2.1.2 PROTEIN.SYNTHESIS.RIBOSOMAL PROTEIN.EUKARYOTIC	76%	-76%
29.2.1.2.1 PROTEIN.SYNTHESIS.RIBOSOMAL PROTEIN.EUKARYOTIC.40S SUBUNIT	78%	-68%
29.2.1.2.2 PROTEIN.SYNTHESIS.RIBOSOMAL PROTEIN.EUKARYOTIC.60S SUBUNIT	75%	-81%
29.2.2 PROTEIN.SYNTHESIS.RIBOSOME BIOGENESIS	-	-
29.2.2.3 PROTEIN.SYNTHESIS.RIBOSOME BIOGENESIS.PRE-RRNA PROCESSING AND MODIFICATIONS	-	-
29.2.2.3.3 PROTEIN.SYNTHESIS.RIBOSOME BIOGENESIS.PRE-RRNA PROCESSING AND MODIFICATIONS.METHYLOTRANSFERASES	-	-
29.2.3 PROTEIN.SYNTHESIS.INITIATION	-	-
29.2.4 PROTEIN.SYNTHESIS.ELONGATION	36%	-
29.3 PROTEIN.TARGETING	-	-
29.3.1 PROTEIN.TARGETING.NUCLEUS	-	-
29.3.2 PROTEIN.TARGETING.MITOCHONDRIA	83%	-
29.3.3 PROTEIN.TARGETING.CHLOROPLAST	-	-58%
29.3.4 PROTEIN.TARGETING.SECRETORY PATHWAY	60%	-
29.3.4.3 PROTEIN.TARGETING.SECRETORY PATHWAY.VACUOLE	-	-
29.3.4.99 PROTEIN.TARGETING.SECRETORY PATHWAY.UNSPECIFIED	58%	-
29.4.1 PROTEIN.POSTRANSLATIONAL MODIFICATION.KINASE	-	-
29.4.1.57 PROTEIN.POSTRANSLATIONAL MODIFICATION.KINASE.RECEPTOR LIKE CYTOPLASMATIC KINASE VII	-	-
29.5.1 PROTEIN.DEGRADATION.SUBTILASES	38%	-
29.5.11.1 PROTEIN.DEGRADATION.UBIQUITIN.UBIQUITIN	62%	-
29.5.11.20 PROTEIN.DEGRADATION.UBIQUITIN.PROTEASOM	85%	-
29.5.11.3 PROTEIN.DEGRADATION.UBIQUITIN.E2	-	-
29.5.11.4 PROTEIN.DEGRADATION.UBIQUITIN.E3	-	-
29.5.11.4.2 PROTEIN.DEGRADATION.UBIQUITIN.E3.RING	-	-
29.5.11.4.3 PROTEIN.DEGRADATION.UBIQUITIN.E3.SCF	-	-
29.5.11.4.3.2 PROTEIN.DEGRADATION.UBIQUITIN.E3.SCF.FBOX	-	-
29.5.11.5 PROTEIN.DEGRADATION.UBIQUITIN.UBIQUITIN PROTEASE	-	-
29.5.2 PROTEIN.DEGRADATION.AUTOPHAGY	-	-
29.5.3 PROTEIN.DEGRADATION.CYSTEINE PROTEASE	-	-
29.5.4 PROTEIN.DEGRADATION.ASPARTATE PROTEASE	-	29%
29.5.5 PROTEIN.DEGRADATION.SERINE PROTEASE	-	-
29.5.7 PROTEIN.DEGRADATION.METALLOPROTEASE	-	-59%
29.5.9 PROTEIN.DEGRADATION.AAA TYPE	45%	-
29.6 PROTEIN.FOLDING	-	-34%
29.7 PROTEIN.GLYCOSYLATION	69%	-
29.8 PROTEIN.ASSEMBLY AND COFACTOR LIGATION	-41%	-59%
30.1 SIGNALLING.IN SUGAR AND NUTRIENT PHYSIOLOGY	-	-

Supplementary Table 1 (Continued)

BIN NAME	Early	Late
30.1.1 SIGNALLING.IN SUGAR AND NUTRIENT PHYSIOLOGY.MISC	-	-
30.11 SIGNALLING.LIGHT	-	-30%
30.2 SIGNALLING.RECEPTOR KINASES	36%	-
30.2.1 SIGNALLING.RECEPTOR KINASES.LEUCINE RICH REPEAT I	63%	-
30.2.11 SIGNALLING.RECEPTOR KINASES.LEUCINE RICH REPEAT XI	59%	-
30.2.12 SIGNALLING.RECEPTOR KINASES.LEUCINE RICH REPEAT XII	50%	-
30.2.17 SIGNALLING.RECEPTOR KINASES.DUF 26	43%	-
30.2.19 SIGNALLING.RECEPTOR KINASES.LEGUME-LECTIN	-	-
30.2.2 SIGNALLING.RECEPTOR KINASES.LEUCINE RICH REPEAT II	47%	-
30.2.24 SIGNALLING.RECEPTOR KINASES.S-LOCUS GLYCOPROTEIN LIKE	-	-
30.2.25 SIGNALLING.RECEPTOR KINASES.WALL ASSOCIATED KINASE	-	-44%
30.2.3 SIGNALLING.RECEPTOR KINASES.LEUCINE RICH REPEAT III	-	-
30.2.8 SIGNALLING.RECEPTOR KINASES.LEUCINE RICH REPEAT VIII	41%	-
30.2.8.2 SIGNALLING.RECEPTOR KINASES.LEUCINE RICH REPEAT VIII.TYPE 2	52%	-
30.2.99 SIGNALLING.RECEPTOR KINASES.MISC	48%	-
30.3 SIGNALLING.CALCIUM	-	-
30.4 SIGNALLING.PHOSPHINOSITIDES	-	-
30.5 SIGNALLING.G-PROTEINS	-	-
30.6 SIGNALLING.MAP KINASES	-	-
31.1 CELL.ORGANISATION	-	-
31.2 CELL.DIVISION	-	-
31.3 CELL.CYCLE	-	-
31.3.1 CELL.CYCLE.PEPTIDYLPROLYL ISOMERASE	-	-
31.4 CELL.VESICLE TRANSPORT	67%	-
31.5 CELL.CELL DEATH	-21%	-
33 DEVELOPMENT	-	-
33.1 DEVELOPMENT.STORAGE PROTEINS	33%	47%
33.2 DEVELOPMENT.LATE EMBRYOGENESIS ABUNDANT	-	-
33.3 DEVELOPMENT.SQUAMOSA PROMOTER BINDING LIKE (SPL)	20%	-
33.99 DEVELOPMENT.UNSPECIFIED	-	-
34.1 TRANSPORT.P- AND V-ATPASES	-	41%
34.12 TRANSPORT.METAL	28%	-
34.13 TRANSPORT.PEPTIDES AND OLIGOPEPTIDES	-22%	-53%
34.14 TRANSPORT.UNSPECIFIED CATIONS	-28%	-
34.15 TRANSPORT.POTASSIUM	-	-45%
34.16 TRANSPORT.ABC TRANSPORTERS AND MULTIDRUG RESISTANCE SYSTEMS	-	-47%
34.19 TRANSPORT.MAJOR INTRINSIC PROTEINS	47%	-
34.2 TRANSPORT.SUGARS	-	-
34.3 TRANSPORT.AMINO ACIDS	-	-

Supplementary Table 1 (Continued)

BIN NAME	Early	Late
34.7 TRANSPORT.PHOSPHATE	-27%	-47%
34.8 TRANSPORT.METABOLITE TRANSPORTERS AT THE ENVELOPE MEMBRANE	-	-
34.9 TRANSPORT.METABOLITE TRANSPORTERS AT THE MITOCHONDRIAL MEMBRANE	-	-
34.99 TRANSPORT.MISC	-	-
35.1.27 NOT ASSIGNED.NO ONTOLOGY.TETRATRICOPEPTIDE REPEAT (TPR)	-	-
35.1.3 NOT ASSIGNED.NO ONTOLOGY.ARMADILLO/BETA-CATENIN REPEAT FAMILY PROTEIN	-	-
35.1.41 NOT ASSIGNED.NO ONTOLOGY.HYDROXYPROLINE RICH PROTEINS	-	-
35.1.5 NOT ASSIGNED.NO ONTOLOGY.PENTATRICOPEPTIDE (PPR) REPEAT-CONTAINING PROTEIN	-	-56%

References

[1] C. van Leeuwen and P. Darriet, "The Impact of Climate Change on Viticulture and Wine Quality," Journal of Wine Economics, vol. 11, no. 1, pp. 150–167, May 2016, doi: 10.1017/jwe.2015.21.

[2] K. Vishwakarma et al., "Abscisic Acid Signaling and Abiotic Stress Tolerance in Plants: A Review on Current Knowledge and Future Prospects," Front. Plant Sci., vol. 8, Feb. 2017, doi: 10.3389/fpls.2017.00161.

[3] B. Brandt et al., "Reconstitution of abscisic acid activation of SLAC1 anion channel by CPK6 and OST1 kinases and branched ABI1 PP2C phosphatase action," Proc. Natl. Acad. Sci. U.S.A., vol. 109, no. 26, pp. 10593–10598, Jun. 2012, doi: 10.1073/pnas.1116590109.

[4] Y. Wang, Z.-H. Chen, B. Zhang, A. Hills, and M. R. Blatt, "PYR/PYL/RCAR Abscisic Acid Receptors Regulate K+ and Cl− Channels through Reactive Oxygen Species-Mediated Activation of Ca2+ Channels at the Plasma Membrane of Intact Arabidopsis Guard Cells," Plant Physiol., vol. 163, no. 2, pp. 566–577, Oct. 2013, doi: 10.1104/pp.113.219758.

[5] Y. Fujita, M. Fujita, K. Shinozaki, and K. Yamaguchi-Shinozaki, "ABA-mediated transcriptional regulation in response to osmotic stress in plants," J. Plant Res., vol. 124, no. 4, pp. 509–525, Jul. 2011, doi: 10.1007/s10265-011-0412-3.

[6] J. Mizoi et al., "Heat-induced inhibition of phosphorylation of the stress-protective transcription factor DREB2A promotes thermotolerance of Arabidopsis thaliana," Journal of Biological Chemistry, vol. 294, no. 3, pp. 902–917, Jan. 2019, doi: 10.1074/jbc.RA118.002662.

[7] J. Speirs, A. Binney, M. Collins, E. Edwards, and B. Loveys, "Expression of ABA synthesis and metabolism genes under different irrigation strategies and atmospheric VPDs is associated with stomatal conductance in grapevine (Vitis vinifera L. cv Cabernet Sauvignon)," J. Exp. Bot., vol. 64, no. 7, pp. 1907–1916, Apr. 2013, doi: 10.1093/jxb/ert052.

[8] J. G. Pérez-Pérez, J. Puertolas, A. Albacete, and I. C. Dodd, "Alternation of wet and dry sides during partial rootzone drying irrigation enhances leaf ethylene evolution," Environmental and Experimental Botany, vol. 176, p. 104095, Aug. 2020, doi: 10.1016/j.envexpbot.2020.104095.

[9] L. Sack, G. P. John, and T. N. Buckley, "ABA Accumulation in Dehydrating Leaves Is Associated with Decline in Cell Volume, Not Turgor Pressure," Plant Physiol., vol. 176, no. 1, pp. 489–495, Jan. 2018, doi: 10.1104/pp.17.01097.

[10] S. Tombesi, A. Nardini, D. Farinelli, and A. Palliotti, "Relationships between stomatal behavior, xylem vulnerability to cavitation and leaf water relations

in two cultivars of Vitis vinifera," Physiologia Plantarum, vol. 152, no. 3, pp. 453–464, 2014, doi: 10.1111/ppl.12180.

[11] S. Tombesi et al., "Stomatal closure is induced by hydraulic signals and maintained by ABA in drought-stressed grapevine," Sci. Rep., vol. 5, no. 1, p. 12449, Jul. 2015, doi: 10.1038/srep12449.

[12] F. Takahashi et al., "A small peptide modulates stomatal control via abscisic acid in long-distance signalling," Nature, vol. 556, no. 7700, pp. 235–238, Apr. 2018, doi: 10.1038/s41586-018-0009-2.

[13] T. C. Hsiao and L. Xu, "Sensitivity of growth of roots versus leaves to water stress: biophysical analysis and relation to water transport," J. Exp. Bot., vol. 51, no. 350, pp. 1595–1616, Sep. 2000, doi: 10.1093/jexbot/51.350.1595.

[14] A. R. Reddy, K. V. Chaitanya, and M. Vivekanandan, "Drought-induced responses of photosynthesis and antioxidant metabolism in higher plants," Journal of Plant Physiol., vol. 161, no. 11, pp. 1189–1202, Nov. 2004, doi: 10.1016/j.jplph.2004.01.013.

[15] A. Zavafer, M. H. Cheah, W. Hillier, W. S. Chow, and S. Takahashi, "Photodamage to the oxygen evolving complex of photosystem II by visible light," Sci. Rep., vol. 5, no. 1, p. 16363, Nov. 2015, doi: 10.1038/srep16363.

[16] K. K. Niyogi, X.-P. Li, V. Rosenberg, and H.-S. Jung, "Is PsbS the site of non-photochemical quenching in photosynthesis?," J. Exp. Bot., vol. 56, no. 411, pp. 375–382, Jan. 2005, doi: 10.1093/jxb/eri056.

[17] R. Szymańska, I. Ślesak, A. Orzechowska, and J. Kruk, "Physiological and biochemical responses to high light and temperature stress in plants," Environmental and Experimental Botany, vol. 139, pp. 165–177, Jul. 2017, doi: 10.1016/j.envexpbot.2017.05.002.

[18] J. Kromdijk et al., "Improving photosynthesis and crop productivity by accelerating recovery from photoprotection," Science, vol. 354, no. 6314, pp. 857–861, Nov. 2016, doi: 10.1126/science.aai8878.

[19] T. Shikanai, "Cyclic Electron Transport Around Photosystem I: Genetic Approaches," Annual Review of Plant Biology, vol. 58, pp. 199–217, 2007, doi: 10.1146/annurev.arplant.58.091406.110525.

[20] U. Hochberg, A. Degu, A. Fait, and S. Rachmilevitch, "Near isohydric grapevine cultivar displays higher photosynthetic efficiency and photorespiration rates under drought stress as compared with near anisohydric grapevine cultivar," Physiologia Plantarum, vol. 147, no. 4, pp. 443–452, Apr. 2013, doi: 10.1111/j.1399-3054.2012.01671.x.

[21] K. Das and A. Roychoudhury, "Reactive oxygen species (ROS) and response of antioxidants as ROS-scavengers during environmental stress in plants," Front. Environ. Sci., vol. 2, Dec. 2014, doi: 10.3389/fenvs.2014.00053.

[22] M. Farooq, A. Wahid, N. Kobayashi, D. Fujita, and S. M. A. Basra, "Plant drought stress: effects, mechanisms and management," Agron. Sustain. Dev., vol. 29, no. 1, pp. 185–212, Mar. 2009, doi: 10.1051/agro:2008021.

[23] J. Moustaka et al., "Anthocyanin accumulation in poinsettia leaves and its functional role in photo-oxidative stress," Environmental and Experimental Botany, vol. 175, p. 104065, Jul. 2020, doi: 10.1016/j.envexpbot.2020.104065.

[24] M. Gorantla et al., "Identification of stress-responsive genes in an indica rice (Oryza sativa L.) using ESTs generated from drought-stressed seedlings," J. Exp. Bot., vol. 58, no. 2, pp. 253–265, Jan. 2007, doi: 10.1093/jxb/erl213.

[25] E. R. Waters and E. Vierling, "Plant small heat shock proteins – evolutionary and functional diversity," New Phytologist, vol. 227, no. 1, pp. 24–37, Jul. 2020, doi: 10.1111/nph.16536.

[26] G. Charrier et al., "Drought will not leave your glass empty: Low risk of hydraulic failure revealed by long-term drought observations in world's top wine regions," Science Advances, vol. 4, no. 1, p. eaao6969, Jan. 2018, doi: 10.1126/sciadv.aao6969.

[27] M. Sodini et al., "Deficit Irrigation Strategies Modulate Grape Maturation and Volatile Aroma Composition in Pinot Gris Wines," Agronomy, vol. 16, no. 13, p. 1232, Jan. 2026, doi: 10.3390/agronomy16131232.

[28] M. M. Chaves et al., "Grapevine under deficit irrigation: hints from physiological and molecular data," Ann. Bot., vol. 105, no. 5, pp. 661–676, May 2010, doi: 10.1093/aob/mcq030.

[29] F. Tardieu and T. Simonneau, "Variability among species of stomatal control under fluctuating soil water status and evaporative demand: modelling isohydric and anisohydric behaviours," J. Exp. Bot., vol. 49, no. Special Issue, pp. 419–432, Mar. 1998, doi: 10.1093/jxb/49.Special_Issue.419.

[30] G. Charrier et al., "Evidence for Hydraulic Vulnerability Segmentation and Lack of Xylem Refilling under Tension," Plant Physiol., vol. 172, no. 3, pp. 1657–1668, Nov. 2016, doi: 10.1104/pp.16.01079.

[31] A. Lavoie-Lamoureux, D. Sacco, P.-A. Risse, and C. Lovisolo, "Factors influencing stomatal conductance in response to water availability in grapevine: a meta-analysis," Physiologia Plantarum, vol. 159, no. 4, pp. 468–482, 2017, doi: 10.1111/ppl.12530.

[32] J. Bota, M. Tomás, J. Flexas, H. Medrano, and J. M. Escalona, "Differences among grapevine cultivars in their stomatal behavior and water use efficiency under progressive water stress," Agricultural Water Management, vol. 164, pp. 91–99, Jan. 2016, doi: 10.1016/j.agwat.2015.07.016.

[33] A. D. Levin, L. E. Williams, and M. A. Matthews, "A continuum of stomatal responses to water deficits among 17 wine grape cultivars (Vitis vinifera)," Functional Plant Biology, vol. 47, no. 1, pp. 11–25, 2020, doi: 10.1071/FP19073.

[34] E. Marguerit, O. Brendel, E. Lebon, C. van Leeuwen, and N. Ollat, "Rootstock control of scion transpiration and its acclimation to water deficit are controlled by different genes," New Phytologist, vol. 194, no. 2, pp. 416–429, 2012, doi: 10.1111/j.1469-8137.2012.04059.x.

[35] R. Munns and A. Termaat, "Whole-Plant Responses to Salinity," Australian Journal of Plant Physiol., vol. 13, no. 1, pp. 143–160, Feb. 1986, doi: 10.1071/PP9860143.

[36] R. R. Walker, M. Sedgley, M. A. Blesing, and T. J. Douglas, "Anatomy, Ultrastructure and Assimilate Concentrations of Roots of Citrus Genotypes Differing in Ability for Salt Exclusion," J. Exp. Bot., vol. 35, no. 10, pp. 1481–1494, Oct. 1984, doi: 10.1093/jxb/35.10.1481.

[37] R. Munns, "Comparative physiology of salt and water stress," Plant, Cell & Environment, vol. 25, no. 2, pp. 239–250, Feb. 2002, doi: 10.1046/j.0016-8025.2001.00808.x.

[38] Z. C. Chen, N. Yamaji, M. Fujii-Kashino, and J. F. Ma, "A Cation-Chloride Cotransporter Gene Is Required for Cell Elongation and Osmoregulation in Rice," Plant Physiol., vol. 171, no. 1, pp. 494–507, May 2016, doi: 10.1104/pp.16.00017.

[39] P. H. Homann, "The relation between the chloride status of the photosynthetic water splitting complex and the inhibitory effectiveness of amines," Photosynth. Res., vol. 10, no. 3, pp. 497–505, Jan. 1986, doi: 10.1007/BF00118316.

[40] Y. Hu and U. Schmidhalter, "Interactive effects of salinity and macronutrient level on wheat. II. Composition," Journal of Plant Nutrition, vol. 20, no. 9, pp. 1169–1182, Sep. 1997, doi: 10.1080/01904169709365325.

[41] A. Herdean et al., "The Arabidopsis Thylakoid Chloride Channel AtCLCe Functions in Chloride Homeostasis and Regulation of Photosynthetic Electron Transport," Front. Plant Sci., vol. 7, Feb. 2016, doi: 10.3389/fpls.2016.00115.

[42] K. Yamane, M. Kawasaki, M. Taniguchi, and H. Miyake, "Differential effect of NaCl and polyethylene glycol on the ultrastructure of chloroplasts in rice seedlings," Journal of Plant Physiol., vol. 160, no. 5, pp. 573–575, Jan. 2003, doi: 10.1078/0176-1617-00948.

[43] G. R. Cramer et al., "Water and salinity stress in grapevines: early and late changes in transcript and metabolite profiles," Funct. Integr. Genomics, vol. 7, no. 2, pp. 111–134, Apr. 2007, doi: 10.1007/s10142-006-0039-y.

[44] E. Blumwald, "Sodium transport and salt tolerance in plants," Current Opinion in Cell Biology, vol. 12, no. 4, pp. 431–434, Aug. 2000, doi: 10.1016/S0955-0674(00)00112-5.

[45] W.-G. Choi, M. Toyota, S.-H. Kim, R. Hilleary, and S. Gilroy, "Salt stress-induced Ca2+ waves are associated with rapid, long-distance root-to-shoot signaling in plants," Proc. Natl. Acad. Sci. U.S.A., vol. 111, no. 17, pp. 6497–6502, Apr. 2014, doi: 10.1073/pnas.1319955111.

[46] G. Miller et al., "The plant NADPH oxidase RBOHD mediates rapid systemic signaling in response to diverse stimuli," Sci. Signal, vol. 2, no. 84, p. ra45, Aug. 2009, doi: 10.1126/scisignal.2000448.

[47] L. Ma et al., "The SOS2-SCaBP8 Complex Generates and Fine-Tunes an AtANN4-Dependent Calcium Signature under Salt Stress," Developmental Cell, vol. 48, no. 5, pp. 697–709.e5, Mar. 2019, doi: 10.1016/j.devcel.2019.02.010.

[48] J. Liu, M. Ishitani, U. Halfter, C.-S. Kim, and J.-K. Zhu, "The Arabidopsis thaliana SOS2 gene encodes a protein kinase that is required for salt tolerance," Proc. Natl. Acad. Sci. U.S.A., vol. 97, no. 7, pp. 3730–3734, Mar. 2000, doi: 10.1073/pnas.97.7.3730.

[49] H. Shi, F. J. Quintero, J. M. Pardo, and J.-K. Zhu, "The Putative Plasma Membrane Na+/H+ Antiporter SOS1 Controls Long-Distance Na+ Transport in Plants," Plant Cell, vol. 14, no. 2, pp. 465–477, Feb. 2002, doi: 10.1105/tpc.010371.

[50] F. J. Quintero et al., "Activation of the plasma membrane Na/H antiporter Salt-Overly-Sensitive 1 (SOS1) by phosphorylation of an auto-inhibitory C-terminal domain," Proc. Natl. Acad. Sci. U.S.A., vol. 108, no. 6, pp. 2611–2616, Feb. 2011, doi: 10.1073/pnas.1018921108.

[51] B.-G. Kim et al., "The calcium sensor CBL10 mediates salt tolerance by regulating ion homeostasis in Arabidopsis," The Plant Journal, vol. 52, no. 3, pp. 473–484, 2007, doi: 10.1111/j.1365-313X.2007.03249.x.

[52] B. Li et al., "Identification of a Stelar-Localized Transport Protein That Facilitates Root-to-Shoot Transfer of Chloride in Arabidopsis," Plant Physiol., vol. 170, no. 2, pp. 1014–1029, Feb. 2016, doi: 10.1104/pp.15.01163.

[53] P. Cubero-Font et al., "Silent S-Type Anion Channel Subunit SLAH1 Gates SLAH3 Open for Chloride Root-to-Shoot Translocation," Current Biology, vol. 26, no. 16, pp. 2213–2220, Aug. 2016, doi: 10.1016/j.cub.2016.06.045.

[54] S. W. Henderson et al., "Grapevine and Arabidopsis Cation-Chloride Cotransporters Localize to the Golgi and Trans-Golgi Network and Indirectly Influence Long-Distance Ion Transport and Plant Salt Tolerance," Plant Physiol., vol. 169, no. 3, pp. 2215–2229, Nov. 2015, doi: 10.1104/pp.15.00499.

[55] R. Storey, D. P. Schachtman, and M. R. Thomas, "Root structure and cellular chloride, sodium and potassium distribution in salinized grapevines," Plant, Cell & Environment, vol. 26, no. 6, pp. 789–800, 2003, doi: 10.1046/j.1365-3040.2003.01005.x.

[56] V. Demidchik and M. Tester, "Sodium Fluxes through Nonselective Cation Channels in the Plasma Membrane of Protoplasts from Arabidopsis Roots," Plant Physiol., vol. 128, no. 2, pp. 379–387, Feb. 2002, doi: 10.1104/pp.010524.

[57] I. Pottosin and O. Dobrovinskaya, "Non-selective cation channels in plasma and vacuolar membranes and their contribution to K+ transport," Journal of Plant Physiol., vol. 171, no. 9, pp. 732–742, May 2014, doi: 10.1016/j.jplph.2013.11.013.

[58] H. Wei, X. Wang, Y. He, H. Xu, and L. Wang, "Clock component OsPRR73 positively regulates rice salt tolerance by modulating OsHKT2;1-mediated sodium homeostasis," EMBO J., vol. 40, no. 3, p. EMBJ2020105086, Dec. 2020, doi: 10.15252/embj.2020105086.

[59] R. J. Davenport, A. Muñoz-Mayor, D. Jha, P. A. Essah, A. Rus, and M. Tester, "The Na+ transporter AtHKT1;1 controls retrieval of Na+ from the xylem in Arabidopsis," Plant, Cell & Environment, vol. 30, no. 4, pp. 497–507, Apr. 2007, doi: 10.1111/j.1365-3040.2007.01637.x.

[60] P. Berthomieu et al., "Functional analysis of AtHKT1 in Arabidopsis shows that Na+ recirculation by the phloem is crucial for salt tolerance," EMBO J., vol. 22, no. 9, pp. 2004–2014, May 2003, doi: 10.1093/emboj/cdg207.

[61] M. Hanana, O. Cagnac, T. Yamaguchi, S. Hamdi, A. Ghorbel, and E. Blumwald, "Molecular biology and transport properties of grapevine Na+/H+ antiporter," in Biosaline Agriculture and High Salinity Tolerance, C. Abdelly, M. Öztürk, M. Ashraf, and C. Grignon, Eds., Basel: Birkhäuser, 2008, pp. 305–315, doi: 10.1007/978-3-7643-8554-5_28.

[62] R. R. Walker, D. H. Blackmore, H. Gong, S. W. Henderson, M. Gilliham, and A. R. Walker, "Analysis of the salt exclusion phenotype in rooted leaves of grapevine (Vitis spp.)," Australian Journal of Grape and Wine Research, vol. 24, no. 3, pp. 317–326, 2018, doi: 10.1111/ajgw.12334.

[63] S. W. Henderson, U. Baumann, D. H. Blackmore, A. R. Walker, R. R. Walker, and M. Gilliham, "Shoot chloride exclusion and salt tolerance in grapevine is associated with differential ion transporter expression in roots," BMC Plant Biol., vol. 14, no. 1, p. 273, Oct. 2014, doi: 10.1186/s12870-014-0273-8.

[64] S. W. Henderson et al., "Functional differences in transport properties of natural HKT1;1 variants influence shoot Na+ exclusion in grapevine rootstocks," New Phytologist, vol. 217, no. 3, pp. 1113–1127, Feb. 2018, doi: 10.1111/nph.14888.

[65] Y. Wu et al., "The grapevine NaE sodium exclusion locus encodes sodium transporters with diverse transport properties and localisation," Journal of Plant Physiol., vol. 246–247, p. 153113, Mar. 2020, doi: 10.1016/j.jplph.2020.153113.

[66] X. Zhang, R. R. Walker, R. M. Stevens, and L. D. Prior, "Yield-salinity relationships of different grapevine (Vitis vinifera L.) scion-rootstock combinations," Australian Journal of Grape and Wine Research, vol. 8, no. 3, pp. 150–156, 2002, doi: 10.1111/j.1755-0238.2002.tb00250.x.

[67] L. Martin, H. Vila, R. Bottini, and F. Berli, "Rootstocks increase grapevine tolerance to NaCl through ion compartmentalization and exclusion," Acta Physiol. Plant., vol. 42, no. 9, p. 145, Sep. 2020, doi: 10.1007/s11738-020-03136-7.

[68] F. Meggio et al., "Biochemical and physiological responses of two grapevine rootstock genotypes to drought and salt treatments: Response of two genotypes to drought and salinity," Australian Journal of Grape and Wine Research, vol. 20, no. 2, pp. 310–323, Jun. 2014, doi: 10.1111/ajgw.12071.

[69] N. Ahmed et al., "Micronutrients and their effects on Horticultural crop quality, productivity and sustainability," Sci. Hortic., vol. 323, p. 112512, Jan. 2024, doi: 10.1016/j.scienta.2023.112512.

[70] R. Hell and U. W. Stephan, "Iron uptake, trafficking and homeostasis in plants," Planta, vol. 216, no. 4, pp. 541–551, Feb. 2003, doi: 10.1007/s00425-002-0920-4.

[71] E.-J. Hsieh and B. M. Waters, "Alkaline stress and iron deficiency regulate iron uptake and riboflavin synthesis gene expression differently in root and leaf

tissue: implications for iron deficiency chlorosis," J. Exp. Bot., vol. 67, no. 19, pp. 5671–5685, Oct. 2016, doi: 10.1093/jxb/erw328.

[72] J. Fu et al., "Physiological and molecular processes of plant tolerance to bicarbonate-induced alkaline stress," Stress Biology, vol. 6, no. 1, p. 53, Jul. 2026, doi: 10.1007/s44154-026-00325-1.

[73] P. J. Lea and R. A. Azevedo, "Nitrogen use efficiency. 1. Uptake of nitrogen from the soil," Annals of Applied Biology, vol. 149, no. 3, pp. 243–247, 2006, doi: 10.1111/j.1744-7348.2006.00101.x.

[74] X. F. Zhu, X. Y. Dong, Q. Wu, and R. F. Shen, "Ammonium regulates Fe deficiency responses by enhancing nitric oxide signaling in Arabidopsis thaliana," Planta, vol. 250, no. 4, pp. 1089–1102, Oct. 2019, doi: 10.1007/s00425-019-03202-6.

[75] S. Santi and W. Schmidt, "Dissecting iron deficiency-induced proton extrusion in Arabidopsis roots," New Phytologist, vol. 183, no. 4, pp. 1072–1084, Sep. 2009, doi: 10.1111/j.1469-8137.2009.02908.x.

[76] A. Martín-Barranco, J. Spielmann, G. Dubeaux, G. Vert, and E. Zelazny, "Dynamic Control of the High-Affinity Iron Uptake Complex in Root Epidermal Cells," Plant Physiol., vol. 184, no. 3, pp. 1236–1250, Nov. 2020, doi: 10.1104/pp.20.00234.

[77] M. Justi, C. A. Silva, and S. D. Rosa, "Organic acids as complexing agents for iron and their effects on the nutrition and growth of maize and soybean," Archives of Agronomy and Soil Science, vol. 68, no. 10, pp. 1369–1384, Aug. 2022, doi: 10.1080/03650340.2021.1893308.

[78] A. Vannozzi et al., "Transcriptional Characterization of a Widely-Used Grapevine Rootstock Genotype under Different Iron-Limited Conditions," Front. Plant Sci., vol. 7, Jan. 2017, doi: 10.3389/fpls.2016.01994.

[79] D. Selote, R. Samira, A. Matthiadis, J. W. Gillikin, and T. A. Long, "Iron-Binding E3 Ligase Mediates Iron Response in Plants by Targeting Basic Helix-Loop-Helix Transcription Factors," Plant Physiol., vol. 167, no. 1, pp. 273–286, Jan. 2015, doi: 10.1104/pp.114.250837.

[80] H.-Q. Ling, P. Bauer, Z. Bereczky, B. Keller, and M. Ganal, "The tomato fer gene encoding a bHLH protein controls iron-uptake responses in roots," Proc. Natl. Acad. Sci. U.S.A., vol. 99, no. 21, pp. 13938–13943, Oct. 2002, doi: 10.1073/pnas.212448699.

[81] B. Schwarz and P. Bauer, "FIT, a regulatory hub for iron deficiency and stress signaling in roots, and FIT-dependent and -independent gene signatures," J. Exp. Bot., vol. 71, no. 5, pp. 1694–1705, Mar. 2020, doi: 10.1093/jxb/eraa012.

[82] Y. Li et al., "IRON MAN interacts with BRUTUS to maintain iron homeostasis in Arabidopsis," Proc. Natl. Acad. Sci. U.S.A., vol. 118, no. 39, p. e2109063118, Sep. 2021, doi: 10.1073/pnas.2109063118.

[83] G. A. Vert, J.-F. Briat, and C. Curie, "Dual Regulation of the Arabidopsis High-Affinity Root Iron Uptake System by Local and Long-Distance Signals," Plant Physiol., vol. 132, no. 2, pp. 796–804, Jun. 2003, doi: 10.1104/pp.102.016089.

[84] P. De Nisi, G. Vigani, M. Dell'Orto, and G. Zocchi, "Application of the split root technique to study iron uptake in cucumber plants," Plant Physiology and Biochemistry, vol. 57, pp. 168–174, Aug. 2012, doi: 10.1016/j.plaphy.2012.05.022.

[85] Y. Enomoto, H. Hodoshima, H. Shimada, K. Shoji, T. Yoshihara, and F. Goto, "Long-distance signals positively regulate the expression of iron uptake genes in tobacco roots," Planta, vol. 227, no. 1, pp. 81–89, Dec. 2007, doi: 10.1007/s00425-007-0596-x.

[86] M. J. García et al., "Shoot to root communication is necessary to control the expression of iron-acquisition genes in Strategy I plants," Planta, vol. 237, no. 1, pp. 65–75, Jan. 2013, doi: 10.1007/s00425-012-1757-0.

[87] Z. Zhai et al., "OPT3 Is a Phloem-Specific Iron Transporter That Is Essential for Systemic Iron Signaling and Redistribution of Iron and Cadmium in Arabidopsis," Plant Cell, vol. 26, no. 5, pp. 2249–2264, May 2014, doi: 10.1105/tpc.114.123737.

[88] J.-C. Chia et al., "Loss of OPT3 function decreases phloem copper levels and impairs crosstalk between copper and iron homeostasis and shoot-to-root signaling in Arabidopsis thaliana," Plant Cell, vol. 35, no. 6, pp. 2157–2185, Jun. 2023, doi: 10.1093/plcell/koad053.

[89] J. I. Covarrubias and A. D. Rombolà, "Organic acids metabolism in roots of grapevine rootstocks under severe iron deficiency," Plant Soil, vol. 394, no. 1, pp. 165–175, Sep. 2015, doi: 10.1007/s11104-015-2530-5.

[90] R. Ksouri, S. M'rah, M. Gharsalli, and M. Lachaâl, "Biochemical Responses to True and Bicarbonate-Induced Iron Deficiency in Grapevine Genotypes," Journal of Plant Nutrition, vol. 29, no. 2, pp. 305–315, Feb. 2006, doi: 10.1080/01904160500476897.

[91] J. I. Covarrubias and A. D. Rombolà, "Physiological and biochemical responses of the iron chlorosis tolerant grapevine rootstock 140 Ruggeri to iron deficiency and bicarbonate," Plant Soil, vol. 370, no. 1, pp. 305–315, Sep. 2013, doi: 10.1007/s11104-013-1623-2.

[92] B. P. M. Ngou, P. Ding, and J. D. G. Jones, "Thirty years of resistance: Zig-zag through the plant immune system," Plant Cell, vol. 34, no. 5, pp. 1447–1478, Apr. 2022, doi: 10.1093/plcell/koac041.

[93] Y. Lu and K. Tsuda, "Intimate Association of PRR- and NLR-Mediated Signaling in Plant Immunity," MPMI, vol. 34, no. 1, pp. 3–14, Jan. 2021, doi: 10.1094/MPMI-08-20-0239-IA.

[94] K. Tsuda and F. Katagiri, "Comparing signaling mechanisms engaged in pattern-triggered and effector-triggered immunity," Current Opinion in Plant Biology, vol. 13, no. 4, pp. 459–465, Aug. 2010, doi: 10.1016/j.pbi.2010.04.006.

[95] M. Bernoux, H. Zetzsche, and J. Stuttmann, "Connecting the dots between cell surface- and intracellular-triggered immune pathways in plants," Current Opinion in Plant Biology, vol. 69, p. 102276, Oct. 2022, doi: 10.1016/j.pbi.2022.102276.

[96] J.-B. Morel and J. L. Dangl, "The hypersensitive response and the induction of cell death in plants," Cell Death Differ., vol. 4, no. 8, pp. 671–683, Dec. 1997, doi: 10.1038/sj.cdd.4400309.

[97] B. T. Ross, N. K. Zidack, and M. L. Flenniken, "Extreme Resistance to Viruses in Potato and Soybean," Front. Plant Sci., vol. 12, p. 658981, Apr. 2021, doi: 10.3389/fpls.2021.658981.

[98] J. D. G. Jones, B. J. Staskawicz, and J. L. Dangl, "The plant immune system: From discovery to deployment," Cell, vol. 187, no. 9, pp. 2095–2116, Apr. 2024, doi: 10.1016/j.cell.2024.03.045.

[99] B. P. M. Ngou, H.-K. Ahn, P. Ding, and J. D. G. Jones, "Mutual potentiation of plant immunity by cell-surface and intracellular receptors," Nature, vol. 592, no. 7852, pp. 110–115, Apr. 2021, doi: 10.1038/s41586-021-03315-7.

[100] M. Yuan et al., "Pattern-recognition receptors are required for NLR-mediated plant immunity," Nature, vol. 592, no. 7852, pp. 105–109, Apr. 2021, doi: 10.1038/s41586-021-03316-6.

[101] R. N. Pruitt et al., "The EDS1–PAD4–ADR1 node mediates Arabidopsis pattern-triggered immunity," Nature, vol. 598, no. 7881, pp. 495–499, Oct. 2021, doi: 10.1038/s41586-021-03829-0.

[102] H. Tian et al., "Activation of TIR signalling boosts pattern-triggered immunity," Nature, vol. 598, no. 7881, pp. 500–503, Oct. 2021, doi: 10.1038/s41586-021-03987-1.

[103] R. Bari and J. D. G. Jones, "Role of plant hormones in plant defence responses," Plant Mol. Biol., vol. 69, no. 4, pp. 473–488, Mar. 2009, doi: 10.1007/s11103-008-9435-0.

[104] S. Huang, X. Zhang, and W. G. D. Fernando, "Directing Trophic Divergence in Plant-Pathogen Interactions: Antagonistic Phytohormones With NO Doubt?," Front. Plant Sci., vol. 11, p. 600063, Dec. 2020, doi: 10.3389/fpls.2020.600063.

[105] Y.-C. Chen et al., "N-hydroxy-pipecolic acid is a mobile metabolite that induces systemic disease resistance in Arabidopsis," Proc. Natl. Acad. Sci. U.S.A., vol. 115, no. 21, pp. E4920–E4929, May 2018, doi: 10.1073/pnas.1805291115.

[106] I. Yildiz et al., "The mobile SAR signal N-hydroxypipecolic acid induces NPR1-dependent transcriptional reprogramming and immune priming," Plant Physiol., vol. 186, no. 3, pp. 1679–1705, Jul. 2021, doi: 10.1093/plphys/kiab166.

[107] P. Zhang, E. Jackson, X. Li, and Y. Zhang, "Salicylic acid and jasmonic acid in plant immunity," Hortic. Res., vol. 12, no. 7, p. uhaf082, Jul. 2025, doi: 10.1093/hr/uhaf082.

[108] K. Zhang, R. Halitschke, C. Yin, C.-J. Liu, and S.-S. Gan, "Salicylic acid 3-hydroxylase regulates Arabidopsis leaf longevity by mediating salicylic acid catabolism," Proc. Natl. Acad. Sci. U.S.A., vol. 110, no. 36, pp. 14807–14812, Sep. 2013, doi: 10.1073/pnas.1302702110.

[109] Y. Zhang et al., "S5H/DMR6 Encodes a Salicylic Acid 5-Hydroxylase That Fine-Tunes Salicylic Acid Homeostasis," Plant Physiol., vol. 175, no. 3, pp. 1082–1093, Nov. 2017, doi: 10.1104/pp.17.00695.

[110] C. Pirrello et al., "Grapevine DMR6-1 Is a Candidate Gene for Susceptibility to Downy Mildew," Biomolecules, vol. 12, no. 2, p. 182, 2022, doi: 10.3390/biom12020182.

[111] T. Zeilmaker et al., "DOWNY MILDEW RESISTANT 6 and DMR6-LIKE OXYGENASE 1 are partially redundant but distinct suppressors of immunity in Arabidopsis," The Plant Journal, vol. 81, no. 2, pp. 210–222, Jan. 2015, doi: 10.1111/tpj.12719.

[112] N. P. Kieu, M. Lenman, E. S. Wang, B. L. Petersen, and E. Andreasson, "Mutations introduced in susceptibility genes through CRISPR/Cas9 genome editing confer increased late blight resistance in potatoes," Sci. Rep., vol. 11, no. 1, p. 4487, Feb. 2021, doi: 10.1038/s41598-021-83972-w.

[113] M. Ferrero et al., "Enhancing tolerance to Phytophthora spp. in eggplant through DMR6–1 CRISPR/Cas9 knockout," Plant Stress, vol. 14, p. 100691, Dec. 2024, doi: 10.1016/j.stress.2024.100691.

[114] L. Giacomelli et al., "Simultaneous editing of two DMR6 genes in grapevine results in reduced susceptibility to downy mildew," Front. Plant Sci., vol. 14, Aug. 2023, doi: 10.3389/fpls.2023.1242240.

[115] S. Djennane et al., "CRISPR/Cas9 editing of Downy mildew resistant 6 (DMR6-1) in grapevine leads to reduced susceptibility to Plasmopara viticola," J. Exp. Bot., vol. 75, no. 7, pp. 2100–2112, Mar. 2024, doi: 10.1093/jxb/erad487.

[116] C. C. Holm, M. Havenga, J. G. Lashbrooke, J. T. Burger, and M. Campa, "CRISPR/Cas9-genome editing identifies the dual role of VvDMR6.1 in downy mildew resistance and response to water limitation in grapevine," Plant Stress, vol. 20, p. 101306, Mar. 2026, doi: 10.1016/j.stress.2026.101306.

[117] W. Wei and Y. Zhao, "Phytoplasma Taxonomy: Nomenclature, Classification, and Identification," Biology, vol. 11, no. 8, p. 1119, Aug. 2022, doi: 10.3390/biology11081119.

[118] F. Quaglino et al., "'Candidatus Phytoplasma solani', a novel taxon associated with stolbur- and bois noir-related diseases of plants," International Journal of Systematic and Evolutionary Microbiology, vol. 63, no. Pt_8, pp. 2879–2894, 2013, doi: 10.1099/ijs.0.044750-0.

[119] F. Quaglino et al., "Identification and ecology of alternative insect vectors of 'Candidatus Phytoplasma solani' to grapevine," Sci. Rep., vol. 9, no. 1, p. 19522, Dec. 2019, doi: 10.1038/s41598-019-56076-9.

[120] M. Kube, J. Mitrovic, B. Duduk, R. Rabus, and E. Seemüller, "Current View on Phytoplasma Genomes and Encoded Metabolism," The Scientific World Journal, vol. 2012, no. 1, p. 185942, 2012, doi: 10.1100/2012/185942.

[121] M. S. Music, I. Samarzija, S. A. Hogenhout, M. Haryono, S.-T. Cho, and C.-H. Kuo, "The genome of 'Candidatus Phytoplasma solani' strain SA-1 is highly dynamic and prone to adopting foreign sequences," Systematic and Applied

Microbiology, vol. 42, no. 2, pp. 117–127, Mar. 2019, doi: 10.1016/j.syapm.2018.10.008.

[122] M. Drcelic, A. Skiljaica, B. Polak, N. Bauer, and M. Seruga Music, "'Candidatus Phytoplasma solani' Predicted Effector SAP11-like Alters Morphology of Transformed Arabidopsis Plants and Interacts with AtTCP2 and AtTCP4 Plant Transcription Factors," Pathogens, vol. 13, no. 10, p. 893, Oct. 2024, doi: 10.3390/pathogens13100893.

[123] P. Pecher et al., "Phytoplasma SAP11 effector destabilization of TCP transcription factors differentially impact development and defence of Arabidopsis versus maize," PLOS Pathogens, vol. 15, no. 9, p. e1008035, Sep. 2019, doi: 10.1371/journal.ppat.1008035.

[124] A. M. MacLean et al., "Phytoplasma effector SAP54 hijacks plant reproduction by degrading MADS-box proteins and promotes insect colonization in a RAD23-dependent manner," PLOS Biol., vol. 12, no. 4, p. e1001835, Apr. 2014, doi: 10.1371/journal.pbio.1001835.

[125] M. Correa Marrero et al., "Protein interaction mapping reveals widespread targeting of development-related host transcription factors by phytoplasma effectors," The Plant Journal, vol. 117, no. 4, pp. 1281–1297, 2024, doi: 10.1111/tpj.16546.

[126] M. Hren et al., "'Bois noir' phytoplasma induces significant reprogramming of the leaf transcriptome in the field grown grapevine," BMC Genomics, vol. 10, no. 1, p. 460, Oct. 2009, doi: 10.1186/1471-2164-10-460.

[127] M. Bertamini and N. Nedunchezhian, "Effects of Phytoplasma [Stolbur-Subgroup (Bois Noir-BN)] on Photosynthetic Pigments, Saccharides, Ribulose 1,5-Bisphosphate Carboxylase, Nitrate and Nitrite Reductases, and Photosynthetic Activities in Field-Grown Grapevine (Vitis vinifera L. cv. Chardonnay) Leaves," Photosynthetica, vol. 39, no. 1, pp. 119–122, Mar. 2001, doi: 10.1023/A:1012412406727.

[128] M. Bertamini, N. Nedunchezhian, F. Tomasi, and M. S. Grando, "Phytoplasma [Stolbur-subgroup (Bois Noir-BN)] infection inhibits photosynthetic pigments, ribulose-1,5-bisphosphate carboxylase and photosynthetic activities in field grown grapevine (Vitis vinifera L. cv. Chardonnay) leaves," Physiological and Molecular Plant Pathology, vol. 61, no. 6, pp. 357–366, Dec. 2002, doi: 10.1006/pmpp.2003.0449.

[129] D. Rusjan, H. Halbwirth, K. Stich, M. Mikulič-Petkovšek, and R. Veberič, "Biochemical response of grapevine variety 'Chardonnay' (Vitis vinifera L.) to infection with grapevine yellows (Bois noir)," Eur. J. Plant Pathol., vol. 134, no. 2, pp. 231–237, Oct. 2012, doi: 10.1007/s10658-012-9988-2.

[130] N. Prezelj et al., "Metabolic Consequences of Infection of Grapevine (Vitis vinifera L.) cv. 'Modra frankinja' with Flavescence Dorée Phytoplasma," Front. Plant Sci., vol. 7, p. 711, May 2016, doi: 10.3389/fpls.2016.00711.

[131] C. Negro et al., "Biochemical Changes in Leaves of Vitis vinifera cv. Sangiovese Infected by Bois Noir Phytoplasma," Pathogens, vol. 9, no. 4, p. 269, Apr. 2020, doi: 10.3390/pathogens9040269.

[132] C. Bernardini et al., "Increased susceptibility to Chrysanthemum Yellows phytoplasma infection in Atcals7ko plants is accompanied by enhanced expression of carbohydrate transporters," Planta, vol. 256, no. 2, p. 43, 2022, doi: 10.1007/s00425-022-03954-8.

[133] F. D. Marco et al., "Involvement of SUT1 and SUT2 Sugar Transporters in the Impairment of Sugar Transport and Changes in Phloem Exudate Contents in Phytoplasma-Infected Plants," Int. J. Mol. Sci., vol. 22, no. 2, p. 745, Jan. 2021, doi: 10.3390/ijms22020745.

[134] D. Rusjan, R. Veberič, and M. Mikulič-Petkovšek, "The response of phenolic compounds in grapes of the variety 'Chardonnay' (Vitis vinifera L.) to the infection by phytoplasma Bois noir," Eur. J. Plant Pathol., vol. 133, no. 4, pp. 965–974, Aug. 2012, doi: 10.1007/s10658-012-9967-7.

[135] A. Sugio, H. N. Kingdom, A. M. MacLean, V. M. Grieve, and S. A. Hogenhout, "Phytoplasma protein effector SAP11 enhances insect vector reproduction by manipulating plant development and defense hormone biosynthesis," Proc. Natl. Acad. Sci. U.S.A., vol. 108, no. 48, pp. E1254–E1263, Nov. 2011, doi: 10.1073/pnas.1105664108.

[136] B. Romero, A. Mithöfer, C. Olivier, T. Wist, and S. M. Prager, "The Role of Plant Defense Signaling Pathways in Phytoplasma-Infected and Uninfected Aster Leafhoppers' Oviposition, Development, and Settling Behavior," J. Chem. Ecol., vol. 50, no. 5, pp. 276–289, Jun. 2024, doi: 10.1007/s10886-024-01488-9.

[137] A. Rotter et al., "Statistical modeling of long-term grapevine response to 'Candidatus Phytoplasma solani' infection in the field," Eur. J. Plant Pathol., vol. 150, no. 3, pp. 653–668, Mar. 2018, doi: 10.1007/s10658-017-1310-x.

[138] A. R. Paolacci et al., "Jasmonate-mediated defence responses, unlike salicylate-mediated responses, are involved in the recovery of grapevine from bois noir disease," BMC Plant Biol., vol. 17, no. 1, p. 118, Jul. 2017, doi: 10.1186/s12870-017-1069-4.

[139] W. Jiang, H. Zhou, H. Bi, M. Fromm, B. Yang, and D. P. Weeks, "Demonstration of CRISPR/Cas9/sgRNA-mediated targeted gene modification in Arabidopsis, tobacco, sorghum and rice," Nucl. Acids Res., vol. 41, no. 20, p. e188, Nov. 2013, doi: 10.1093/nar/gkt780.

[140] D. Zhang, Z. Zhang, T. Unver, and B. Zhang, "CRISPR/Cas: A powerful tool for gene function study and crop improvement," Journal of Advanced Research, vol. 29, pp. 207–221, Mar. 2021, doi: 10.1016/j.jare.2020.10.003.

[141] J. W. Woo et al., "DNA-free genome editing in plants with preassembled CRISPR-Cas9 ribonucleoproteins," Nat. Biotechnol., vol. 33, no. 11, pp. 1162–1164, Nov. 2015, doi: 10.1038/nbt.3389.

[142] G. Campos, C. Chialva, S. Miras, and D. Lijavetzky, "New Technologies and Strategies for Grapevine Breeding Through Genetic Transformation," Front. Plant Sci., vol. 12, Nov. 2021, doi: 10.3389/fpls.2021.767522.

[143] G. Gambino, P. Ruffa, R. Vallania, and I. Gribaudo, "Somatic embryogenesis from whole flowers, anthers and ovaries of grapevine (Vitis spp.)," Plant Cell Tiss.

Organ Cult., vol. 90, no. 1, pp. 79–83, Jul. 2007, doi: 10.1007/s11240-007-9256-x.

[144] S. A. Dhekney, Z. T. Li, M. E. Compton, and D. J. Gray, "Optimizing Initiation and Maintenance of Vitis Embryogenic Cultures," HortScience, vol. 44, no. 5, pp. 1400–1406, Aug. 2009, doi: 10.21273/HORTSCI.44.5.1400.

[145] I. Nakajima et al., "CRISPR/Cas9-mediated targeted mutagenesis in grape," PLOS ONE, vol. 12, no. 5, p. e0177966, May 2017, doi: 10.1371/journal.pone.0177966.

[146] R. Strah et al., "Combined omics data reveal multilevel response to water deficit in grapevine disease-resistant varieties," Front. Plant Sci., vol. 17, Jul. 2026, doi: 10.3389/fpls.2026.1818883.

[147] I. Buesa et al., "Physiological and Transcriptional Responses to Saline Irrigation of Young 'Tempranillo' Vines Grafted Onto Different Rootstocks," Front. Plant Sci., vol. 13, Jun. 2022, doi: 10.3389/fpls.2022.866053.

[148] S. Khalil et al., "The activation of iron deficiency responses of grapevine rootstocks is dependent to the availability of the nitrogen forms," BMC Plant Biol., vol. 24, no. 1, p. 218, Mar. 2024, doi: 10.1186/s12870-024-04906-y.

[149] S. Khalil et al., "Lime-induced iron deficiency stimulates a stronger response in tolerant grapevine rootstocks compared to low iron availability," Plant Stress, vol. 16, p. 100841, Jun. 2025, doi: 10.1016/j.stress.2025.100841.

[150] M. Dermastia et al., "Differential Response of Grapevine to Infection with 'Candidatus Phytoplasma solani' in Early and Late Growing Season through Complex Regulation of mRNA and Small RNA Transcriptomes," Int. J. Mol. Sci., vol. 22, no. 7, p. 3531, 2021, doi: 10.3390/ijms22073531.

[151] L. Bavaresco et al., "Grapevine breeding programs in Italy," in Grapevine Breeding Programs for the Wine Industry, A. Reynolds, Ed., ser. Woodhead Publishing Series in Food Science, Technology and Nutrition. Oxford: Woodhead Publishing, 2015, pp. 135–157, doi: 10.1016/B978-1-78242-075-0.00007-7.

[152] R. Braidotti et al., "Multi-hormonal analysis and aquaporins regulation reveal new insights on drought tolerance in grapevine," Journal of Plant Physiol., vol. 296, p. 154243, May 2024, doi: 10.1016/j.jplph.2024.154243.

[153] R. López-Urrea, A. Montoro, F. Mañas, P. López-Fuster, and E. Fereres, "Evapotranspiration and crop coefficients from lysimeter measurements of mature 'Tempranillo' wine grapes," Agricultural Water Management, vol. 112, pp. 13–20, Sep. 2012, doi: 10.1016/j.agwat.2012.05.009.

[154] D. R. Hoagland and D. I. Arnon, The Water-Culture Method for Growing Plants Without Soil. Berkeley, CA: University of California, College of Agriculture, 1950. Accessed: Sep. 16, 2026. [Online]. Available: http://archive.org/details/watercultureme3450hoag

[155] J. I. Covarrubias, C. Retamales, S. Donnini, A. D. Rombolà, and C. Pastenes, "Contrasting physiological responses to iron deficiency in Cabernet Sauvignon grapevines grafted on two rootstocks," Sci. Hortic., vol. 199, pp. 1–8, Feb. 2016, doi: 10.1016/j.scienta.2015.12.013.

[156] A. Aryan, G. Brader, J. Mörtel, M. Pastar, and M. Riedle-Bauer, "An abundant 'Candidatus Phytoplasma solani' tuf b strain is associated with grapevine, stinging nettle and Hyalesthes obsoletus," Eur. J. Plant Pathol., vol. 140, no. 2, pp. 213–227, Oct. 2014, doi: 10.1007/s10658-014-0455-0.

[157] A. Carra, G. Gambino, and A. Schubert, "A cetyltrimethylammonium bromide-based method to extract low-molecular-weight RNA from polysaccharide-rich plant tissues," Anal. Biochem., vol. 360, no. 2, pp. 318–320, Jan. 2007, doi: 10.1016/j.ab.2006.09.022.

[158] A. Canaguier et al., "A new version of the grapevine reference genome assembly (12X.v2) and of its annotation (VCost.v3)," Genomics Data, vol. 14, pp. 56–62, Dec. 2017, doi: 10.1016/j.gdata.2017.09.002.

[159] R Core Team, R: A Language and Environment for Statistical Computing. Vienna, Austria: R Foundation for Statistical Computing, 2020. [Online]. Available: https://www.R-project.org/

[160] M. E. Ritchie et al., "limma powers differential expression analyses for RNA-sequencing and microarray studies," Nucl. Acids Res., vol. 43, no. 7, pp. e47–e47, Apr. 2015, doi: 10.1093/nar/gkv007.

[161] M. D. Robinson, D. J. McCarthy, and G. K. Smyth, "edgeR : a Bioconductor package for differential expression analysis of digital gene expression data," Bioinformatics, vol. 26, no. 1, pp. 139–140, Jan. 2010, doi: 10.1093/bioinformatics/btp616.

[162] H. Wickham, *ggplot2*. in Use R! Cham: Springer International Publishing, 2016. doi: 10.1007/978-3-319-24277-4.

[163] A. Subramanian et al., "Gene set enrichment analysis: A knowledge-based approach for interpreting genome-wide expression profiles," Proc. Natl. Acad. Sci. U.S.A., vol. 102, no. 43, pp. 15545–15550, Oct. 2005, doi: 10.1073/pnas.0506580102.

[164] Ž. Ramšak et al., "GoMapMan: integration, consolidation and visualization of plant gene annotations within the MapMan ontology," Nucl. Acids Res., vol. 42, no. D1, pp. D1167–D1175, Jan. 2014, doi: 10.1093/nar/gkt1056.

[165] L. Torregrosa, "A simple and efficient method to obtain stable embryogenic cultures from anthers of Vitis vinifera L.," Vitis, vol. 37, May 1998.

[166] J.-P. Concordet and M. Haeussler, "CRISPOR: intuitive guide selection for CRISPR/Cas9 genome editing experiments and screens," Nucl. Acids Res., vol. 46, no. W1, pp. W242–W245, Jul. 2018, doi: 10.1093/nar/gky354.

[167] E. Bertini, G. B. Tornielli, M. Pezzotti, and S. Zenoni, "Regeneration of plants from embryogenic callus-derived protoplasts of Garganega and Sangiovese grapevine (Vitis vinifera L.) cultivars," Plant Cell Tiss. Organ Cult., vol. 138, no. 2, pp. 239–246, Aug. 2019, doi: 10.1007/s11240-019-01619-1.

[168] S. Najafi, E. Bertini, E. D'Incà, M. Fasoli, and S. Zenoni, "DNA-free genome editing in grapevine using CRISPR/Cas9 ribonucleoprotein complexes followed by protoplast regeneration," Hortic. Res., vol. 10, no. 1, p. uhac240, Jan. 2023, doi: 10.1093/hr/uhac240.

[169] R. Strah, E. Bertini, S. Zenoni, M. P. Novak, M. Pezzotti, and M. Dermastia, "Protocols for Grapevine Transformation: Tissue Preparation, Protoplast Isolation, and Cultivation," in Phytoplasma: Methods and Protocols, K. Janik and M. Tabarelli, Eds., New York, NY: Springer US, 2026, pp. 133–149, doi: 10.1007/978-1-0716-5104-9_11.

[170] M. Karimi, D. Inzé, and A. Depicker, "GATEWAY vectors for Agrobacterium-mediated plant transformation," Trends in Plant Science, vol. 7, no. 5, pp. 193–195, May 2002, doi: 10.1016/S1360-1385(02)02251-3.

[171] J. P. Nitsch and C. Nitsch, "Haploid Plants from Pollen Grains," Science, vol. 163, no. 3862, pp. 85–87, Jan. 1969, doi: 10.1126/science.163.3862.85.

[172] R. Chee, R. Pool, and D. Bucher, "A Method for Large Scale in vitro Propagation of Vitis," 1984. Accessed: Sep. 16, 2026. [Online]. Available: https://hdl.handle.net/1813/5140

[173] C. Lovisolo and A. Schubert, "Effects of water stress on vessel size and xylem hydraulic conductivity in Vitis vinifera L.," J. Exp. Bot., vol. 49, no. 321, pp. 693–700, Apr. 1998, doi: 10.1093/jxb/49.321.693.

[174] E. Gerzon et al., "Grapevine Anatomy as a Possible Determinant of Isohydric or Anisohydric Behavior," Am. J. Enol. Vitic., vol. 66, no. 3, pp. 340–347, Aug. 2015, doi: 10.5344/ajev.2015.14090.

[175] A. Degu et al., "Swift metabolite changes and leaf shedding are milestones in the acclimation process of grapevine under prolonged water stress," BMC Plant Biol., vol. 19, no. 1, p. 69, Feb. 2019, doi: 10.1186/s12870-019-1652-y.

[176] R. Falchi et al., "Summer drought stress: differential effects on cane anatomy and non-structural carbohydrate content in overwintering Cabernet Sauvignon and Syrah vines," in BIO Web of Conferences, EDP Sciences, 2019, p. 03007, doi: 10.1051/bioconf/20191303007.

[177] L. Rossdeutsch et al., "ABA-mediated responses to water deficit separate grapevine genotypes by their genetic background," BMC Plant Biol., vol. 16, p. 91, Apr. 2016, doi: 10.1186/s12870-016-0778-4.

[178] Y. Cohen, M. Reuveni, L. Gur, and S. Ovadia, "Survival in the field of Pseudoperonospora cubensis and Plasmopara viticola after extreme hot and dry weather conditions in Israel," Phytoparasitica, vol. 48, no. 5, pp. 699–703, Nov. 2020, doi: 10.1007/s12600-020-00839-y.

[179] G. A. Gambetta, J. C. Herrera, S. Dayer, Q. Feng, U. Hochberg, and S. D. Castellarin, "The physiology of drought stress in grapevine: towards an integrative definition of drought tolerance," J. Exp. Bot., vol. 71, no. 16, pp. 4658–4676, Aug. 2020, doi: 10.1093/jxb/eraa245.

[180] U. Hochberg, A. Perry, S. Rachmilevitch, A. Ben-Gal, and O. Sperling, "Instantaneous and lasting effects of drought on grapevine water use," Agricultural and Forest Meteorology, vol. 338, p. 109521, Jul. 2023, doi: 10.1016/j.agrformet.2023.109521.

[181] A. Deloire, A. Carbonneau, Z. Wang, and H. Ojeda, "Vine and water: a short review," OENO One, vol. 38, no. 1, pp. 1–13, Mar. 2004, doi: 10.20870/oeno-one.2004.38.1.932.

[182] L. W. de Almeida, L. Torregrosa, G. Dournes, A. Pellegrino, H. Ojeda, and A. Roland, "New Fungus-Resistant Grapevine Vitis and V. vinifera L. × M. rotundifolia Derivative Hybrids Display a Drought-Independent Response in Thiol Precursor Levels," J. Agric. Food Chem., vol. 72, no. 4, pp. 1855–1863, Jan. 2024, doi: 10.1021/acs.jafc.2c08595.

[183] H. J. W. Dace, A. E. Adetunji, J. P. Moore, J. M. Farrant, and H. W. M. Hilhorst, "A review of the role of metabolites in vegetative desiccation tolerance of angiosperms," Current Opinion in Plant Biology, vol. 75, p. 102410, Oct. 2023, doi: 10.1016/j.pbi.2023.102410.

[184] R. Angelovici, G. Galili, A. R. Fernie, and A. Fait, "Seed desiccation: a bridge between maturation and germination," Trends in Plant Science, vol. 15, no. 4, pp. 211–218, Apr. 2010, doi: 10.1016/j.tplants.2010.01.003.

[185] A. I. ElSayed, M. S. Rafudeen, and D. Golldack, "Physiological aspects of raffinose family oligosaccharides in plants: protection against abiotic stress," Plant Biology, vol. 16, no. 1, pp. 1–8, Jan. 2014, doi: 10.1111/plb.12053.

[186] S. Sengupta, S. Mukherjee, P. Basak, and A. L. Majumder, "Significance of galactinol and raffinose family oligosaccharide synthesis in plants," Front. Plant Sci., vol. 6, Aug. 2015, doi: 10.3389/fpls.2015.00656.

[187] M. M. Chaves and M. M. Oliveira, "Mechanisms underlying plant resilience to water deficits: prospects for water-saving agriculture," J. Exp. Bot., vol. 55, no. 407, pp. 2365–2384, Nov. 2004, doi: 10.1093/jxb/erh269.

[188] S. Dal Santo et al., "Distinct transcriptome responses to water limitation in isohydric and anisohydric grapevine cultivars," BMC Genomics, vol. 17, no. 1, p. 815, Oct. 2016, doi: 10.1186/s12864-016-3136-x.

[189] C. R. Catacchio et al., "Transcriptomic and genomic structural variation analyses on grape cultivars reveal new insights into the genotype-dependent responses to water stress," Sci. Rep., vol. 9, no. 1, p. 2809, Feb. 2019, doi: 10.1038/s41598-019-39010-x.

[190] N. Cochetel et al., "Drought tolerance of the grapevine, Vitis champinii cv. Ramsey, is associated with higher photosynthesis and greater transcriptomic responsiveness of abscisic acid biosynthesis and signaling," BMC Plant Biol., vol. 20, no. 1, p. 55, Feb. 2020, doi: 10.1186/s12870-019-2012-7.

[191] U. Hochberg et al., "Metabolite profiling and network analysis reveal coordinated changes in grapevine water stress response," BMC Plant Biol., vol. 13, no. 1, p. 184, Nov. 2013, doi: 10.1186/1471-2229-13-184.

[192] K. Urano et al., "Characterization of the ABA-regulated global responses to dehydration in Arabidopsis by metabolomics," The Plant Journal, vol. 57, no. 6, pp. 1065–1078, 2009, doi: 10.1111/j.1365-313X.2008.03748.x.

[193] T. Obata and A. R. Fernie, "The use of metabolomics to dissect plant responses to abiotic stresses," Cell. Mol. Life Sci., vol. 69, no. 19, pp. 3225–3243, Oct. 2012, doi: 10.1007/s00018-012-1091-5.

[194] K. Nahar, M. Hasanuzzaman, and M. Fujita, "Roles of Osmolytes in Plant Adaptation to Drought and Salinity," in Osmolytes and Plants Acclimation to Changing Environment: Emerging Omics Technologies, N. Iqbal, R. Nazar,

and N. A. Khan, Eds., New Delhi: Springer India, 2016, pp. 37–68, doi: 10.1007/978-81-322-2616-1_4.

[195] M. S. Haider et al., "Insights into grapevine defense response against drought as revealed by biochemical, physiological and RNA-Seq analysis," Sci. Rep., vol. 7, no. 1, p. 13134, Oct. 2017, doi: 10.1038/s41598-017-13464-3.

[196] C. Chen, X. Cui, P. Zhang, Z. Wang, and J. Zhang, "Expression of the pyrroline-5-carboxylate reductase (P5CR) gene from the wild grapevine Vitis yeshanensis promotes drought resistance in transgenic Arabidopsis," Plant Physiology and Biochemistry, vol. 168, pp. 188–201, Nov. 2021, doi: 10.1016/j.plaphy.2021.10.004.

[197] P. Zhang, X. Cui, C. Chen, and J. Zhang, "Overexpression of the VyP5CR gene increases drought tolerance in transgenic grapevine (V. vinifera L.)," Sci. Hortic., vol. 316, p. 112019, Jun. 2023, doi: 10.1016/j.scienta.2023.112019.

[198] P. P. Lehr, E. Hernández-Montes, J. Ludwig-Müller, M. Keller, and C. Zörb, "Abscisic acid and proline are not equivalent markers for heat, drought and combined stress in grapevines," Australian Journal of Grape and Wine Research, vol. 28, no. 1, pp. 119–130, 2022, doi: 10.1111/ajgw.12523.

[199] J. W. Tan et al., "Global transcriptome and gene co-expression network analyses reveal regulatory and non-additive effects of drought and heat stress in grapevine," Front. Plant Sci., vol. 14, Feb. 2023, doi: 10.3389/fpls.2023.1096225.

[200] F. Takahashi, T. Kuromori, K. Urano, K. Yamaguchi-Shinozaki, and K. Shinozaki, "Drought Stress Responses and Resistance in Plants: From Cellular Responses to Long-Distance Intercellular Communication," Front. Plant Sci., vol. 11, Sep. 2020, doi: 10.3389/fpls.2020.556972.

[201] A. M. Kinnersley and F. J. Turano, "Gamma Aminobutyric Acid (GABA) and Plant Responses to Stress," Critical Reviews in Plant Sciences, vol. 19, no. 6, pp. 479–509, Nov. 2000, doi: 10.1080/07352680091139277.

[202] H. Jia et al., "Sucrose functions as a signal involved in the regulation of strawberry fruit development and ripening," New Phytologist, vol. 198, no. 2, pp. 453–465, 2013, doi: 10.1111/nph.12176.

[203] T. Hirayama and K. Shinozaki, "Research on plant abiotic stress responses in the post-genome era: past, present and future," The Plant Journal, vol. 61, no. 6, pp. 1041–1052, 2010, doi: 10.1111/j.1365-313X.2010.04124.x.

[204] L. Fang et al., "Expression of Vitis amurensis NAC26 in Arabidopsis enhances drought tolerance by modulating jasmonic acid synthesis," J. Exp. Bot., vol. 67, no. 9, pp. 2829–2845, Apr. 2016, doi: 10.1093/jxb/erw122.

[205] V. S. Khadka et al., "Transcriptomic response is more sensitive to water deficit in shoots than roots of Vitis riparia (Michx.)," BMC Plant Biol., vol. 19, p. 72, Feb. 2019, doi: 10.1186/s12870-019-1664-7.

[206] W. J. Sweet, J. C. Morrison, J. M. Labavitch, and M. A. Matthews, "Altered Synthesis and Composition of Cell Wall of Grape (Vitis vinifera L.) Leaves during Expansion and Growth-Inhibiting Water Deficits," Plant Cell Physiol.,

vol. 31, no. 4, pp. 407–414, Jan. 1990, doi: 10.1093/oxfordjournals.pcp.a077924.

[207] H. Le Gall, F. Philippe, J.-M. Domon, F. Gillet, J. Pelloux, and C. Rayon, "Cell Wall Metabolism in Response to Abiotic Stress," Plants, vol. 4, no. 1, pp. 112–166, Mar. 2015, doi: 10.3390/plants4010112.

[208] Y. Osakabe, K. Yamaguchi-Shinozaki, K. Shinozaki, and L.-S. P. Tran, "Sensing the environment: key roles of membrane-localized kinases in plant perception and response to abiotic stress," J. Exp. Bot., vol. 64, no. 2, pp. 445–458, Jan. 2013, doi: 10.1093/jxb/ers354.

[209] D. W. Hopper, R. Ghan, K. A. Schlauch, and G. R. Cramer, "Transcriptomic network analyses of leaf dehydration responses identify highly connected ABA and ethylene signaling hubs in three grapevine species differing in drought tolerance," BMC Plant Biol., vol. 16, p. 118, May 2016, doi: 10.1186/s12870-016-0804-6.

[210] C. Li et al., "A GDSL-motif esterase/acyltransferase/lipase is responsible for leaf water retention in barley," Plant Direct, vol. 1, no. 5, p. e00025, 2017, doi: 10.1002/pld3.25.

[211] J. Tang et al., "GDSL lipase occluded stomatal pore 1 is required for wax biosynthesis and stomatal cuticular ledge formation," New Phytologist, vol. 228, no. 6, pp. 1880–1896, 2020, doi: 10.1111/nph.16741.

[212] H. Chen et al., "Recent Advances in Biosynthesis and Bioactivity of Plant Caffeoylquinic Acids," Current Issues in Molecular Biology, vol. 47, no. 11, p. 942, Nov. 2025, doi: 10.3390/cimb47110942.

[213] A. V. Alber et al., "Evolution of coumaroyl conjugate 3-hydroxylases in land plants: lignin biosynthesis and defense," The Plant Journal, vol. 99, no. 5, pp. 924–936, 2019, doi: 10.1111/tpj.14373.

[214] B. Yadav, A. Jogawat, M. S. Rahman, and O. P. Narayan, "Secondary metabolites in the drought stress tolerance of crop plants: A review," Gene Reports, vol. 23, p. 101040, Jun. 2021, doi: 10.1016/j.genrep.2021.101040.

[215] L. Almagro et al., "Dissecting the Transcriptional Response to Elicitors in Vitis vinifera Cells," PLOS ONE, vol. 9, no. 10, p. e109777, Oct. 2014, doi: 10.1371/journal.pone.0109777.

[216] M. Priya et al., "Drought and heat stress-related proteins: an update about their functional relevance in imparting stress tolerance in agricultural crops," Theor. Appl. Genet., vol. 132, no. 6, pp. 1607–1638, Jun. 2019, doi: 10.1007/s00122-019-03331-2.

[217] M. H. Arisha et al., "RNA-sequencing analysis revealed genes associated drought stress responses of different durations in hexaploid sweet potato," Sci. Rep., vol. 10, no. 1, p. 12573, Jul. 2020, doi: 10.1038/s41598-020-69232-3.

[218] X. Yang, M. Lu, Y. Wang, Y. Wang, Z. Liu, and S. Chen, "Response Mechanism of Plants to Drought Stress," Horticulturae, vol. 7, no. 3, p. 50, Mar. 2021, doi: 10.3390/horticulturae7030050.

[219] S. Saito et al., "Arabidopsis CYP707As Encode (+)-Abscisic Acid 8'-Hydroxylase, a Key Enzyme in the Oxidative Catabolism of Abscisic Acid," Plant Physiol., vol. 134, no. 4, pp. 1439–1449, Apr. 2004, doi: 10.1104/pp.103.037614.

[220] F. Gaiotti, L. Nerva, G. Fila, L. Lovat, N. Belfiore, and W. Chitarra, "Comparative effects of drought stress on leaf gas exchange, foliar ABA and leaf orientation in four grapevine cultivars grown in Northern Italy," Physiologia Plantarum, vol. 175, no. 6, p. e14063, 2023, doi: 10.1111/ppl.14063.

[221] L. Guan et al., "Transcriptome Sequence Analysis Elaborates a Complex Defensive Mechanism of Grapevine (Vitis vinifera L.) in Response to Salt Stress," Int. J. Mol. Sci., vol. 19, no. 12, p. 4019, Dec. 2018, doi: 10.3390/ijms19124019.

[222] A. Upadhyay et al., "Global transcriptome analysis of grapevine (Vitis vinifera L.) leaves under salt stress reveals differential response at early and late stages of stress in table grape cv. Thompson Seedless," Plant Physiology and Biochemistry, vol. 129, pp. 168–179, Aug. 2018, doi: 10.1016/j.plaphy.2018.05.032.

[223] H. Gong et al., "Contrast in chloride exclusion between two grapevine genotypes and its variation in their hybrid progeny," J. Exp. Bot., vol. 62, no. 3, pp. 989–999, Jan. 2011, doi: 10.1093/jxb/erq326.

[224] M. Corso et al., "Comprehensive transcript profiling of two grapevine rootstock genotypes contrasting in drought susceptibility links the phenylpropanoid pathway to enhanced tolerance," J. Exp. Bot., vol. 66, no. 19, pp. 5739–5752, Sep. 2015, doi: 10.1093/jxb/erv274.

[225] Q. Fu, Y. Tan, H. Zhai, and Y. Du, "Evaluation of salt resistance mechanisms of grapevine hybrid rootstocks," Sci. Hortic., vol. 243, pp. 148–158, Jan. 2019, doi: 10.1016/j.scienta.2018.07.034.

[226] B. Ç. Aydemir et al., "Salt stress induces endoplasmic reticulum stress-responsive genes in a grapevine rootstock," PLOS ONE, vol. 15, no. 7, p. e0236424, Jul. 2020, doi: 10.1371/journal.pone.0236424.

[227] D. Bianchi, L. Caramanico, D. Grossi, L. Brancadoro, and G. D. Lorenzis, "How Do Novel M-Rootstock (Vitis Spp.) Genotypes Cope with Drought?," Plants, vol. 9, no. 10, p. 1385, Oct. 2020, doi: 10.3390/plants9101385.

[228] N. Franck et al., "Contrasting grapevines grafted into naturalized rootstock suggest scion-driven transcriptomic changes in response to water deficit," Sci. Hortic., vol. 262, p. 109031, Feb. 2020, doi: 10.1016/j.scienta.2019.109031.

[229] J. P. Baggett et al., "Is foliar Cl- concentration the cause of photosynthetic decline in grapevine during mild salinity?," OENO One, vol. 55, no. 4, pp. 33–48, Oct. 2021, doi: 10.20870/oeno-one.2021.55.4.4795.

[230] V. Urdanoz and R. Aragüés, "Three-year field response of drip-irrigated grapevine (Vitis vinifera L., cv. Tempranillo) to soil salinity," Plant Soil, vol. 324, no. 1, pp. 219–230, Nov. 2009, doi: 10.1007/s11104-009-9948-6.

[231] L. Lucini, B. Miras-Moreno, M. Busconi, A. Marocco, M. Gatti, and S. Poni, "Molecular basis of rootstock-related tolerance to water deficit in Vitis vinifera L. cv. Sangiovese: A physiological and metabolomic combined

approach," Plant Science, vol. 299, p. 110600, Oct. 2020, doi: 10.1016/j.plantsci.2020.110600.

[232] B. Prinsi, O. Failla, A. Scienza, and L. Espen, "Root Proteomic Analysis of Two Grapevine Rootstock Genotypes Showing Different Susceptibility to Salt Stress," Int. J. Mol. Sci., vol. 21, no. 3, p. 1076, Jan. 2020, doi: 10.3390/ijms21031076.

[233] S. Dal Santo et al., "Grapevine field experiments reveal the contribution of genotype, the influence of environment and the effect of their interaction (G×E) on the berry transcriptome," The Plant Journal, vol. 93, no. 6, pp. 1143–1159, 2018, doi: 10.1111/tpj.13834.

[234] A. Zombardo et al., "Transcriptomic and biochemical investigations support the role of rootstock-scion interaction in grapevine berry quality," BMC Genomics, vol. 21, no. 1, p. 468, Jul. 2020, doi: 10.1186/s12864-020-06795-5.

[235] G. Ozdemir and B. Devrim, "Effects of Different Iron Applications on Root Ferric Chelate Reductase Activity of Öküzgözü and Boğazkere Grape Varieties," presented at the International Engineering and Natural Sciences Conference, Nov. 2018. Accessed: Sep. 16, 2026. [Online]. Available: https://www.researchgate.net/publication/329863982_EFFECTS_OF_DIFFERENT_IRON_APPLICATIONS_ON_ROOT_FERRIC_CHELATE_REDUCTASE_ACTIVITY_OF_OKUZGOZU_AND_BOGAZKERE_GRAPE_VARIETIES

[236] G. Li, H. J. Kronzucker, and W. Shi, "The Response of the Root Apex in Plant Adaptation to Iron Heterogeneity in Soil," Front. Plant Sci., vol. 7, Mar. 2016, doi: 10.3389/fpls.2016.00344.

[237] X.-M. Liu et al., "ZAT11, a zinc finger transcription factor, is a negative regulator of nickel ion tolerance in Arabidopsis," Plant Cell Rep., vol. 33, no. 12, pp. 2015–2021, Dec. 2014, doi: 10.1007/s00299-014-1675-7.

[238] M. Xie, J. Sun, D. Gong, and Y. Kong, "The Roles of Arabidopsis C1-2i Subclass of C2H2-type Zinc-Finger Transcription Factors," Genes (Basel), vol. 10, no. 9, p. 653, Aug. 2019, doi: 10.3390/genes10090653.

[239] X. Zhang, D. Zhang, W. Sun, and T. Wang, "The Adaptive Mechanism of Plants to Iron Deficiency via Iron Uptake, Transport, and Homeostasis," Int. J. Mol. Sci., vol. 20, no. 10, p. 2424, Jan. 2019, doi: 10.3390/ijms20102424.

[240] C. W. Jin, G. Y. You, Y. F. He, C. Tang, P. Wu, and S. J. Zheng, "Iron Deficiency-Induced Secretion of Phenolics Facilitates the Reutilization of Root Apoplastic Iron in Red Clover," Plant Physiol., vol. 144, no. 1, pp. 278–285, May 2007, doi: 10.1104/pp.107.095794.

[241] L. Marastoni et al., "Changes in physiological activities and root exudation profile of two grapevine rootstocks reveal common and specific strategies for Fe acquisition," Sci. Rep., vol. 10, no. 1, p. 18839, Nov. 2020, doi: 10.1038/s41598-020-75317-w.

[242] W. Schmidt and T. J. Buckhout, "A hitchhiker's guide to the Arabidopsis ferrome," Plant Physiology and Biochemistry, vol. 49, no. 5, pp. 462–470, May 2011, doi: 10.1016/j.plaphy.2010.12.001.

[243] G. Vert et al., "IRT1, an Arabidopsis Transporter Essential for Iron Uptake from the Soil and for Plant Growth," Plant Cell, vol. 14, no. 6, pp. 1223–1233, Jun. 2002, doi: 10.1105/tpc.001388.

[244] A. Zamboni et al., "Genome-wide microarray analysis of tomato roots showed defined responses to iron deficiency," BMC Genomics, vol. 13, no. 1, p. 101, Mar. 2012, doi: 10.1186/1471-2164-13-101.

[245] M. Krausko, M. Labajová, D. Peterková, and J. Jásik, "Specific expression of AtIRT1 in phloem companion cells suggests its role in iron translocation in aboveground plant organs," Plant Signal. Behav., vol. 16, no. 9, p. 1925020, 2021, doi: 10.1080/15592324.2021.1925020.

[246] Y. Wang et al., "Effects of Iron Deficiency Stress on Plant Growth and Quality in Flowering Chinese Cabbage and Its Adaptive Response," Agronomy, vol. 12, no. 4, p. 875, Apr. 2022, doi: 10.3390/agronomy12040875.

[247] S. Lee, F. K. Ricachenevsky, and T. Punshon, "Functional overlap of two major facilitator superfamily transporter, ZIF1, and ZIFL1 in zinc and iron homeostasis," Biochemical and Biophysical Research Communications, vol. 560, pp. 7–13, Jun. 2021, doi: 10.1016/j.bbrc.2021.04.120.

[248] T.-Y. Wu, W. Gruissem, and N. K. Bhullar, "Facilitated citrate-dependent iron translocation increases rice endosperm iron and zinc concentrations," Plant Science, vol. 270, pp. 13–22, May 2018, doi: 10.1016/j.plantsci.2018.02.002.

[249] F. Divol, D. Couch, G. Conéjéro, H. Roschzttardtz, S. Mari, and C. Curie, "The Arabidopsis YELLOW STRIPE LIKE4 and 6 transporters control iron release from the chloroplast," Plant Cell, vol. 25, no. 3, pp. 1040–1055, Mar. 2013, doi: 10.1105/tpc.112.107672.

[250] M. Carli, S. Risoli, G. Lorenzini, E. Pellegrini, C. Nali, and L. Cotrozzi, "Biometric, Physiological, Biochemical, and Molecular Responses of Grapevine to Flavescence Dorée Phytoplasma Infection: A Comprehensive Meta-Analysis," Phytopathology, vol. 116, no. 9, 2026, doi: 10.1094/PHYTO-04-26-0103-R.

[251] B. E. Maust, F. Espadas, C. Talavera, M. Aguilar, J. M. Santamaría, and C. Oropeza, "Changes in Carbohydrate Metabolism in Coconut Palms Infected with the Lethal Yellowing Phytoplasma," Phytopathology, vol. 93, no. 8, pp. 976–981, Aug. 2003, doi: 10.1094/PHYTO.2003.93.8.976.

[252] Y.-P. Gai et al., "Metabolomic analysis reveals the potential metabolites and pathogenesis involved in mulberry yellow dwarf disease," Plant, Cell & Environment, vol. 37, no. 6, pp. 1474–1490, 2014, doi: 10.1111/pce.12255.

[253] M. A. Ballicora, A. A. Iglesias, and J. Preiss, "ADP-Glucose Pyrophosphorylase: A Regulatory Enzyme for Plant Starch Synthesis," Photosynth. Res., vol. 79, no. 1, pp. 1–24, Jan. 2004, doi: 10.1023/B:PRES.0000011916.67519.58.

[254] M. Dermastia et al., "Candidate pathogenicity factor/effector proteins of 'Candidatus Phytoplasma solani' modulate plant carbohydrate metabolism, accelerate the ascorbate–glutathione cycle, and induce autophagosomes," Front. Plant Sci., vol. 14, p. 1232367, Aug. 2023, doi: 10.3389/fpls.2023.1232367.

[255] C. Mittelberger, B. Hause, and K. Janik, "The 'Candidatus Phytoplasma mali' effector protein SAP11CaPm interacts with MdTCP16, a class II CYC/TB1 transcription factor that is highly expressed during phytoplasma infection," PLOS ONE, vol. 17, no. 12, p. e0272467, Dec. 2022, doi: 10.1371/journal.pone.0272467.

[256] A. Sugio, A. M. MacLean, and S. A. Hogenhout, "The small phytoplasma virulence effector SAP11 contains distinct domains required for nuclear targeting and CIN-TCP binding and destabilization," New Phytologist, vol. 202, no. 3, pp. 838–848, 2014, doi: 10.1111/nph.12721.

[257] Z. Mou, W. Fan, and X. Dong, "Inducers of Plant Systemic Acquired Resistance Regulate NPR1 Function through Redox Changes," Cell, vol. 113, no. 7, pp. 935–944, Jun. 2003, doi: 10.1016/S0092-8674(03)00429-X.

[258] M. Kinkema, W. Fan, and X. Dong, "Nuclear Localization of NPR1 Is Required for Activation of PR Gene Expression," Plant Cell, vol. 12, no. 12, pp. 2339–2350, Dec. 2000, doi: 10.1105/tpc.12.12.2339.

[259] M. Malnoy et al., "DNA-Free Genetically Edited Grapevine and Apple Protoplast Using CRISPR/Cas9 Ribonucleoproteins," Front. Plant Sci., vol. 7, Dec. 2016, doi: 10.3389/fpls.2016.01904.

[260] D. M. Tricoli and J. M. Debernardi, "An efficient protoplast-based genome editing protocol for Vitis species," Hortic. Res., vol. 11, no. 1, p. uhad266, Jan. 2024, doi: 10.1093/hr/uhad266.

[261] G. Gambino et al., "Genome editing of a recalcitrant wine grape genotype by lipofectamine-mediated delivery of CRISPR/Cas9 ribonucleoproteins to protoplasts," The Plant Journal, vol. 119, no. 1, pp. 404–412, 2024, doi: 10.1111/tpj.16770.

[262] C. Böttcher et al., "Efficient DNA-Free Protoplast Gene Editing of Elite Winegrape Cultivars for the Generation of Clones With Reduced Downy Mildew Susceptibility," Australian Journal of Grape and Wine Research, vol. 2025, no. 1, p. 8867814, 2025, doi: 10.1155/ajgw/8867814.

[263] G. Gambino, M. Minuto, P. Boccacci, I. Perrone, R. Vallania, and I. Gribaudo, "Characterization of expression dynamics of WOX homeodomain transcription factors during somatic embryogenesis in Vitis vinifera," J. Exp. Bot., vol. 62, no. 3, pp. 1089–1101, Jan. 2011, doi: 10.1093/jxb/erq349.

Bibliography

Publications Related to the Thesis

Journal Articles

Rebeka Strah, Rachele Falchi, Chao Song, Andrej Blejec, Živa Ramšak, Kristina Gruden, Enrico Peterlunger, Aaron Fait, Maruša Pompe Novak, Paolo Sivilotti, "Combined omics data reveal multilevel response to water deficit in grapevine disease-resistant varieties", *Frontiers in plant science*, 2026, vol. 17

Sarhan Khalil, Rebeka Strah, Arianna Lodovici, Petr Vojta, Jörg Ziegler, Maruša Pompe Novak, Laura Zanin, Nicola Tomasi, Astrid Forneck, Michaela Griesser, "Lime-induced iron deficiency stimulates a stronger response in tolerant grapevine rootstocks compared to low iron availability", *Plant stress*, Jun. 2025, vol. 16.

Sarhan Khalil, Rebeka Strah, Arianna Lodovici, Petr Vojta, Federica De Berardinis, Jörg Ziegler, Maruša Pompe Novak, Laura Zanin, Nicola Tomasi, Astrid Forneck, Michaela Griesser, "The activation of iron deficiency responses of grapevine rootstocks is dependent to the availability of the nitrogen forms", *BMC plant biology*, 2024, vol. 24

Ignacio Buesa, Juan G. Pérez-Pérez, Fernando Visconti, Rebeka Strah, Diego S. Intrigliolo, Luis Bonet, Kristina Gruden, Maruša Pompe Novak, Jose M. de Paz, "Physiological and transcriptional responses to saline irrigation of young 'Tempranillo' vines grafted onto different rootstocks", *Frontiers in plant science*, Jun. 2022, vol. 13.

Marina Dermastia, Blaž Škrlj, Rebeka Strah, Barbara Anžič, Špela Tomaž, Maja Križnik, Christina Schönhuber, Monika Riedle-Bauer, Živa Ramšak, Marko Petek, Aleš Kladnik, Nada Lavrač, Kristina Gruden, Thomas Roitsch, Günter Brader, Maruša Pompe Novak, "Differential response of grapevine to Infection with 'Candidatus Phytoplasma solani' in early and late growing season through complex regulation of mRNA and small RNA transcriptomes", *International journal of molecular sciences*, 1 Apr. 2021, vol. 22.

Rebeka Strah, Edoardo Bertini, Sara Zenoni, Maruša Pompe Novak, Mario Pezzotti, Marina Dermastia, "Protocols for grapevine transformation : tissue preparation, protoplast isolation, and cultivation", In: *Phytoplasma : methods and protocols*, Katrin Janik (ed.), Mattia Tabarelli (ed.), 1st ed., New York: Springer Nature, cop. 2026, str. 133-149, ilustr., Methods in molecular biology, 3008, ISBN 978-1-0716-5103-2, https://link.springer.com/protocol/10.1007/978-1-0716-5104-9_11.

Conference Paper

Rebeka Strah, Rachele Falchi, Chao Song, Andrej Blejec, Živa Ramšak, Kristina Gruden, Enrico Peterlunger, Aaron Fait, Maruša Pompe Novak, Paolo Sivilotti, "How

Cabernet Volos and Fleurtai respond to water deficits – integrating transcriptomic and metabolomic data", In: 1st Alpe Adria Plant Physiology Meeting: abstract book: Udine - Rauscedo, 5th/6th March 2026.

Rebeka Strah, Edoardo Bertini, Sara Zenoni, Maruša Pompe Novak, Marina Dermastia, "Regenerating single cells of grapevine cv. Zweiglet into whole plants", In: 16th Jožef Stefan International Postgraduate School Students' Conference, 29th – 31st May, Piran, Slovenia : Book of abstracts : Two decades of discovery: advancing science and solutions, Alnilan Cristina Barros Lobato (ed.), et al., Ljubljana: Jožef Stefan Institute: Jožef Stefan International Postgraduate School, 2024, http://ipssc.mps.si/auxiliary_material/IPSSC24_BoA.pdf.

Paolo Sivilotti, Rachele Falchi, Riccardo Braidotti, Alberto Calderan, Radomira Vankova, Michaela Griesser, Chao Song, Aaron Fait, Rebeka Strah, Andrej Blejec, Živa Ramšak, Kristina Gruden, Maruša Pompe Novak, "Impact of water stress on metabolome and transcriptome of grapevine varieties resistant to diseases", In: 19th CFGBC Symposium: book of abstracts: Slovenia, 6th June 2024, Nejc Nadižar (ed.), Ljubljana: University of Ljubljana, Faculty of Medicine, 2024.

Rebeka Strah, Edoardo Bertini, Sara Zenoni, Maruša Pompe Novak, Marina Dermastia, "Successful regeneration of whole plants from single cells of grapevine cv. Zweiglet", In: 19th CFGBC Symposium: book of abstracts: Slovenia, 6th June 2024, Nejc Nadižar (ed.), Ljubljana: University of Ljubljana, Faculty of Medicine, 2024, str. 44.

Rebeka Strah, Maja Zagorščak, Maja Križnik, Živa Ramšak, Špela Tomaž, Anna Coll Rius, Barbara Dušak, Barbara Anžič, Timotej Čepin, Marko Petek, Aleš Kladnik, Blaž Škrlj, Nada Lavrač, Tjaša Lukan, Kristina Gruden, Maruša Pompe Novak, Marina Dermastia, et al., "Multi-level exploration of interactions between 'Ca. P. solani' and grapevine", In: Proceedings of the 6th European Bois Noir Workshop [and] 1st International Pro-AECOGY Conference : Towards the Prophylactic and Agroecological Control of grapevine yellows : 14-16 May 2024, Bordeaux, France, 6th European Bois Noir Workshop and 1st International Pro-AECOGY Conference, Towards the Prophylactic and Agroecological Control of grapevine yellows, 14-16 May 2024.

Sarhan Khalil, Arianna Lodovici, Rebeka Strah, Astrid Forneck, Laura Zanin, Nicola Tomasi, Maruša Pompe Novak, Michaela Griesser, "Characterization of the adaptive mechanisms of grapevine rootstocks to iron deficiency induced by lime stress", In: Proceedings of the Open International Conference on Grapevine Physiology and Biotechnology 2024: Logroño, La Rioja, Spain, from July 7th to 11th, 2024.

Maruša Pompe Novak, Rebeka Strah, Špela Tomaž, Tjaša Lukan, Anna Coll Rius, Maja Zagorščak, Kristina Gruden, Günter Brader, Marina Dermastia, "The role of phytoplasma effector interaction with phosphoglucomutase in the pathogenicity of 'Candidatus Phytoplasma solani' in grapevine", In: Proceedings of the Open International Conference on Grapevine Physiology and Biotechnology 2024: Logroño, La Rioja, Spain, from July 7th to 11th, 2024.

Rebeka Strah, Edoardo Bertini, Sara Zenoni, Maruša Pompe Novak, Marina Dermastia, "Regenerating embryos from single cells of grapevine cv. Zweiglet", In: 15th Meeting of the Slovenian Biochemical Society with International Participation. Portorož, 20-23 September 2023.

Rebeka Strah, Edoardo Bertini, Sara Zenoni, Maruša Pompe Novak, Marina Dermastia, "Genome editing for phytoplasma-resistant grapevine", In: 14. študentska konferenca Mednarodne podiplomske šole Jožefa Stefana: 2022, Kamnik, Slovenia.

Rebeka Strah, "Metabolic and transcriptomic response to water deficit in two grapevine interspecific hybrids", In: Learning from the drylands - towards ecosystem restoration: abstract book, The 8th International Conference on Drylands, Deserts &

Desertification, November 27–December 1, 2022, The Jacob Blaustein Institutes for Desert Research, Sde Boker Campus, Ben-Gurion University of the Negev.

Katarina Šoln, Nada Žnidaršič, Anna Gasperl, Edith Stabentheiner, Maria Mueller, Rebeka Strah, Špela Baebler, Maruša Pompe Novak, Jasna Dolenc Koce, "Allelopathy of invasive Fallopia plants induced oxidative stress in radish seedlings", In: Plants in Changing Environment: International Conference of the Slovenian Society of Plant Biology: Biotechnical Faculty, University of Ljubljana, September 15-16, 2022, Ljubljana, Slovenia.

Maruša Pompe Novak, Rebeka Strah, Špela Tomaž, Maja Križnik, Živa Ramšak, Marko Petek, Marina Dermastia, Kristina Gruden, "Grapevine in changing environment", In: Plants in Changing Environment: International Conference of the Slovenian Society of Plant Biology: Biotechnical Faculty, University of Ljubljana, September 15-16, 2022, Ljubljana, Slovenia.

Other Publications

Katarina Šoln, Rebeka Strah, Anna Gasperl, Špela Baebler, Maruša Pompe Novak, Edith Stabentheiner, Maria Mueller, Jasna Dolenc Koce, "Transcriptome insights reveal root hair inhibition and ROS imbalance in radish seedlings treated with rhizome extracts of invasive Fallopia species", *Plant physiology and biochemistry*, 2025, vol. 229

Marina Dermastia, Špela Tomaž, Rebeka Strah, Tjaša Lukan, Anna Coll Rius, Barbara Dušak, Timotej Čepin, Aleš Kladnik, Maja Zagorščak, Kristina Gruden, Maruša Pompe Novak, et al., "Candidate pathogenicity factor/effector proteins of 'Candidatus Phytoplasma solani' modulate plant carbohydrate metabolism, accelerate the ascorbate–glutathione cycle, and induce autophagosomes", *Frontiers in plant science*, 2023, vol. 14.

Marina Dermastia, Blaž Škrlj, Anita Valmarska, Rebeka Strah, Maruša Pompe Novak, Barbara Anžič, Špela Tomaž, Maja Križnik, Marko Petek, Aleš Kladnik, Nada Lavrač, Kristina Gruden, et al., "Understanding interactions of 'Candidatus Phytoplasma solani' with grapevine through the lens of complex networks", Phytopathogenic mollicutes, Jun. 2023, vol. 13, DOI: 10.5958/2249-4677.2023.00005.1.

Matej Milijaš Jotić, Andraž Marinč, Rebeka Strah, Jure Zaman, "Vpliv nadmorske višine na pojavljanje arbuskularne mikorize pri navadni ajdi (Fagopyrum esculentum)", *Collectanea studentium physiologiae plantarum*, 2019, vol. 10.

Rebeka Strah, Tanja Kunej, "Molecular sexing assays in 114 mammalian species: in silico sequence reanalysis and a unified graphical visualization of diagnostic tests", *Ecology and evolution*, 2019, vol. 9.

Biography

Rebeka Strah obtained her BSc in Biotechnology at the Biotechnical Faculty of University of Ljubljana in 2018, and her MSc in Ecotechnologies at Jožef Stefan International Postgraduate School in 2021. During her undergraduate studies, she worked under the supervision of Prof. Dr. Marina Dermastia and Prof. Dr. Maruša Pompe Novak in phytoplasma effector research and transcriptomic analyses of grapevine. She also worked with Prof. Dr. Tanja Kunej on a review of molecular sexing assays in mammals, which they published. After graduation, she was employed as a research assistant at NIB and enrolled in the doctoral study programme Nanosciences and Nanotechnologies at the Jožef Stefan International Postgraduate School under the supervision of Prof. Dr. Marina Dermastia. At NIB she is mainly involved in the analysis of high-throughput sequencing (HTS) data and systems biology, with a focus on grapevine (*Vitis vinifera* L.) related projects. She complements this work with various molecular biology approaches to validate the information obtained by sequencing. She was involved in the ARIS project InGrapa, which aimed to elucidate how the phytoplasma '*Candidatus* Phytoplasma solani' interacts with grapevine, in which she performed *in planta* localization studies of effector proteins and contributed to the data analysis of a transcriptomic dataset comparing early- and late-season grapevine responses to infection. The results of this project have been published. She was also involved in the Arimnet EnViRoS project, which investigated grapevine responses to various abiotic stresses, in which she contributed to the analysis of various transcriptomics datasets from several grapevine tissues under water deficit or high salinity conditions. The results of this project have been published. She is also involved in grapevine transformation research at NIB. In the first year of her PhD studies, she attended a six-month short-term scientific mission at the University of Verona, under the supervision of Prof. Dr. Sara Zenoni, where she learned the procedures for grapevine whole-plant regeneration from single cells, and successfully transferred the knowledge to her home institution. She was involved in the ARIS project Crisphy, where the main aim was to produce genome-edited grapevines with the use of the latest DNA-free CRISPR-Cas9 approach. Some, but not all, results of this project have been published. She presented her work at several national and international conferences, where she participated with posters and short talks. She is active at different science popularisation events, such as the Slovenian Science Fair, Fascination of Plants Day, and Researchers' Night. She is also active in education. She was habilitated as an assistant at the University of Nova Gorica in 2025 and is teaching a practical course at the School for Viticulture and Enology at the University of Nova Gorica and a practical course at the Landscape Governance College in Novo Mesto.